nature chemistry

Article

https://doi.org/10.1038/s41557-023-01315-w

Aromatic pentaamide macrocycles bind anions with high affinity for transport across biomembranes

In the format provided by the authors and unedited

1. Supporting Figures and Table

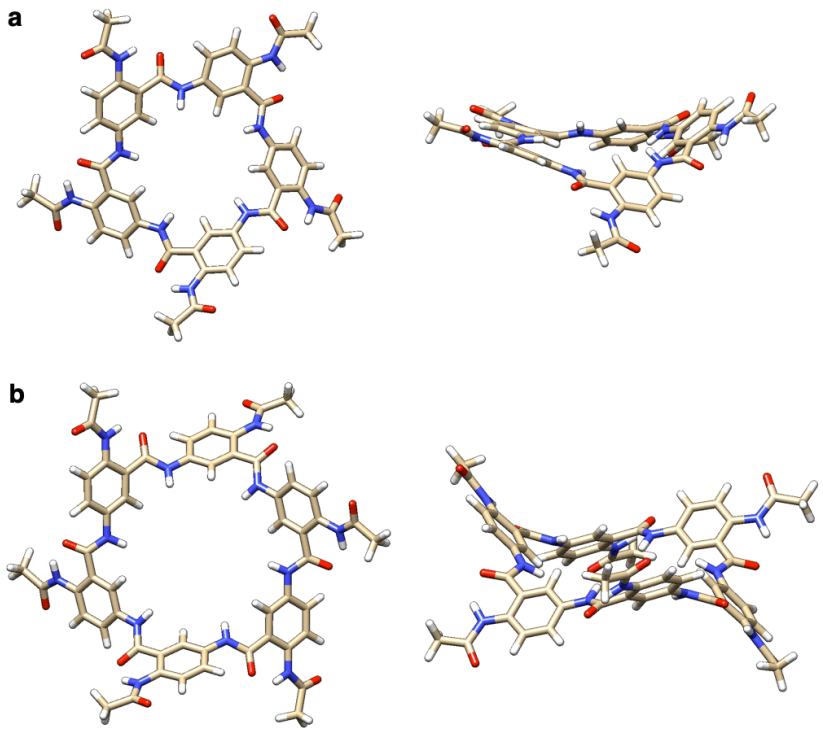

Figure S1 | Top (left) and side (right) views of energy-minimized structures of **a**, the five-residue macrocycle **c5**, and **b**, the six-residue macrocycle **c6**.

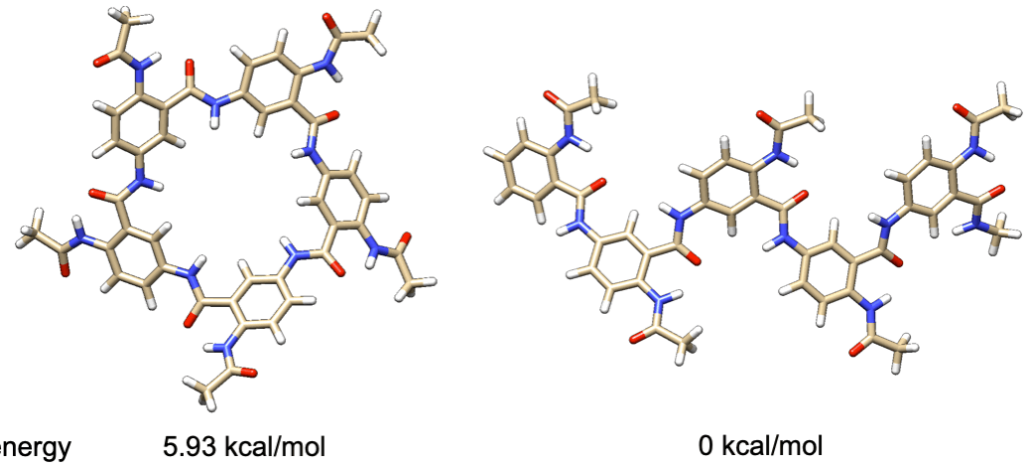

Figure S2 | Formation energy for 'pentamer L5' → 'macrocycle c5' + 'CH_4'. The energy of a CH_4 molecule was added to the energy of the macrocycle **c5** to keep the atom type and atom count equal for comparing the energies of macrocycle **c5** (left) and linear pentamer **L5** (right). The formation of the macrocycle **c5** and a methane molecule is calculated to be 5.93 kcal/mol endothermic with respect to the linear pentamer **L5**.

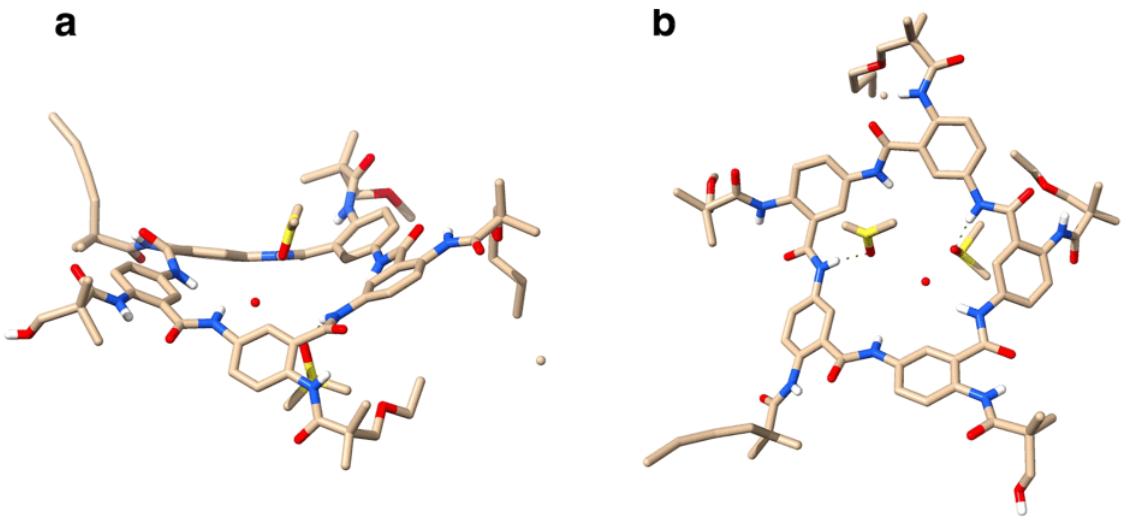

Figure S3 | Crystal structure of macrocycle c5a. a, top view, and **b**, side view. Most of the sidechains are disordered. Two DMSO molecules are H-bonded (dashed lines) are shown.

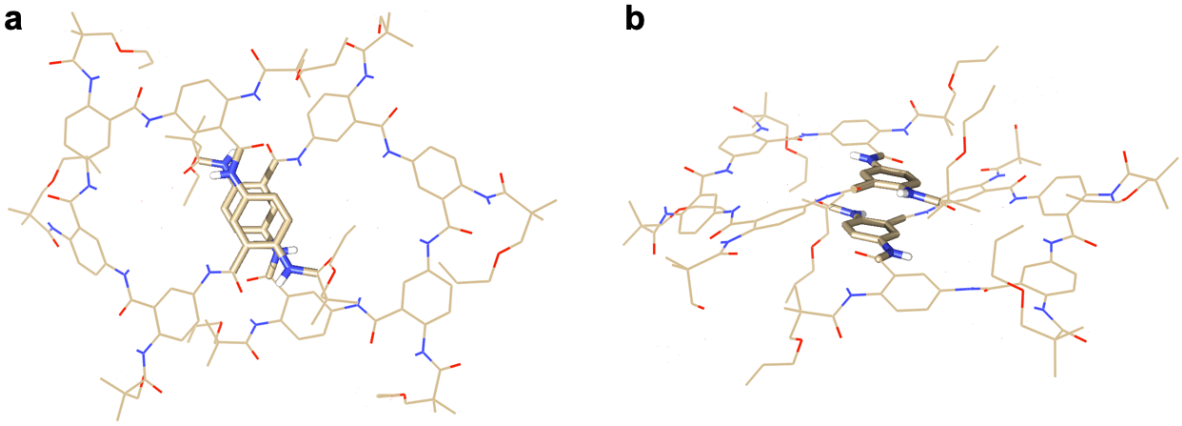

Figure S4 | Packing of two adjacent molecules of macrocycle c5c in the solid state. **a**, top view, and **b**, side view. The two residues that are involved in stacking are shown as sticks and the rest of the bonds are shown as wire. Hydrogen atoms, except for those of amide groups, are omitted for clarity.

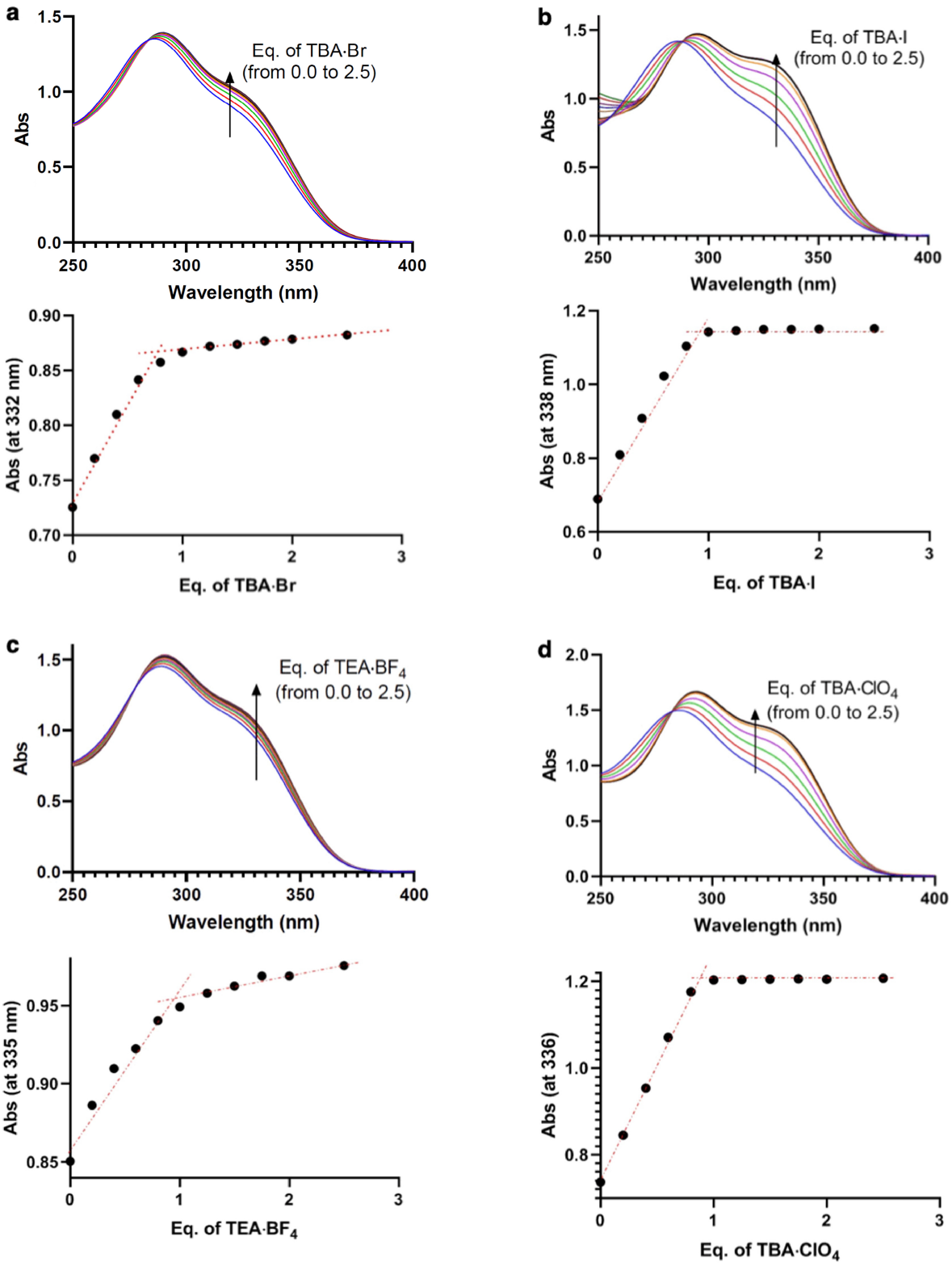

Figure S5(a-d) | **UV-vis titration of c5a** (20 μM) with **a**, TBA^+Br^-, **b**, TBA^+I^-, **c**, $TBA^+BF_4^-$, and **d**, $TBA^+ClO_4^-$, in MeOH:$CHCl_3$ (5:95, v/v)at 25 °C.

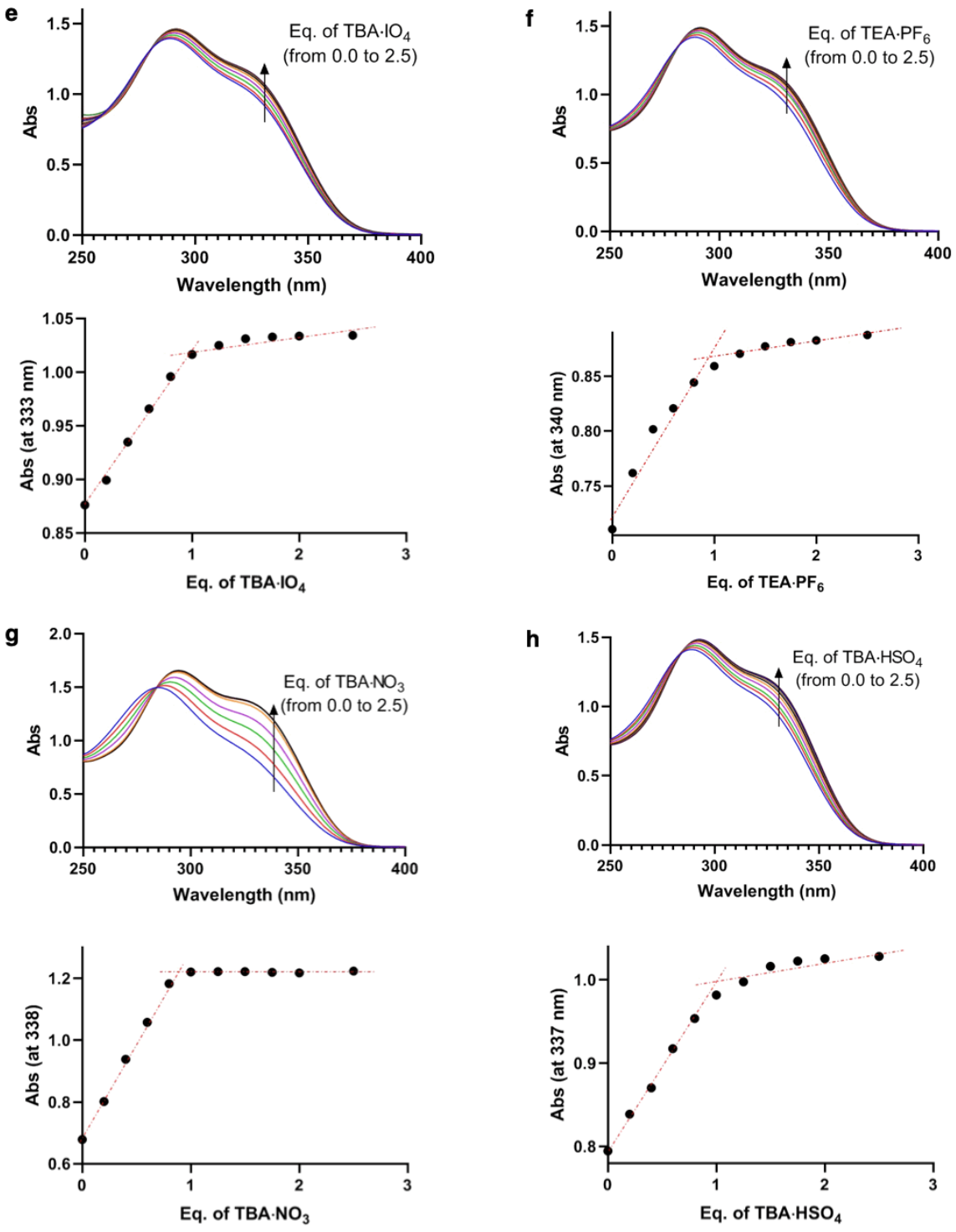

Figure S5(e-h) | **UV-vis titration of c5a** (20 μM) with **e**, $TBA^{+}IO_4^{-}$, **f**, $TEA^{+}PF_6^{-}$, **g**, $TBA^{+}NO_3^{-}$, and **h**, $TBA^{+}HSO_4^{-}$, in MeOH:$CHCl_3$ (5:95, v/v)at 25 °C.

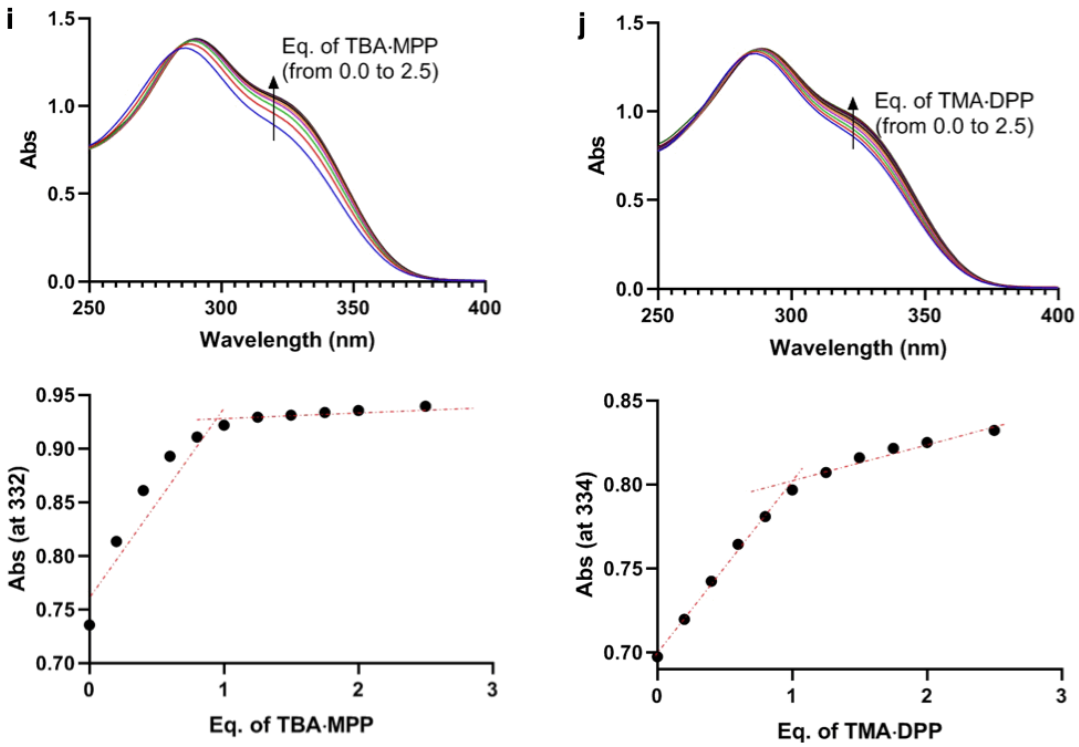

Figure S5(i,j) | **UV-vis titration of c5a** (20 μM) with **i**, TBA^+MPP^-, and **j**, TMA^+DPP^-, in MeOH:$CHCl_3$ (5:95, v/v)at 25 °C.

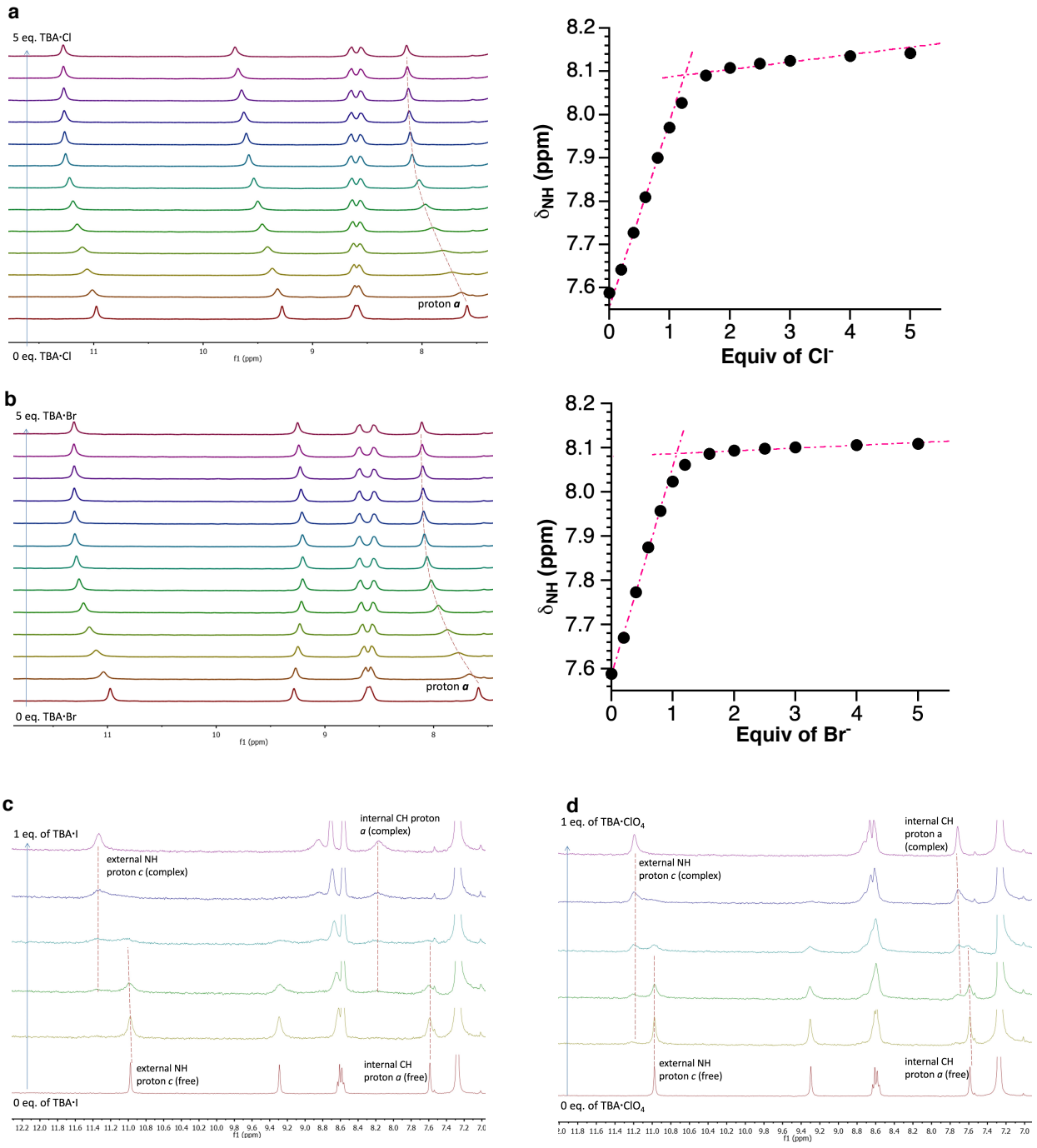

Figure S6 | ^{1}H NMR titration of c5a (0.25 mM) with **a**, TBA^+Cl^-, **b**, TBA^+Br^-, **c**, TBA^+I^-, and **d**, $TBA^+ClO_4^-$, in DMSO-d_6:$CDCl_3$ (1:99, v/v) at 25 °C

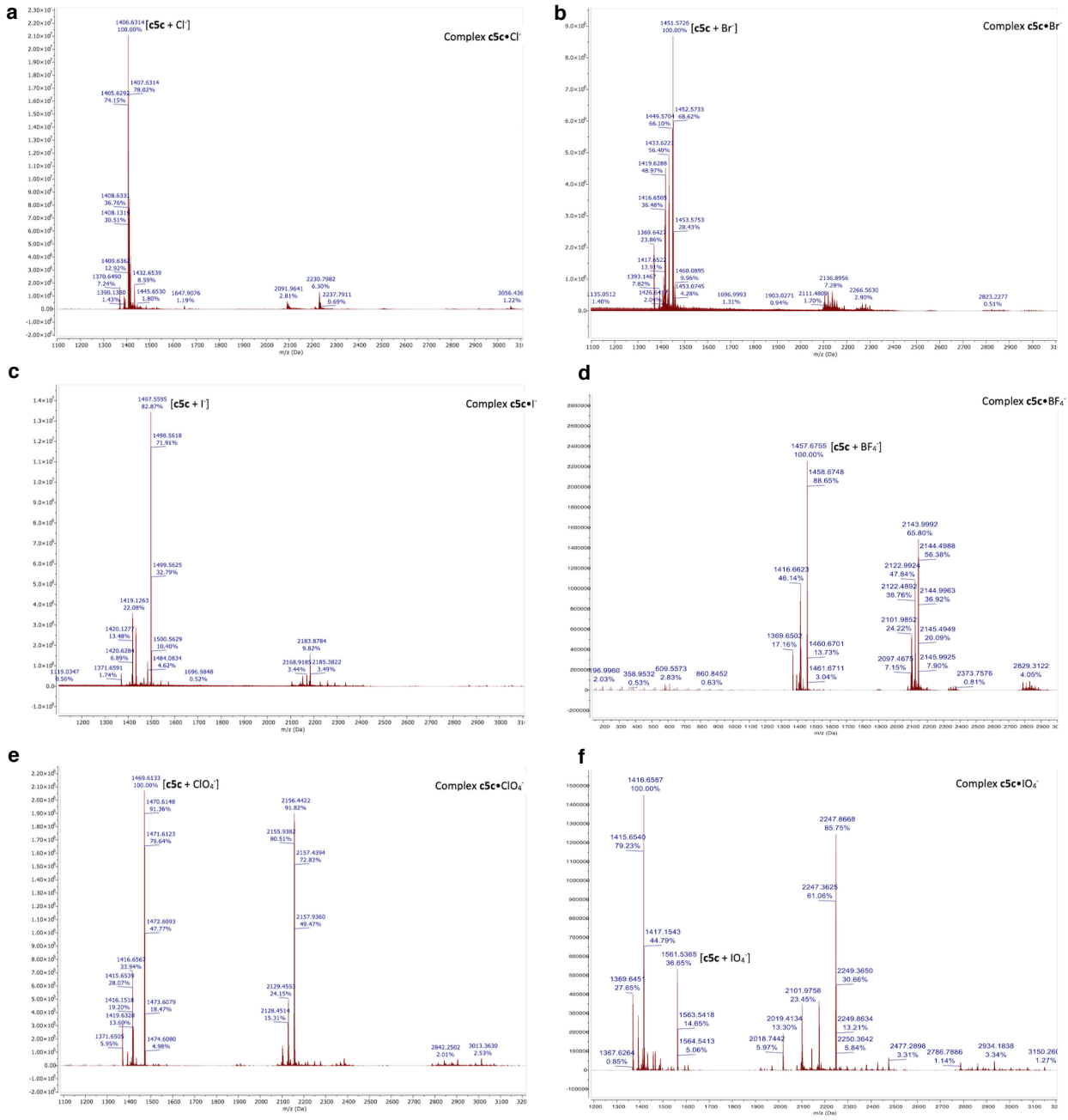

Figure S7(a-f) | High-resolution mass spectra (negative ion mode) the 1:1 complexes of macrocycle **c5c** with **a**, TBA^+Cl^-. If [2 x **c5c** $+Cl^-$] existed, a peak at *m/z* = 2778.6037 would be observed. **b**, TBA^+Br^-. If [2 x **c5c** + $Br]^-$ existed, peak at *m/z* = 2823.0547 would be observed. **c**, TBA^+I^-. If [2 x **c5c** + $I]^-$ existed, peak at *m/z* = 2870.0552 would be observed. **d**, $TBA^+BF_4^-$. If [2 x **c5c** + $BF_4]^-$ existed, a peak at *m/z* = 2828.3209 would be observed. **e**, $TBA^+ClO_4^-$. If [2 x **c5c** + $ClO_4]^-$ existed, a peak at *m/z* = 2946.0635 would be observed. The peak at *m/z* = 1416.1518 corresponds to the 1:1 complex of **c5c** and formate – formic acid was added in the mobile phase. The peak at *m/z* = 2156.4422 cannot be assigned to any complex of **c5a** and ClO_4^- and is most likely from impurity/contaminant from the equipment. **f**, $TBA^+IO_4^-$. If [2 x **c5c** + $IO_4]^-$ existed, a peak at *m/z* = 2934.1838 would be observed. The peak at *m/z* = 1416.6587 corresponds to the 1:1 complex of **c5c** and formate – formic acid was added in the mobile phase.

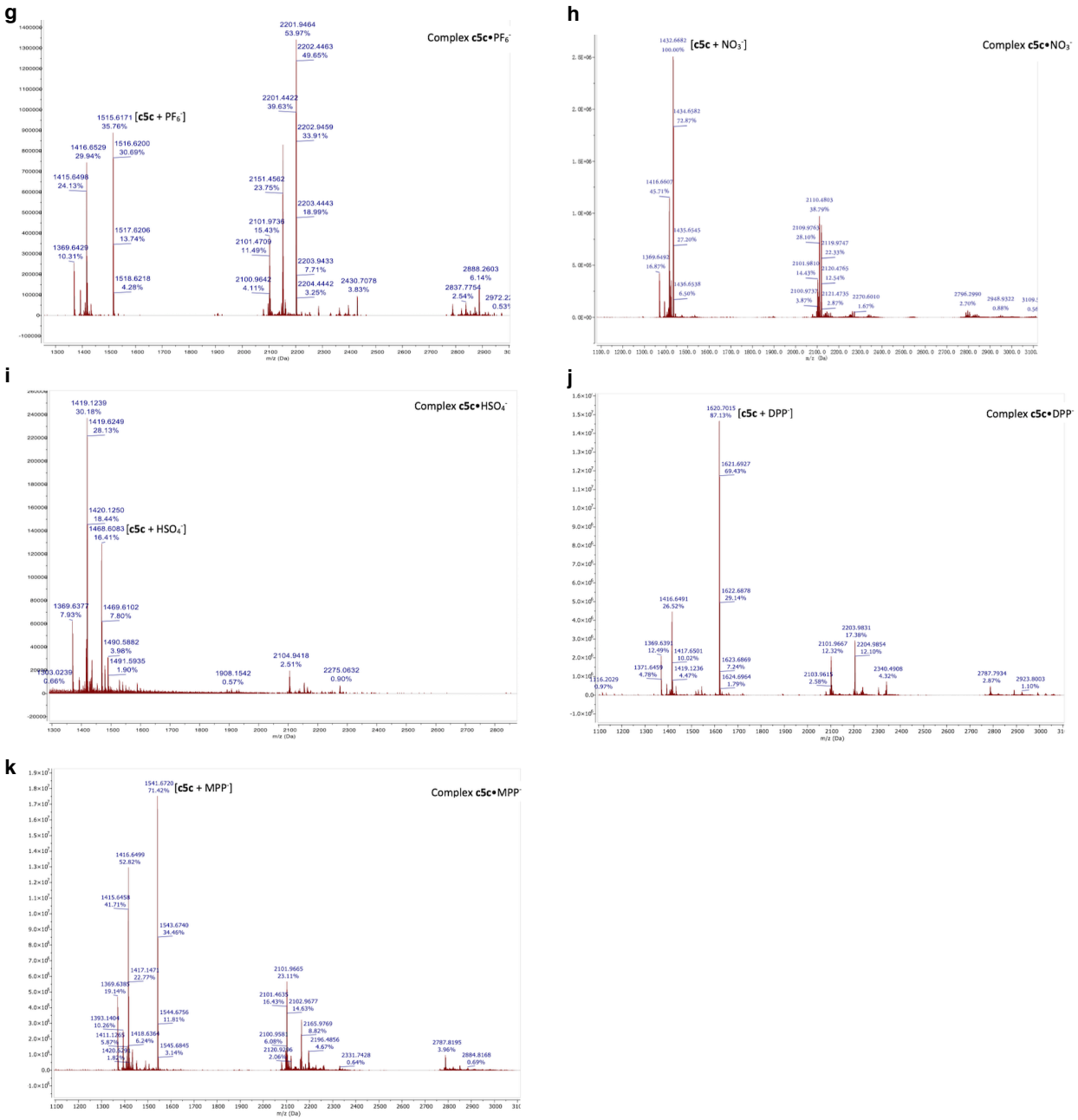

Figure S7(g-k) | High-resolution mass spectra (negative ion mode) the 1:1 complexes of macrocycle **c5c** with **g**, $TEA^+PF_6^-$. (If [2 x **c5c** + PF_6]$^-$ existed, a peak at *m/z* = 2888.1149 would be observed. The peak at *m/z* = 1416.6529 corresponds to the 1:1 complex of **c5c** and formate – formic acid was added in the mobile phase.) **h**, $TBA^+NO_3^-$. If [2 x **c5c** + NO_3]$^-$ existed, a peak at *m/z* = 2803.3058 would be observed. The peak at *m/z* = 1416.6607 corresponds to the 1:1 complex of **c5c** and formate – formic acid was added in the mobile phase. The peaks at *m/z* = 2110 - 2119 cannot be assigned and are likely from impurity/contaminant from the equipment. **i**, $TBA^+HSO_4^-$. If [2 x **c5c** + HSO_4]$^-$ existed, a peak at *m/z* = 2840.2207. would be observed. The peak at *m/z* = 1419.1239 corresponds to [**2 x c5c** + SO_4^{2-}]. **j**, TMA^+DPP^-. If [2 x **c5c** + DPP]$^-$ existed, a peak at *m/z* = 2992.3299 would be observed. The peak at *m/z* = 1416.6491 corresponds to the 1:1 complex of **c5c** and formate – formic acid was added in the mobile phase. **k**, TBA^+MPP^-. If [2 x **c5c** + MPP]$^-$ existed, a peak at *m/z* = 2914.2611 would be observed. The peak at *m/z* = 1416.6499 corresponds to the 1:1 complex of **c5c** and formate – formic acid was added in the mobile phase. The peak at *m/z* = 2101.9665 cannot be assigned to any complex of **c5a** and ClO_4^- and is most likely from impurity/contaminant from the equipment.

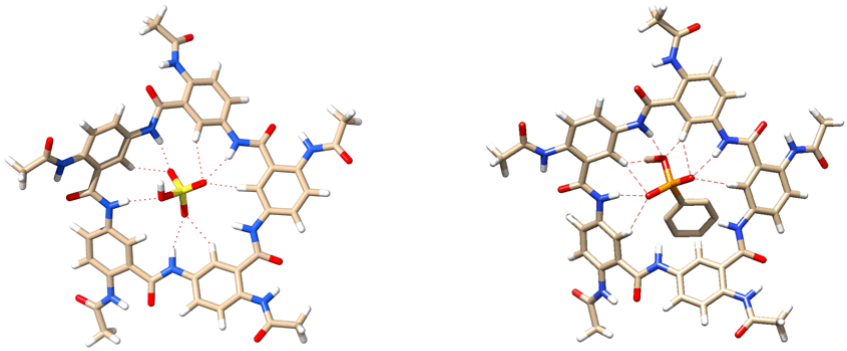

c5•HSO_4^- **c5**•MPP^-

Figure S8 | Optimized structures of the 1:1 complexes of c5 with HSO_4^- and MPP^-. In each complex, the CH/NH protons and the anion that are within van der Waals contact distances ($d_{H\cdots O} \leq 2.8$ Å) are indicated by red dashed lines. The structures were computationally optimized in vacuum.

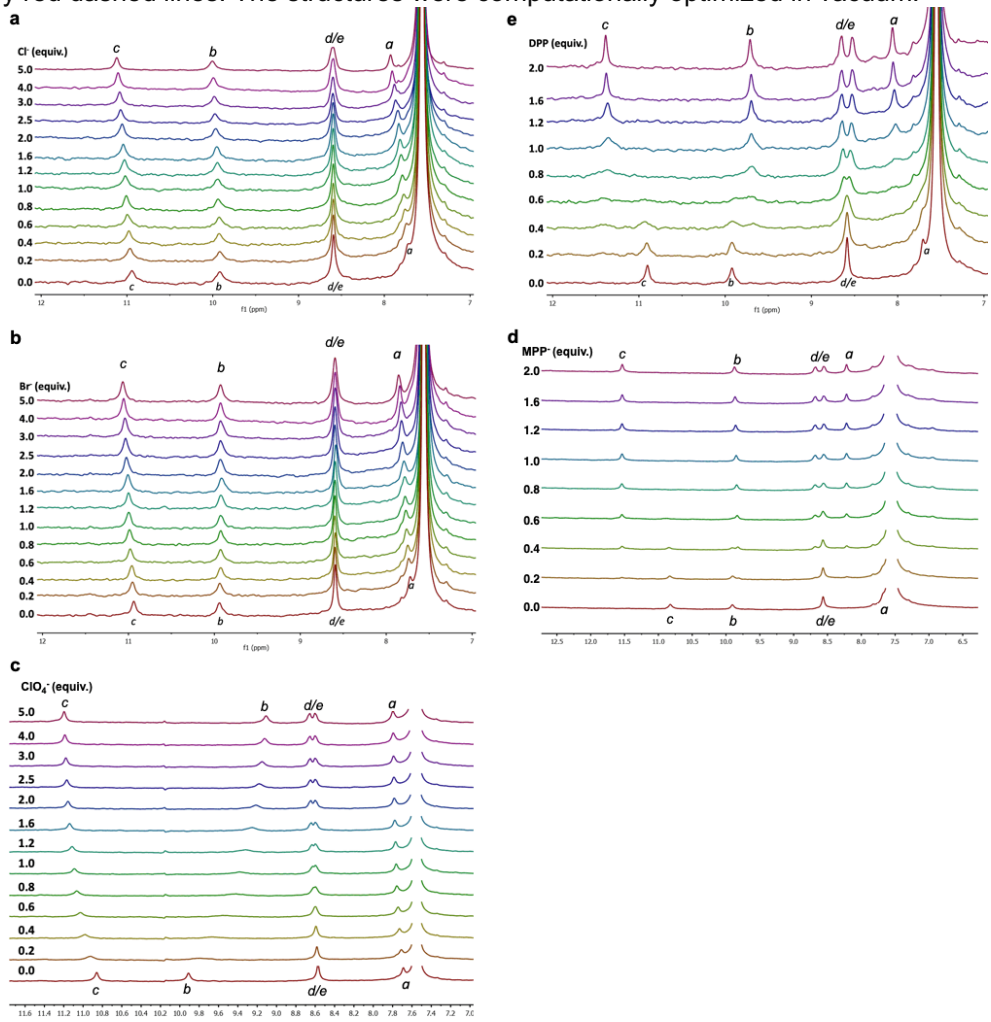

Figure S9 | Partial ^{1}H NMR spectra of c5a (0.1 mM) titrated with **a**, 0 to 5 equiv of TBA^+Cl^-, **b**, 0 to 5 equiv of TBA^+Br^-, **c**, 0 to 5 equiv of $TBA^+ClO_4^-$, **d**, 0 to 2 equiv. of TMA^+DPP^-, and **e**, 0 to 2 equiv of TBA^+MPP^-, in DMSO-d_6 : $CDCl_3$ (15 : 85, v/v).

a (in DMSO:$CHCl_3$ (5:95, v/v) at 25 ^oC)

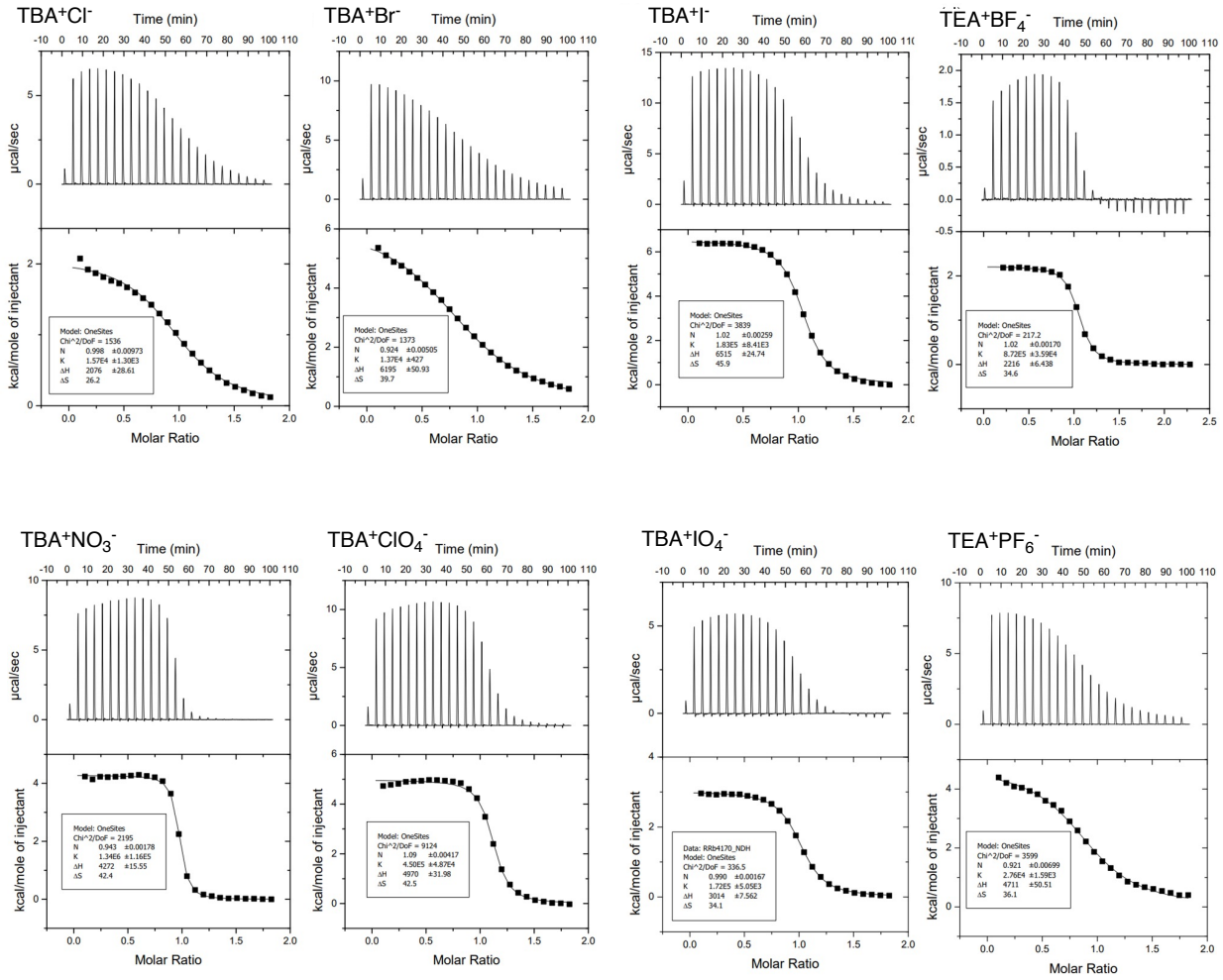

Figure S10a | ITC titration curves (upper panel) and binding isotherms (lower panel) for the complexation of **c5a** (0.5 mM) with the TBA^+ salts (5 mM each) of $Cl^–$, $Br^–$, $I^–$, $BF_4^–$, $NO_3^–$, $ClO_4^–$, $IO_4^–$, and $PF_6^–$ in DMSO:$CHCl_3$ (5:95, v/v) at 25 ^oC.

b (in $CH_3CN:CHCl_3$ (5:95, v/v) at 25 °C

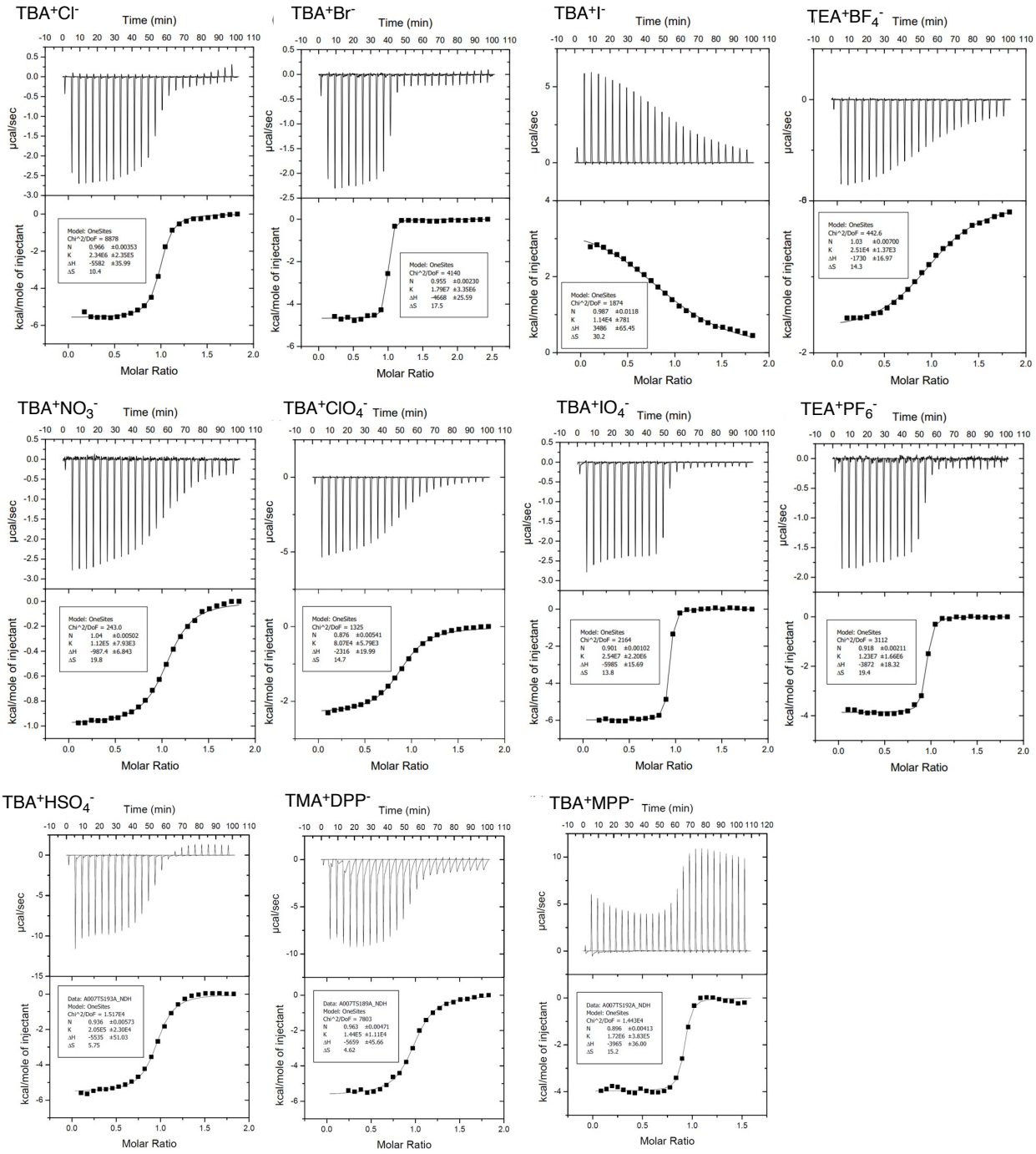

Figure S10b | ITC titration curves (upper panel) and binding isotherms (lower panel) for the complexation of **c5a** with various anions in $CH_3CN:CHCl_3$ (5:95, v/v). Concentrations of **c5a** (in the cell) used in the titrations: 0.075 mM with TBA^+Br^- (1 mM); 0.09 mM with $TBA^+IO_4^-$ (0.9 mM); 0.1 mM with TBA^+Cl^- (1 mM); 0.5 mM with TBA^+I^- (1 mM), $TBA^+BF_4^-$ (5 mM), $TBA^+NO_3^-$ (5 mM), $TBA^+ClO_4^-$ (5 mM), $TBA^+HSO_4^-$ (5 mM), TMA^+DPP^- (5 mM), and TBA^+MPP^- (4 mM). For two-step competition titration experiments, Cl^- (2.5 mM) served as the competitor for the titration of **c5a** with I^-; PF_6^-, served as the competitor for the titration of **c5a** with BF_4^- (PF_6^-: 1 mM), NO_3^- (PF_6^-: 1 mM), ClO_4^- (PF_6^-: 0.5 mM), HSO_4^- (PF_6^-: 2.8 mM), DPP^- (PF_6^-: 5 mM), and MPP^- (PF_6^-: 2.5 mM).

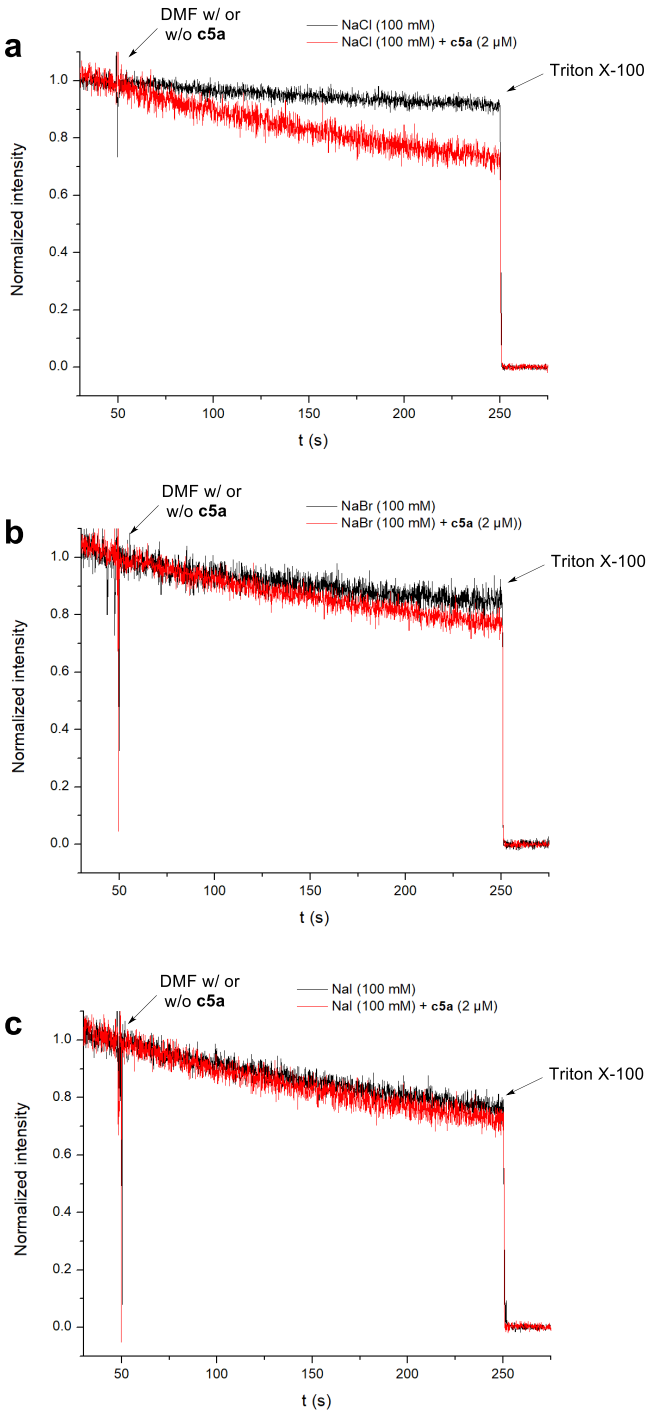

Figure S11 | Halide transport into POPC LUVs mediated by **c5a**. Inside vesicles: 10 mM HEPES, 100 mM $NaNO_3$, 1 mM lucigenin. Outside vesicles: 10 mM HEPES, 100 mM NaX (X =Cl, Br, or I). The emission of the intravesicular lucigenin was monitored at 505 nm (excitation wavelength: 430 nm). After adding **c5a** (final concentration: 2 μM) and monitoring the emission of lucigenin for 200 seconds, the vesicles were lysed by adding 0.1% of Triton X-100.

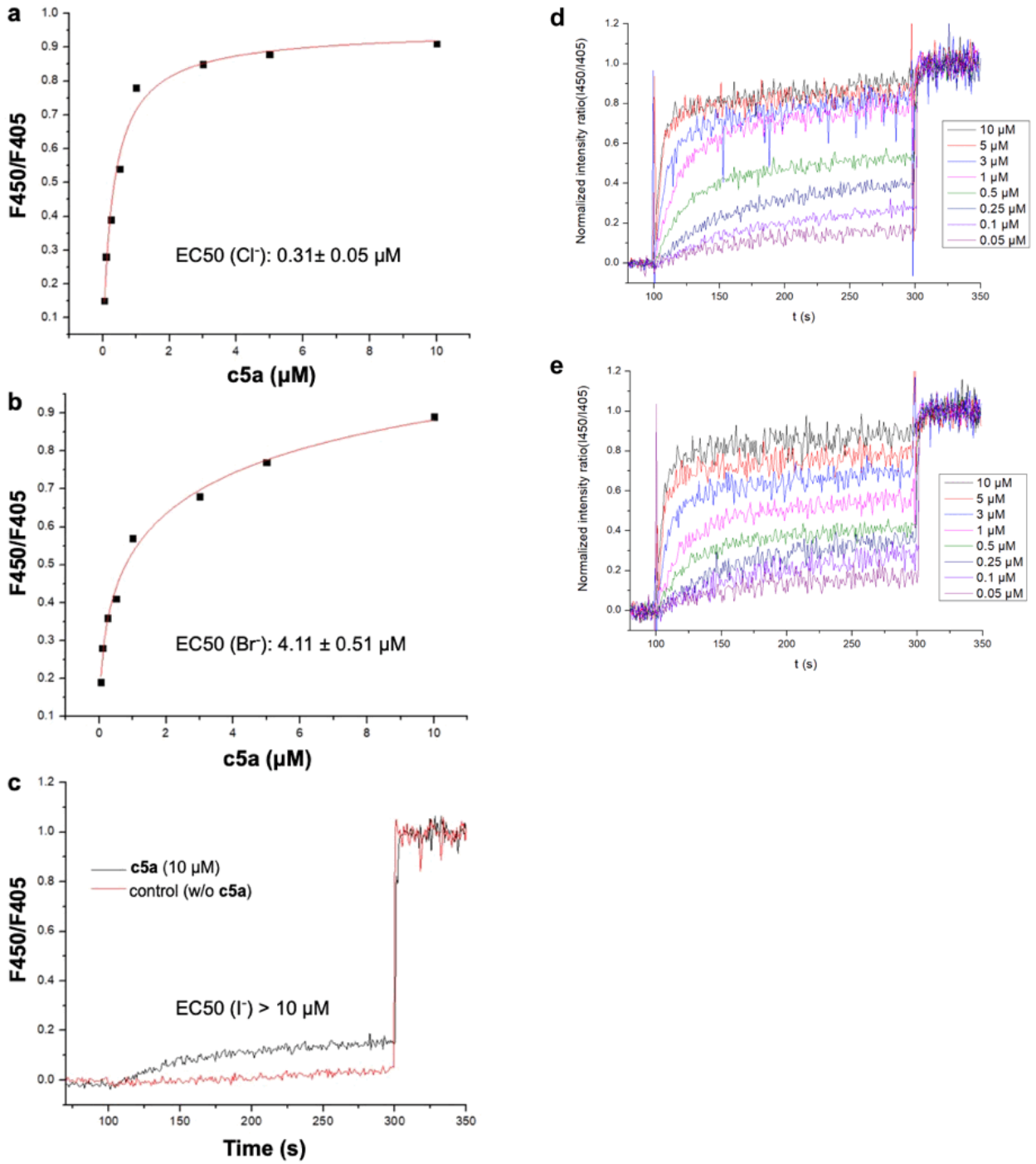

Figure S12 | Dose-response curves and half-maximal effective concentration (EC50) values for the transport of **a**, Cl^-, and **b**, Br^- mediated by macrocycle **c5a** (0.05 to 10 μM, final concentration) reflected by the emission of HPTS (1 mM) entrapped in POPC LUVs. **c**, Fluorescence trace of I^- transport mediated by **c5a** at 10 μM over 200 s. The EC50 for I^- transport by **c5a**, which cannot be determined due to the low transport activity, is estimated to be greater than 10 μM. **d**, Fluorescence trace of Cl^- transport mediated by **c5a** at different concentrations from 0.05 μM to 10 μM over 200 s. **e**, Fluorescence trace of Br^- transport mediated by **c5a** different concentrations from 0.05 μM to 10 μM over 200 s. (emission wavelength: 510 nm; normalized intensity ratio F450/F405: = ratio of fluorescence emission intensities at excitation wavelengths of 450 nm and 405 nm)

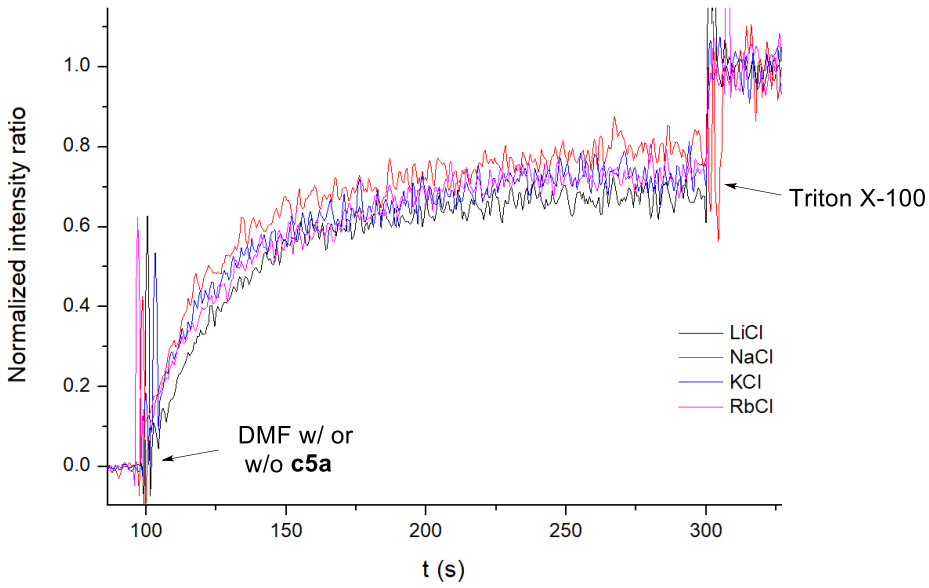

Figure S13 | Ion transport into POPC LUVs mediated by **c5a** at 25 ºC. Inside vesicles: 10 mM HEPES, 100 mM MCl (M = Li, Na, K, Rb), 1 mM HPTS, pH 7.0. Outside vesicles: 10 mM HEPES, 100 mM MCl, pH 7.0. A base pulse (20 ⌈L of 0.5 M NaOH) was applied to each vesicular solution at 50 s, followed by adding 20 ⌈L of c5a in DMF at 100 s. For each group, the vesicles were lysed after 200s by adding 0.1 % Triton X-100 to obtained the maxium emission intensity for normalization. The emission intensities of the intravesicular HPTS at 510 nm, I_{405} and I_{450}, corresponding to two excitation wavelengths (405 and 450 nm) were monitored simultaneously, based on which the normalized intensity ratios (I_{405}/I_{450}) of the two emision intensities were obtained.

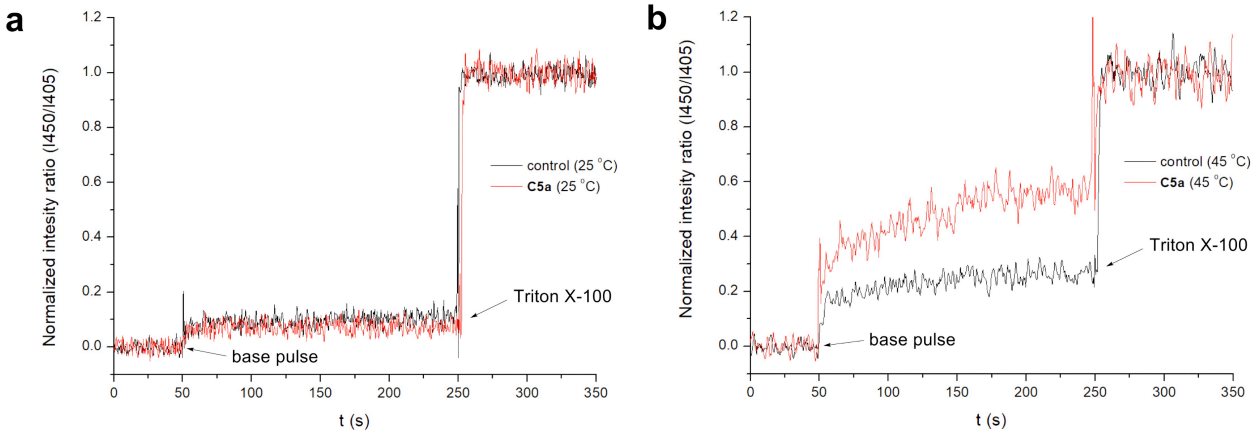

Figure S14 | Chloride transport into DPPC LUVs mediated by **c5a** at 25 ºC and 45 ºC. Inside vesicles: 10 mM HEPES, 100 mM NaCl, 1 mM HPTS, pH 7.0. Outside vesicles: 10 mM HEPES, 100 mM NaCl, pH 7.0. To ensure proper insertion of **c5a**, the LUVs were incubated with **c5a** (final concentration: 2μM) at 45 ºC for 3 min before being kept at 45 ºC or being cooled down to 25 ºC. The LUVs for the control groups do not contain **c5a**. A base pulse (20 uL of NaOH) was applied to each vesicular solution at 25 ºC or 45 ºC. For each group, the vesicles were lysed after 200s by adding 0.1 % Triton X-100 to obtained the maxium emission intensity for normalization. The emission of the intravesicular HPTS was monitored at 505 nm (excitation wavelengths: 405 and 450 nm).

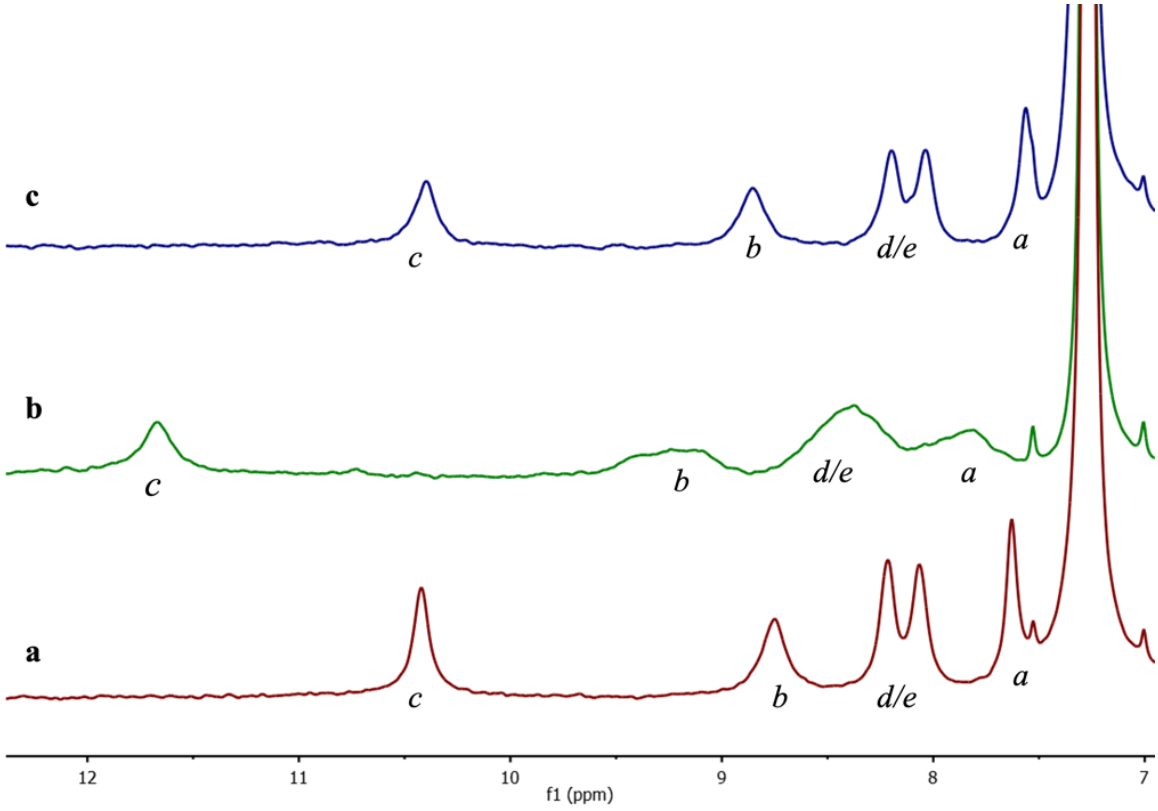

Figure S15 | **^{1}H NMR spectra** of **a**, **c5a**; **b**, **c5b**; and **c**, **c5c** in $CDCl_3$ (0.2 mM, 400 MHz, 25 °C).

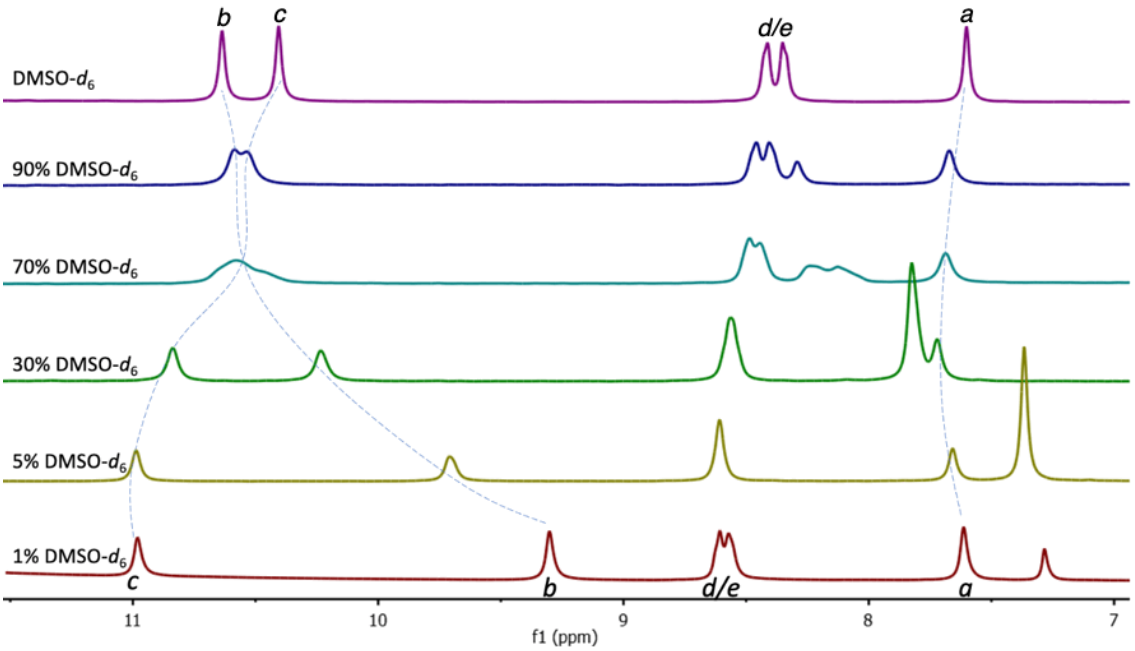

Figure S16 | **^{1}H NMR spectra of c5a** in mixed solvent of DMSO-d_6 and $CDCl_3$ (1.0 mM, 400 MHz, 25 °C).

a (in DMSO-*d*6:$CDCl_3$ (15:85, v/v))

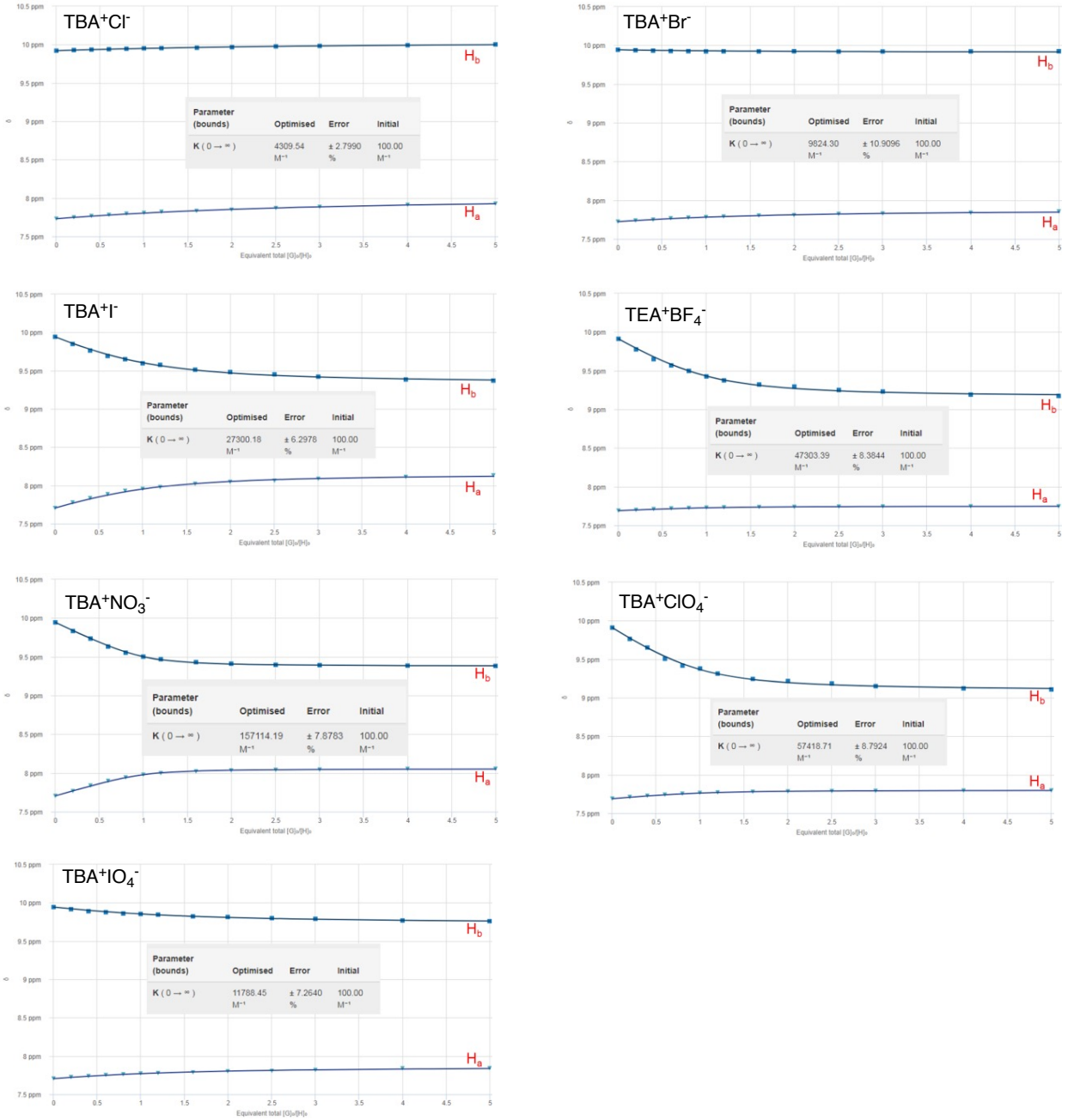

Figure S17a (continued on next page)

b (in $CD_3CN:CDCl_3$ (80:20, v/v)

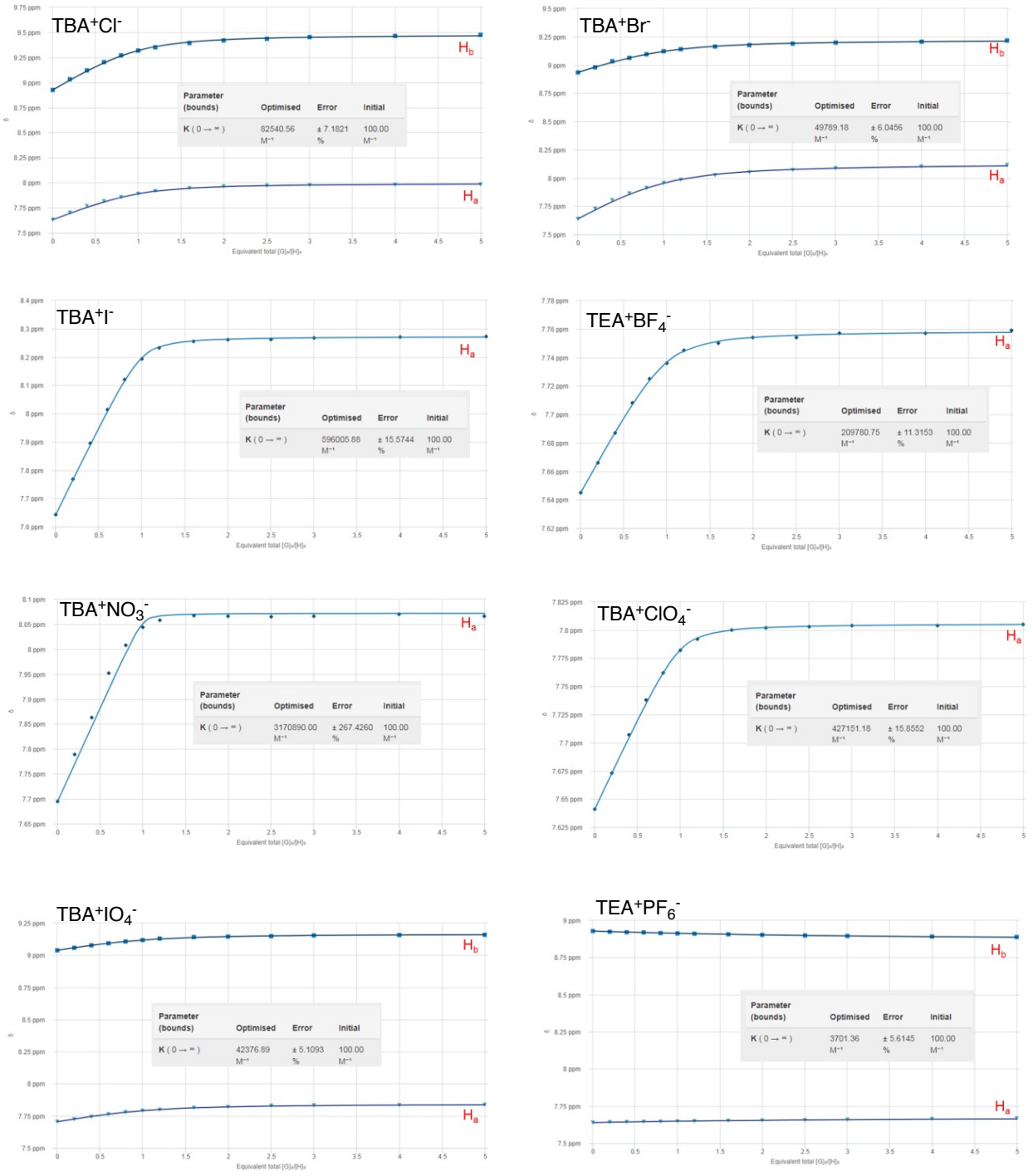

Figure S17b (continued on next page)

c (in DMSO-d_6:$CDCl_3$ (70:30, v/v))

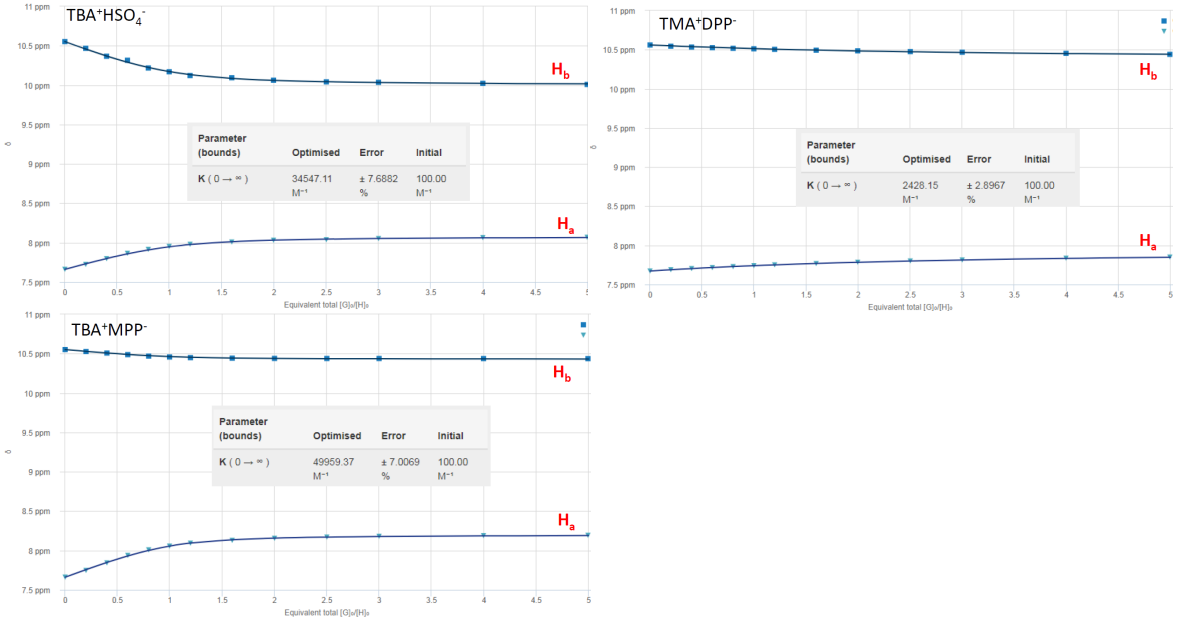

d (in D_2O:acetone-d_6 (20:80, v/v))

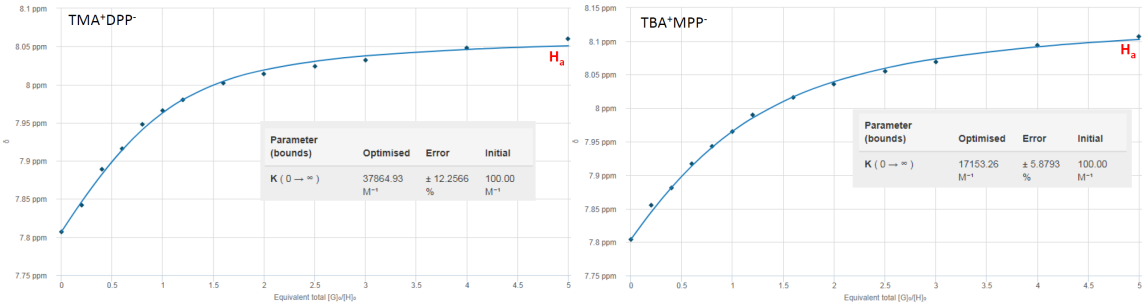

e (in D_2O:acetone-d_6 (60:40, v/v))

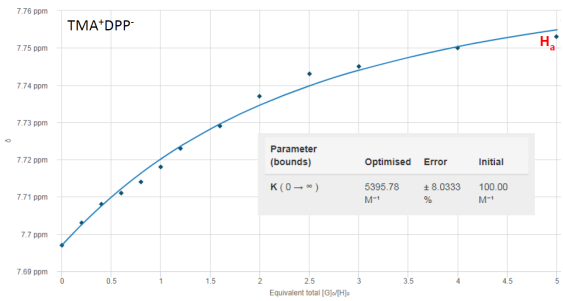

Figure S17(c-e) | Binding isotherms of c5a or c5b (0.1-0.2 mM) titrated with 0-5 equiv of the anions shown in various solvents. In each case, the fitting output is based on the chemical shift changes of CH protons *a* and NH protons *b* (unless indicated otherwise) using the online fitting tool BindFit (v0.5).

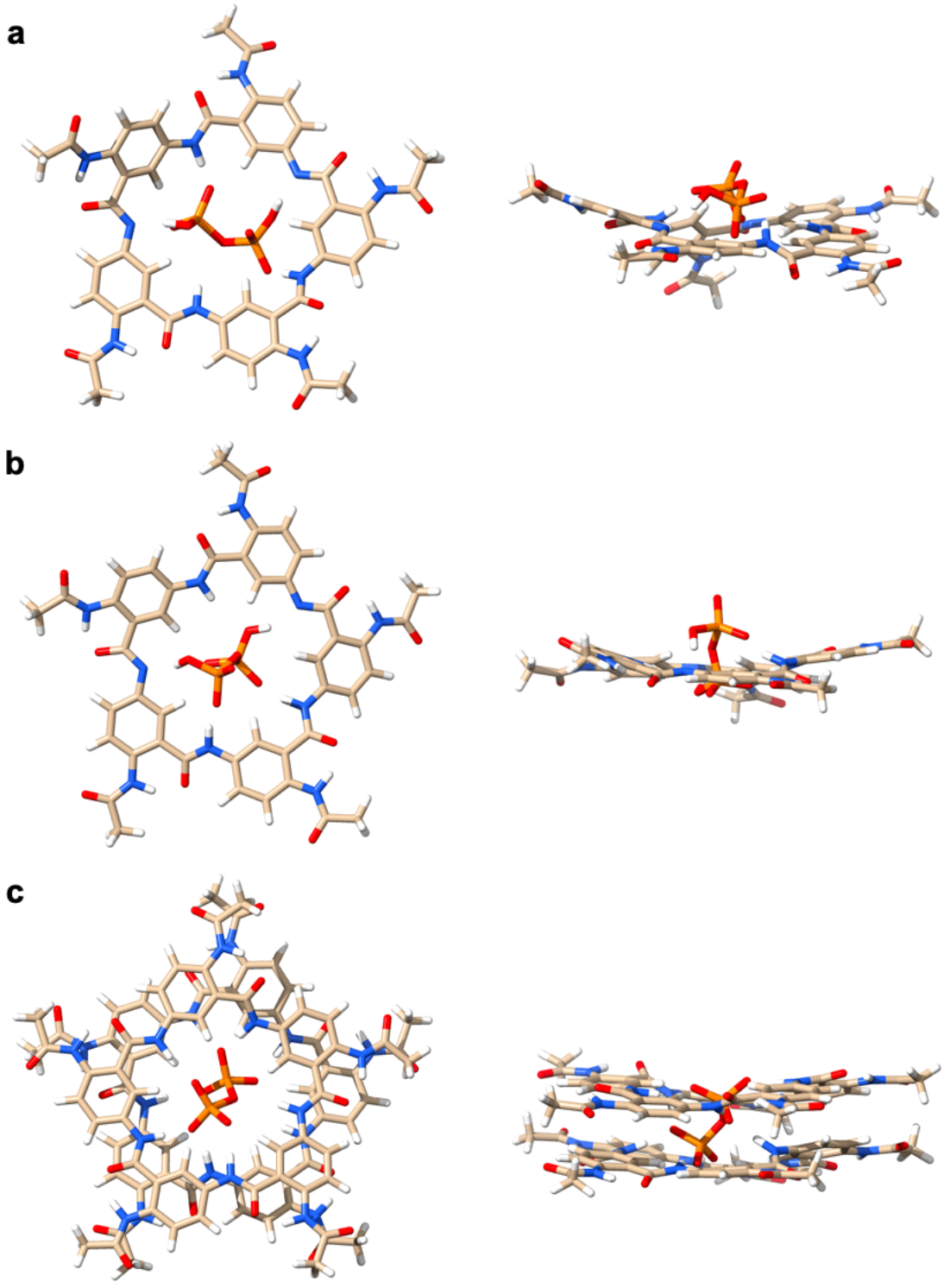

Figure S18 | Top (left) and side (right) views of the energy-minimized structures of **a**, the 1:1 complex of macrocycle **c5** and a horizontally placed pyrophosphate ion; **b**, the 1:1 complex of macrocycle **c5** and a vertically placed pyrophosphate ion; and **c**, the 2:1 complex of macrocycle **c5** and a vertically placed pyrophosphate ion.

a

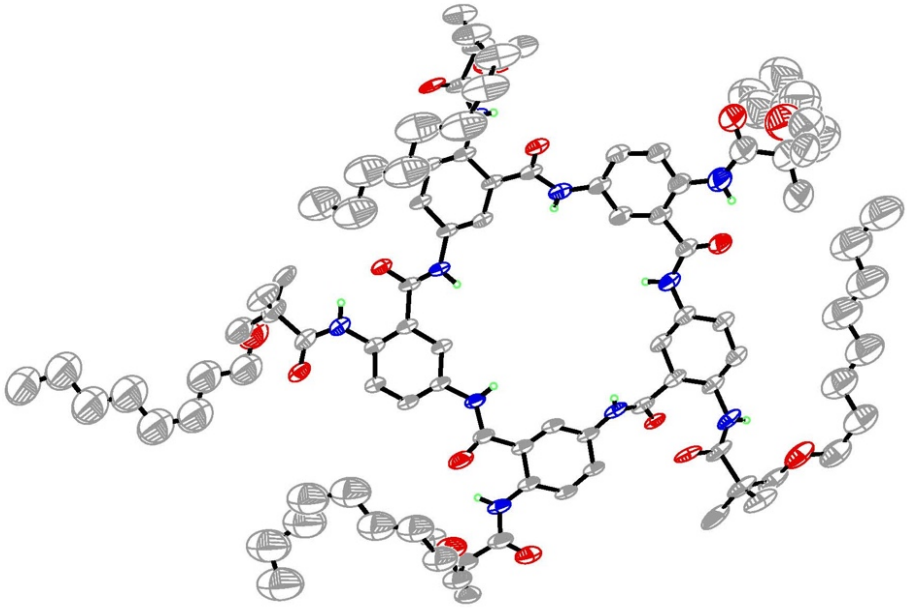

b

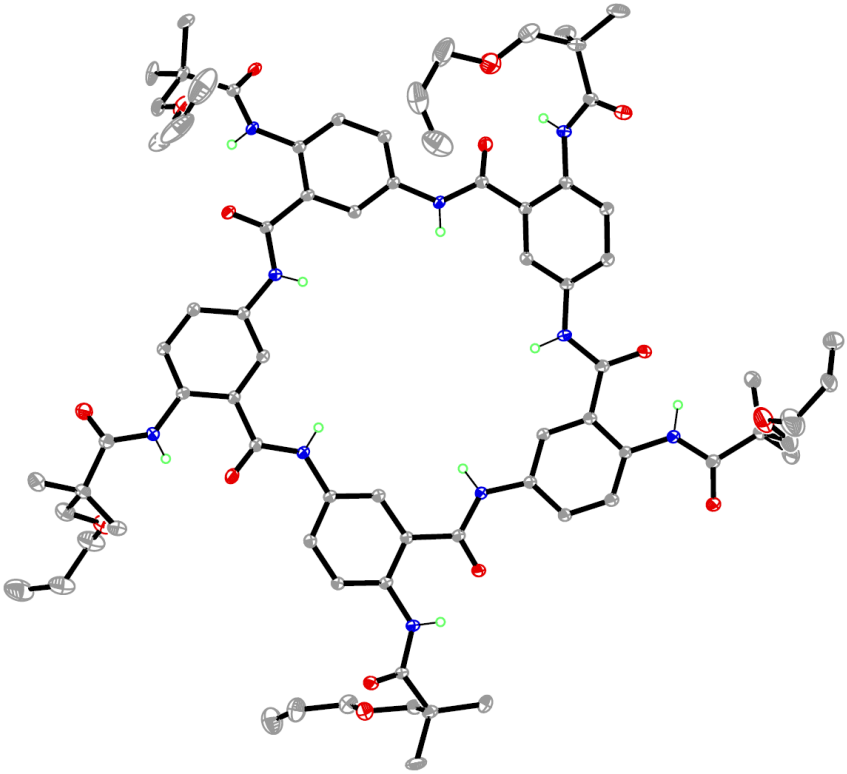

Figure S19. The ORTEP plots of the crystal structures of **a,** macrocycle **c5a**, and **b**, macrocycle **c5c** (CCDC reference number: 2124841), with a 30% probability ellipsoid. All hydrogen atoms, except for those of NH groups, are removed for clarity.

Table S1. Association constants K_a (M^{-1}) for the 1:1 complexes of macrocycles **c5a** with three oxoanions.

	Diameter (Å)	CH_3CN:$CHCl_3$ (5:95, v/v) [a]	CD_3CN:$CDCl_3$ (40:60, v/v) [b]	DMSO-d_6:$CDCl_3$ (70:30, v/v) [c]	D_2O: acetone-d_6 (20:80, v/v) [c]	D_2O: acetone-d_6 (60:40, v/v) [c]
HSO_4^- [d]	4.42	(7.0 ± 1.4) x 10^9	-	(3.52 ± 0.35) x 10^4	-	-
MPP$^-$ [d]	~4.3	(5.2 ± 1.4) x 10^{10}	(3.11 ± 0.57) x 10^8	(4.66 ± 0.55) x 10^4	(1.72 ± 0.10) x 10^4	-
DPP$^-$ [e]	~4.3	(4.3 ± 0.8) x 10^9	(2.99 ± 0.36) x 10^7	(2.43 ± 0.07) x 10^3	(3.79 ± 0.45) x 10^4	(5.40 ± 0.43) x 10^3

[a] Determined by two-step competition ITC experiments with PF_6^- as the competitor.
[b] Determined by two-step competition NMR titration experiments with Cl^- as the competitor at 25 ºC.
[c] Determined by NMR titrations at 25 ºC.
[d] As the TBA^+ salts (TBA^+ = tetrabutylammonium).
[e] As the TMA^+ salt (TMA^+ = tetramethylammonium).

2. Synthesis

Scheme S1. Stepwise synthesis of macrocycle c5a.

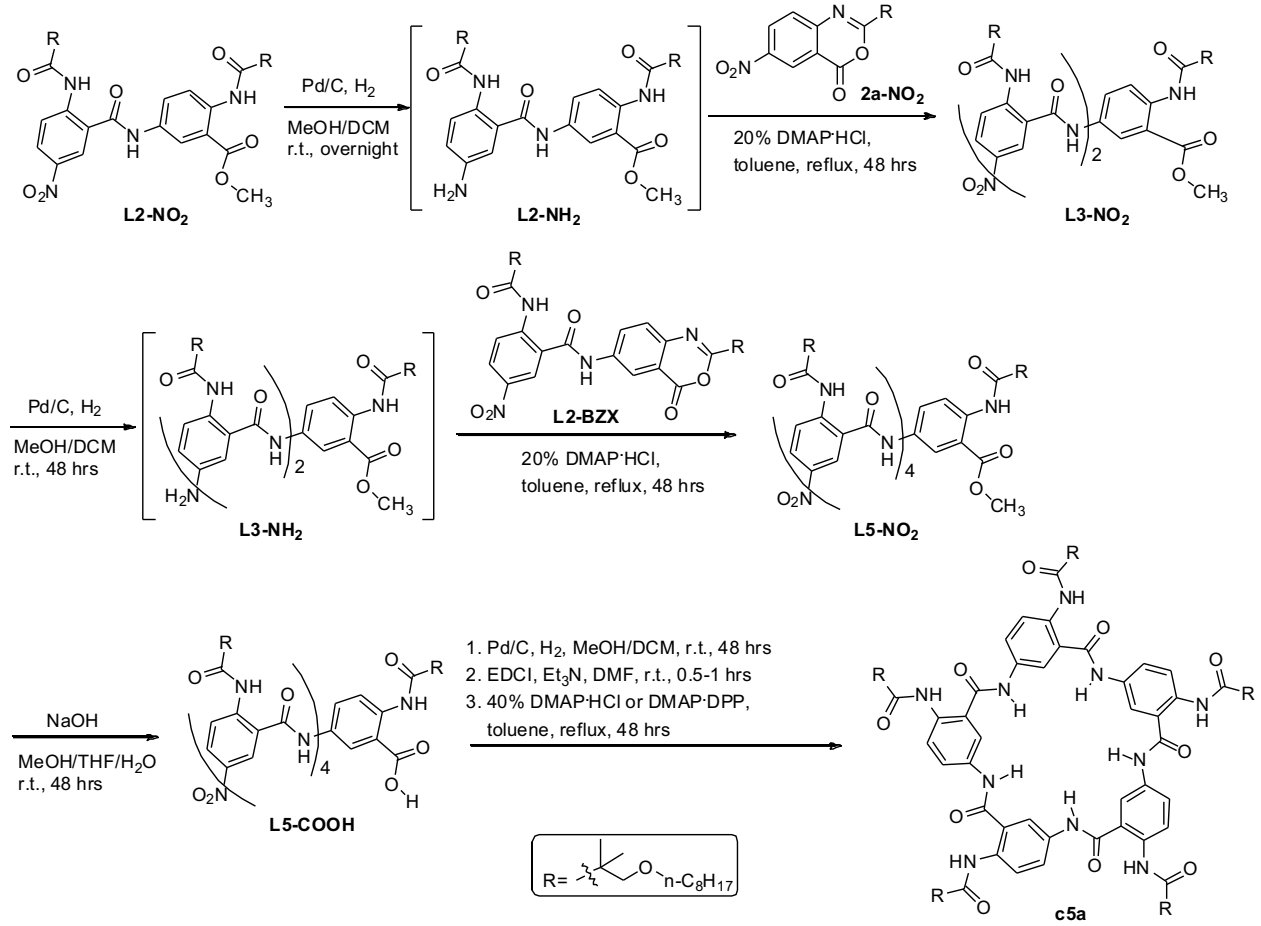

Nitro trimer methyl esterL3-NO_2:The hydrogenation of nitro dimer methyl ester **L2-NO_2** to prepare its corresponding amine **L2-NH_2** was accomplished via the general method. To a solution of the freshly prepared amine **L2-NH_2** (1.85 g, 2.56 mmol) and benzoxazinone monomer **2a-NO_2** (0.96 g, 2.56 mmol) in dry toluene (80 mL) was added 20 mol% of DMAP·HCl. The obtained suspended solution was heated under reflux for 2 days. Then, the organic layer was washed with brine (40 mL x 2 times) and dried over anhydrous Na_2SO_4. After removal of toluene under vacuum, the crude product was subjected to flash silica gel column (hexane/ethyl acetate, from 6/1 to 4/1) to afford the pure **L3-NO_2** as a yellowish solid (2.56 g, 91 %). ^{1}H NMR (400 MHz, $CDCl_3$): δ 11.48 (s, 1H), 11.21 (s, 1H), 10.85 (s, 1H), 9.17 (s, 1H), 8.83 (d, *J* = 7.6 Hz, 1H), 8.74-8.71 (m, 2H), 8.65 (s, 1H), 8.35-8.32 (m, 2H), 8.28 (dd, *J* = 7.6, 2.0 Hz, 1H), 7.86 (d, *J* = 2.0 Hz, 1H), 7.75 (dd, *J* = 7.2, 2.0 Hz, 1H), 7.57 (dd, *J* = 7.2, 2.0 Hz, 1H), 3.92 (s, 3H), 3.55-3.50 (m, 5H), 3.47-3.43 (m, 5H), 3.41-3.37 (m, 4H), 1.61 (m, 2H), 1.54 (m, 2H), 1.45 (m, 4H), 1.34 (m, 12H), 1.29 (m, 12H), 1.23 (m, 14H), 1.12 (m, 12H), 0.90-0.80 (m, 10H). ^{13}C NMR (75 MHz, 5% DMSO-d_6 / 95% $CDCl_3$): δ 176.42, 175.72, 167.91, 166.90, 165.84, 145.43, 141.35, 137.92, 135.77, 132.99, 132.67, 127.16, 126.70, 125.01, 124.18, 123.28, 122.63, 122.37, 121.10, 121.04, 120.84, 115.63, 77.39, 77.16, 77.09, 71.56, 71.54, 52.26, 44.94, 44.72, 44.35, 31.64, 31.60, 29.24, 29.19, 29.18, 29.15, 29.09, 29.10, 29.07, 25.92, 25.86, 25.83, 22.86, 22.76, 22.69, 22.47, 22.46, 13.98, 13.95. HRMS (ESI) m/z: $[M + Na]^+$ Calcd. for $C_{61}H_{92}N_6O_{12}Na$ 1123.6671; Found 1123.6687.

Nitro pentamer methyl ester L5-NO_2: The hydrogenation of nitro trimer methyl ester **L3-NO_2** to prepare its corresponding amine **L3-NH_2** was accomplished via the general method. To a solution of the freshly prepared amine **L3-NH_2** (3.3 g, 3.08 mmol) and benzoxazinone **L2-BZX** (2.34 g, 3.23 mmol) in dry toluene (70 mL) was added 20 mol% of DMAP·HCl. The obtained suspended solution was heated under reflux for 2 days. Then, the organic layer was washed with brine (50 mL x 2 times) and dried over anhydrous Na_2SO_4. After removal of toluene under vacuum, the crude product was dissolved in the hot acetonitrile. The white precipitate formed and was collected via filtration. After drying it in the oven overnight, nitro pentamer methyl ester **L5-NO_2** was obtained as a white solid (5.13 g, 93 %). ^{1}H NMR (400 MHz, DMSO-d_6): δ 11.29 (s, 1H), 11.01 (s, 1H), 10.94 (s, 1H), 10.71 (s, 1H), 10.68 (s, 1H), 10.65 (s, 1H), 10.50 (s, 1H), 10.49 (s, 1H), 10.39 (s, 1H), 8.74-8.71 (m, 2H), 8.57 (d, *J* = 7.2 Hz, 1H), 8.44-8.43 (m, 2H), 8.37 (d, *J* = 6.8 Hz, 1H), 8.34-8.29 (m, 2H), 8.25 (s, 1H), 8.18-8.16 (m, 2H), 7.94 (d, *J* = 7.2 Hz, 1H), 7.81-7.77 (m, 2H), 7.72 (d, *J* = 7.6 Hz, 1H), 3.87 (s, 3H), 3.40 (m, 2H), 3.36 (m, 11H), 3.30 (m, 12H), 1.42 (m, 2H), 1.35 (m, 8H), 1.21 (m, 10H), 1.17 (m, 13H), 1.15 (m, 27H), 1.08 (m, 42H), 0.78 (m, 15H). ^{13}C NMR (75 MHz, DMSO-d_6): δ 175.99, 174.99, 174.97, 174.89, 174.87, 174.61, 168.08, 167.38, 167.35, 167.34, 167.32, 167.27, 166.03, 145.12, 141.65, 137.50, 135.36, 134.86, 134.69, 134.35, 134.00, 133.99, 133.96, 133.92, 133.31, 129.33, 128.04, 126.41, 124.91, 124.88, 124.22, 124.10, 124.06, 124.00, 123.94, 123.88, 122.05, 122.03, 122.01, 121.95, 121.74, 121.72, 121.68, 121.08, 121.07, 121.05, 120.99, 120.97, 120.95, 120.88, 115.91, 109.99, 77.43, 77.40, 77.37, 77.32, 77.28, 77.19, 77.17, 77.13, 77.07, 77.04, 77.01, 76.95, 76.94, 76.92, 76.89, 76.84, 76.82, 71.23, 71.15, 71.14, 71.11, 71.05, 70.99, 70.92, 52.81, 52.78, 44.80, 44.65, 44.63, 44.13, 31.49, 28.98, 25.92, 25.76, 22.89, 22.84, 22.67, 22.57, 22.33, 14.11. HRMS (ESI) m/z: $[M+Na]^+$Calcd. for $C_{101}H_{152}N_{10}O_{18}Na$ 1816.1184; Found 1816.1207.

Nitro pentamer acid L5-COOH: To a solution of **L5-NO_2** (0.96 g, 0.54 mmol) in 50 mL of methanol / THF (v/v, 4/1) was added NaOH (0.10 g in 1 mL of H_2O). The hydrolysis reaction was carried out at room temperature for 4 days. The reaction solution was concentrated under vacuum, to which 1 M HCl aqueous solution was added to adjust the pH value of the solution to 3-4. Meanwhile, the white precipitate formed and was collected via the filtration. The crude product was then washed with acetonitrile. After drying it in the oven overnight, nitro pentamer acid **L5-COOH** was obtained as a white solid (0.86 g, 89 %). ^{1}H NMR (400 MHz, DMSO-d_6): δ 13.70 (broad, 1H), 11.46 (broad, 1H), 11.31 (s, 1H), 11.02 (s, 1H), 10.73 (s, 1H), 10.69 (s, 1H), 10.61 (s, 1H), 10.52 (m, 2H), 10.44 (s, 1H), 8.75-8.72 (m, 2H), 8.61 (d, *J* = 9.2 Hz, 1H), 8.46-8.43 (m, 2H), 8.40-8.31 (m, 3H), 8.27 (s, 1H), 8.19-8.17 (m, 2H), 7.91 (d, *J* = 9.2 Hz, 1H), 7.82-7.72 (m, 3H), 3.40-3.31 (m, 22H), 1.35 (m, 10H), 1.19-1.08 (m, 80H), 0.77 (m, 15H). ^{13}C NMR (75 MHz, DMSO-d_6): δ 176.02, 175.23, 175.01, 174.88, 170.07, 167.35, 167.23, 166.12, 166.04, 145.15, 141.65, 138.06, 135.39, 134.89, 134.75, 133.98, 133.91, 133.68, 133.32, 128.04, 125.97, 124.92, 124.21, 124.05, 123.94, 123.02, 122.03, 121.92, 121.73, 121.08, 120.23, 116.68, 77.51, 77.08, 76.95, 71.18, 70.94, 44.81, 44.70, 44.19, 31.51, 29.05, 28.98, 25.93, 25.77, 22.86, 22.70, 22.57, 22.35, 14.14, HRMS (ESI) m/z: $[M+Na]^+$Calcd. for $C_{100}H_{150}N_{10}O_{18}Na$ 1802.1027; Found 1802.0988.

Macrocycle c5a: Hydrogenation reaction of nitro pentamer acid **L5-COOH** to its corresponding amine was carried out via the general procedure. To a solution of the freshly prepared aromatic amine (0.55 g, 0.31 mmol) in 3 mL of dry DMF was added EDCI (89 mg, 0.46 mmol) and triethylamine (68 mg, 0.62 mmol). The obtained reaction solution was stirred at room temperature for 0.5-1 hrs. Then, all solvent was removed under vacuum. The mixture was used for the cyclization reaction without any further purification. To accomplish the intramolecular cyclization, the mixture was suspended in dry toluene (160 mL), followed by addition of 40 mol% DMAP·HCl or a mixture containing DMAP (15 mg, 0.12 mmol) and DPP (30 mg, 0.12 mmol) (40 mol% DMAP·DPP). The obtained suspended solution was heated under reflux for 48 hrs. Then

the organic layer was washed with brine (50 mL x 2 times) and dried over anhydrous Na_2SO_4. After removal of toluene under vacuum, the crude product was subjected to flash silica gel column (DCM/MeOH, from 50/1 to 30/1) to afford the crude product. The further purification was accomplished by the precipitation of the crude product in hot acetonitrile. Then the white solid was collected via filtration and dried in the oven overnight. The pure **c5a** was obtained as a white solid (0.17 g (32%) when DMAP·HCl was used as the catalyst; 0.19 g (35%) when DMAP·DPP was used as the catalyst), corresponding to overall yields of 22% and 24%, respectively, for **c5a** from the stepwise synthesis starting from the benxazinone monomer. ^{1}H NMR (400 MHz, DMSO-d_6): δ 10.58 (s, 5H), 10.43 (s, 5H), 8.40 (d, J = 9.2 Hz, 5H), 8.33 (d, J = 8.8 Hz, 5H), 7.61 (s, 5H), 3.41 (s, 10H), 3.37 (t, J = 6.4 Hz, 10H), 1.42 (m, 10H), 1.19-1.13 (m, 50H), 1.09 (m, 30H), 0.77 (t, J = 6.8 Hz, 15H). ^{13}C NMR (75 MHz, DMSO-d_6): δ 174.78, 166.94, 134.87, 133.81, 124.71, 123.91, 122.17, 121.28, 77.23, 71.28, 44.31, 31.67, 29.34, 29.23, 29.17, 26.01, 23.01, 22.52, 14.37. HRMS (ESI) m/z: [M+Na]$^+$Calcd. for $C_{100}H_{150}N_{10}O_{15}Na$ 1754.1180; Found 1754.1160.

Scheme S2. Synthesis of macrocycle c5a-c one-pot macrocyclization of monomers (benzoxazinone amines)

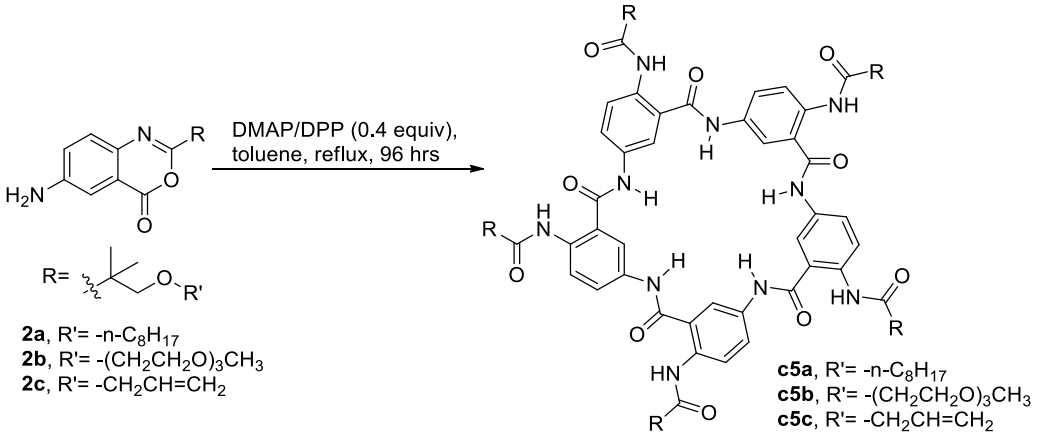

General synthetic procedure for macrocycle c5a-c: To a solution of benzoxazinone amine **2a-c** (0.09 mmol) in dry toluene (45 mL) were added DMAP (4.4 mg, 0.036 mmol) and DPP (9.0 mg, 0.036 mmol). The resulting reaction solution was heated under reflux for 96 hrs. Then, the reaction solution was washed with brine (45 mL x 2 times) and dried over anhydrous Na_2SO_4. Under high vacuum, the reaction solution was concentrated for further purification.

Macrocycle c5a: The crude product was subject to silica gel column (DCM / MeOH, from 50 / 1 to 30 / 1) to offer the pure **c5a** as a white solid (14.0 mg, 45%). The characterization data of **c5a** via the one-pot macrocyclization is consistent to the one obtained via the step-wise synthetic method.

Macrocycle c5b: The crude product was sub
ject to silica gel column (DCM / MeOH, from 40 / 1 to 20 / 1) to offer the pure **c5b** as a white solid (13.0 mg, 38%). ^{1}H NMR (400 MHz, DMSO-d_6): δ 10.65 (s, 5H), 10.45 (s, 5H), 8.37-8.32 (m, 10H), 7.69 (s, 5H), 3.57-3.33 (m, 75H), 3.19 (s, 10H), 1.22 (s, 30H). ^{13}C NMR (75 MHz, DMSO-d_6): δ 174.92, 167.09, 134.96, 133.85, 124.72, 124.27, 122.35, 121.61, 77.56, 71.60, 70.79, 70.18, 70.08, 69.91, 69.81, 58.36, 44.23, 22.82. HRMS (ESI) m/z: [M+Na]$^+$ Calcd. for $C_{95}H_{140}N_{10}O_{30}Na$ 1923.9635; Found 1923.9617.

Macrocycle c5c: The crude product was subject to silica gel column (CH_2Cl_2 / MeOH, from 50 / 1 to 30 / 1) to offer the pure **c5c** as a white solid (9.6 mg, 39%).^{1}H NMR (400 MHz, DMSO-d_6): δ 10.68 (s, 5H), 10.44 (s, 5H), 8.38 (d, *J* = 8.8 Hz, 5H), 8.34 (d, *J* = 8.8 Hz, 5H), 7.63 (s, 5H), 5.86-5.81 (m, 5H), 5.23 (d, *J* = 17.2 Hz, 5H), 5.05 (d, *J* = 10.4 Hz, 5H), 3.98 (d, *J* = 5.6 Hz, 10H), 3.46 (s, 10H), 1.24 (s, 30H). ^{13}C NMR (75 MHz, DMSO-d_6): δ 174.75, 167.00, 147.97, 135.38, 133.75, 124.39, 121.62, 116.84, 84.83, 76.79, 71.88, 44.34, 23.00. HRMS (ESI) m/z: $[M+Na]^+$ Calcd. for $C_{75}H_{90}N_{10}NaO_{15}$ 1393.6485; Found. 1393.6451.

Scheme S3. Synthesis of benzoxazinone amine 2a

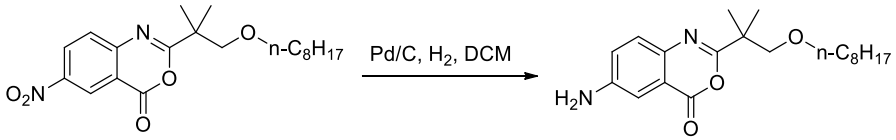

Compound 2a: In the presence of H_2 gas, the solution of **2a-NO$_2$** (0.75 g, 2.0 mmol) and catalytic amount of Pd/C in DCM was stirred at room temperature overnight. All solid was filtered out and resulting filtrate was concentrated under vacuum. The pure benzoxazinone amine **2a** was obtained as a white solid (0.64 g, 93%). ^{1}H NMR (400 MHz, $CDCl_3$): δ 7.42 (d, *J* = 8.4 Hz, 1H), 7.35 (d, *J* = 2.8 Hz, 1H), 7.08 (d, *J* = 8.4 and 2.8 Hz, 1H), 4.02 (broad, 2H), 3.58 (s, 2H), 3.41 (t, *J* = 6.4 Hz, 1H), 1.48 (m, 2H), 1.35 (s, 2H), 1.25-1.17 (m, 10H), 0.85 (t, *J* = 6.8 Hz, 3H). ^{13}C NMR (75 MHz, $CDCl_3$): δ 162.59, 160.59, 146.51, 138.49, 128.05, 123.77, 117.65, 110.56, 77.27, 71.62, 42.36, 31.75, 29.35, 29.32, 29.22, 26.03, 23.07, 22.61, 14.07. MS (ESI) m/z: $[M + H]^+$ Calcd. for $C_{20}H_{31}N_2O_3$, 347.23; Found 347.19.

Scheme S4. Synthesis of benzoxazinone amine 2b

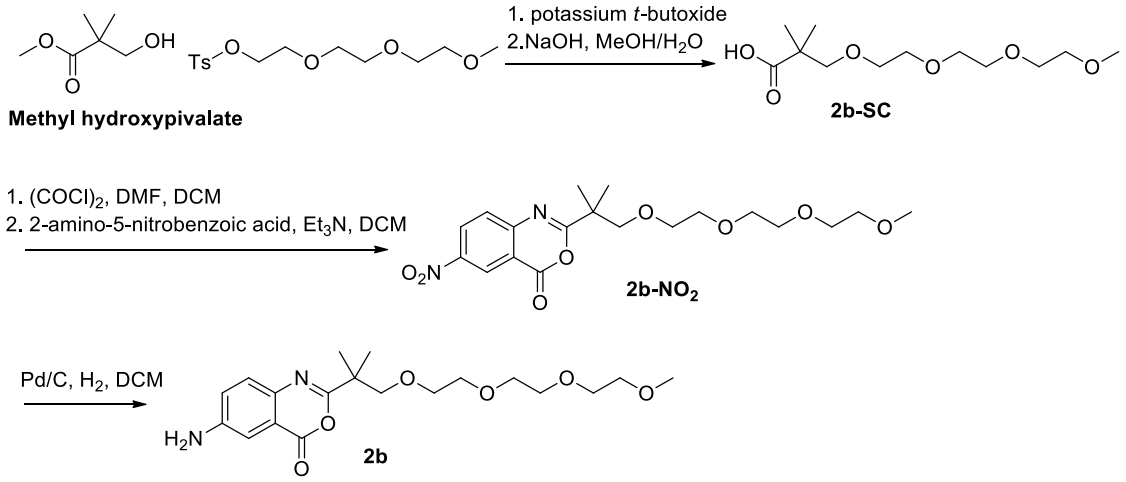

Compound 2b-SC: At 0 °C, to the solution of methyl hydroxypivalate (10.37 g, 1.0 eq) and 2-(2-(2-methoxyethoxy)ethoxy) ethyl 4-methyl benzenesulfonate (25.0 g, 1.0 eq) in dry DMF (75 mL) was added potassium *t*-butoxide (9.69 g, 1.1 eq) portionwise. The reaction mixture was heated to 80 °C for 2 days. The reaction was cooled to room temperature and the solid was filtered off. The reaction solution was concentrated under vacuum and then diluted with ethyl acetate. The resulting solution was washed with 1 M HCl (50 mL x 2 times), water (50 mL x 2 times) and brine (50 mL x 2 times).The organic layer was dried over anhydrous Na_2SO_4 and then removed under vacuum. The crude methyl ester was dissolved in MeOH

(100 mL), followed by an addition of NaOH aqueous solution (5.76 g in 75 mL of H_2O). The obtained reaction solution was stirred at room temperature for 2 days. MeOH was removed under vacuum. The aqueous residue was acidified with diluted HCl aqueous solution. Then, the aqueous solution was extracted with ethyl acetate (50 mL x 3 times). The organic layer was combined and washed with water (50 x 2 times) and brine (50 x 2 times) combined and concentrated to give pure **2b-SC** as an oil (6.9 g, 33% for two steps). ^{1}H NMR (400 MHz, $CDCl_3$): δ 3.68-3.64 (m, 10H), 3.61-3.59 (m, 2H), 3.50 (s, 2H), 3.40 (s, 3H), 1.22 (s, 6H). ^{13}C NMR (75 MHz, $CDCl_3$): δ 181.14, 77.58, 71.77, 70.93, 70.52, 70.49, 70.21, 70.04, 58.74, 43.19, 22.06. HRMS (ESI) m/z: $[M-H]^-$ Calcd. for $C_{12}H_{23}O_6$ 263.1500; Found 263.1498.

Compound 2b-NO_2: To a solution of **2b-SC** (10.56 g, 40 mmol) in dry DCM (50 mL) was added oxalyl chloride (5.59 g, 44 mmol). After addition of one drop of dry DMF as an initiator, the reaction was stirred at room temperature for 5 hours. The corresponding acid chloride was obtained after removal of DCM under vacuum, which was used for the next step without any further purification. To a solution of 2-amino-5-nitrobenzoic acid (2.91 g, 16 mmol) and triethylamine (5.45 g, 50 mmol) in DCM (50 mL) was added freshly prepared acid chloride. The obtained reaction solution was stirred overnight. Then the reaction solution was concentrated under vacuum and the crude product was subject to silica gel column (ethyl acetate / hexanes, from 3 / 1 to 1 / 1). The pure **2b-NO_2** was prepared as a yellow oil (3.88 g, 59%). ^{1}H NMR (400 MHz, $CDCl_3$): δ 9.03 (d, *J* = 2.8 Hz, 1H), 8.58 (dd, *J* = 9.6 and 2.8 Hz, 1H), 7.74 (d, *J* = 9.6 Hz, 1H), 3.69 (s, 2H), 3.60-3.56 (m, 10H), 3.51 (m, 2H), 3.36 (s, 3H), 1.40 (s, 6H). ^{13}C NMR (75 MHz, $CDCl_3$): δ 169.67, 158.02, 150.66, 146.42, 130.34, 128.59, 124.30, 117.24, 77.65, 71.82, 70.99, 70.50, 70.47, 70.39, 70.26, 58.89, 43.28, 22.88. MS (ESI) m/z: $[M + H]^+$ Calcd. for $C_{19}H_{27}N_2O_8$, 411.17; Found 411.06.

Compound 2b: Benzoxazinone amine **2b** was prepared via the same method as the preparation of **2a** without any modification. The **2b** (0.68 g, 89%) was obtained as a yellow oil from **2b-NO_2** (0.82 g, 2.0 mmol). ^{1}H NMR (400 MHz, $CDCl_3$): δ 7.37 (d, *J* = 8.4 Hz, 1H), 7.32 (d, *J* = 2.8 Hz, 1H), 7.06 (d, *J* = 8.4 and 2.8 Hz, 1H), 4.05 (s, 2H), 3.64 (s, 2H), 3.58-3.51 (m, 12H), 3.35 (s, 3H), 1.35 (s, 6H). ^{13}C NMR (75 MHz, $CDCl_3$): δ 162.44, 160.48, 146.53, 138.45, 128.05, 123.77, 117.68, 110.56, 77.79, 71.87, 71.08, 70.56, 70.42, 70.30, 58.97, 42.35, 23.02. MS (ESI) m/z: $[M + H]^+$ Calcd. for $C_{19}H_{29}N_2O_6$, 381.20; Found 381.17.

Scheme S5. Synthesis of benzoxazinone amine 2c

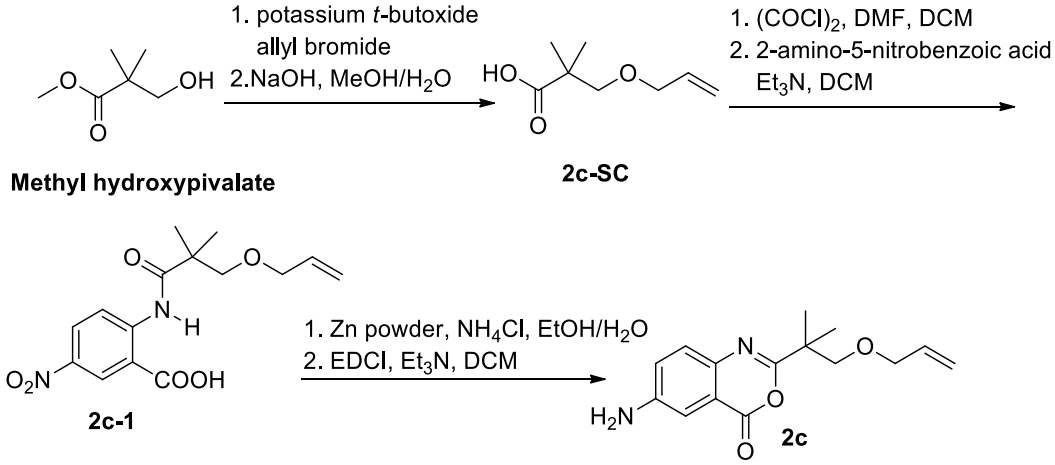

Compound 2c-SC: At 0 °C, to the solution of methyl hydroxypivalate (13.2 g, 100 mmol) and allyl bromide (13.3 g, 110 mmol) was added potassium *t*-butoxide (12.4 g, 110 mmol) portionwise. The reaction mixture was stirred overnight at room temperature. The reaction mixture was diluted with ethyl acetate. The resulting solution was washed with 1 M HCl (50 mL x 2 times), water (50 mL x 2 times) and brine (50 mL x 2 times).The organic layer was dried over anhydrous Na_2SO_4 and then removed under vacuum. The obtained crude methyl ester was dissolved in MeOH (100 mL), followed by an addition of NaOH aqueous solution (4 g in 10 mL of H_2O). The obtained reaction solution was stirred overnight at room temperature. MeOH was removed under vacuum. The aqueous residue was acidified with diluted HCl aqueous solution. Then, the aqueous solution was extracted with ethyl acetate (50 mL x 3 times). The organic layer was combined and washed with water (50 x 2 times) and brine (50 x 2 times) combined and concentrated to give pure **2c-SC** as an oil (6.1 g, 39% for two steps). ^{1}H NMR (400 MHz, $CDCl_3$): δ 5.94-5.84 (m, 1H), 5.30-5.17 (m, 2H), 4.02 (d, *J* = 5.6 Hz, 2H), 3.45 (s, 2H), 1.23 (s, 6H). ^{13}C NMR (75 MHz, $CDCl_3$): δ 183.89, 135.20, 117.42, 77.00, 72.85, 43.89, 22.63. HRMS (ESI) m/z: $[M-H]^-$ Calcd. for $C_8H_{13}O_3$ 157.0870; Found. 157.0868.

Compound 2c-1: To a solution of **2c-SC** (6.1 g, 39 mmol) in dry DCM (50 mL) was added oxalyl chloride (5.2 g, 41 mmol). After addition of one drop of dry DMF as an initiator, the reaction was stirred at room temperature for 5 hours. The corresponding acid chloride was obtained after removal of DCM under vacuum, which was used for the next step without any further purification. To a solution of 2-amino-5-nitrobenzoic acid (6.5 g, 36 mmol) and triethylamine (6.4 g, 59 mmol) in DCM (50 mL) was added freshly prepared acid chloride. The obtained reaction solution was stirred overnight. Then the reaction solution was concentrated under vacuum and the resulting residue was then dissolved in 100 mL of ethyl acetate. The organic layer was washed with dilute HCl aqueous solution (20 mL x 2 times) followed by brine (20 mL x 2 times). The organic layer was then dried over anhydrous Na_2SO_4 and removed under vacuum. The crude product was dissolved in hot ethyl acetate / hexane. Then white precipitate formed and was collected via simple filtration to give pure compound **2c-1** (5.5 g, 56%). ^{1}H NMR (400 MHz, $CDCl_3$): δ 11.50 (s, 1H), 9.03 (d, *J* = 9.6 Hz, 1H), 8.96 (d, *J* = 2.8 Hz, 1H), 8.40 (dd, *J* = 9.6 and 2.8 Hz, 1H), 5.90-5.83 (m, 1H), 5.27-5.15 (m, 2H), 4.04 (d, *J* = 5.6 Hz, 2H), 3.53 (s, 2H), 1.36 (s, 6H). ^{13}C NMR (75 MHz, $CDCl_3$): δ 177.45, 170.88, 147.64, 142.32, 134.71, 130.64, 128.18, 121.68, 118.19, 77.27, 73.06, 45.75, 23.18. HRMS (ESI) m/z: $[M-H]^-$ Calcd. for $C_{15}H_{17}N_2O_6$ 321.1092; Found. 321.1087.

Compound 2c: To a solution of **2c-1** (2.0 g, 7.2 mmol) and zinc powder (1.9 g, 28.8 mmol) in ethanol (40 mL) was added NH_4Cl (2.4 g in 8 mL of H_2O). The reaction solution was heated under reflux for 5 hrs. Then, the hot solution was filtered to remove any insoluble solid. The obtained solution was concentrated and water had to be removed under vacuum to give the dry amine product, which was used in the next step without further purification. To a suspended solution of crude amine in DCM (20 mL) was added EDCI (1.4 g, 7.2 mmol) and triethylamine (1.6 g, 14.4 mmol). The reaction was stirred overnight at room temperature. After removal of DCM, the reaction residue was subject to silica gel column (hexane / ethyl acetate, from 5 / 1 to 3 / 1). The benzoxazinone amine **2c** was obtained as a yellowish solid (0.77 g, 39% for two steps). ^{1}H NMR (400 MHz, $CDCl_3$): δ 7.42 (d, *J* = 8.4 Hz, 1H), 7.37 (d, *J* = 2.8 Hz, 1H), 7.09 (dd, *J* = 8.4 and 2.8 Hz, 1H), 5.89-5.80 (m, 1H), 5.31-5.12 (m, 2H), 4.00-3.98 (m, 4H), 3.61 (s, 2H), 1.37 (s, 6H). ^{13}C NMR (75 MHz, $CDCl_3$): δ 162.51, 160.54, 146.40, 138.60, 134.77, 128.15, 123.81, 117.74, 116.77, 110.68, 76.64, 72.32, 42.30, 23.11. MS (ESI) m/z: $[M + H]^+$ Calcd. for $C_{15}H_{19}N_2O_3$, 275.32; Found 275.68.

3. Characterization Data (^{1}H, ^{13}C, and mass spectra)

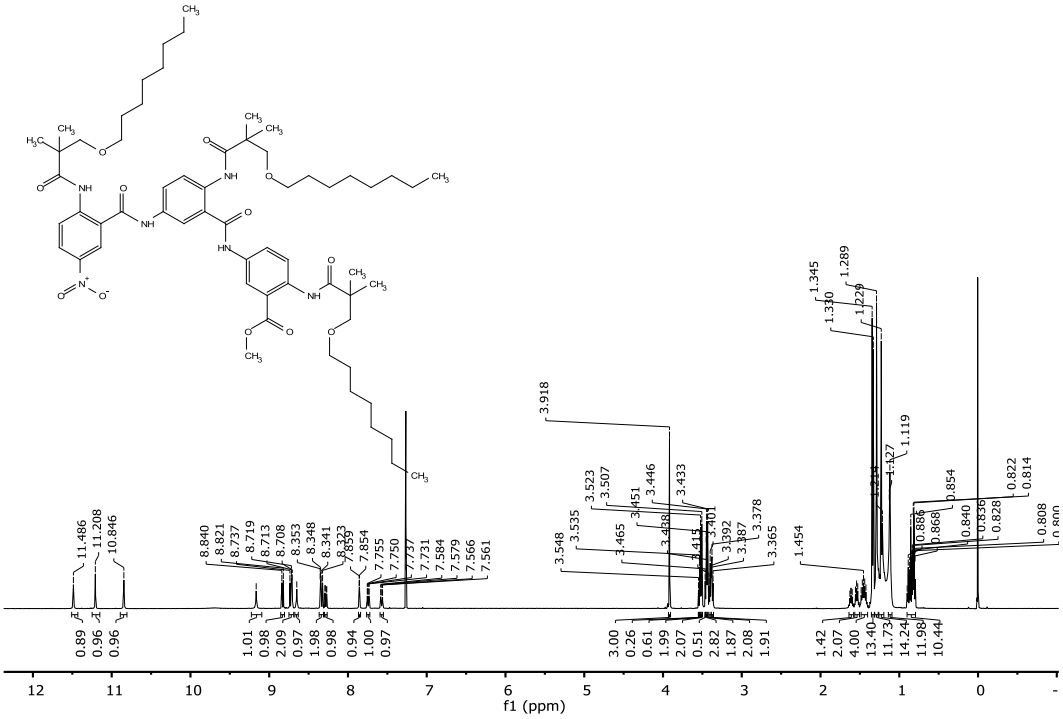

Figure S20 | **^{1}H NMR spectrum** of compound **L3-NO$_2$** ($CDCl_3$, 400 MHz, 25 °C)

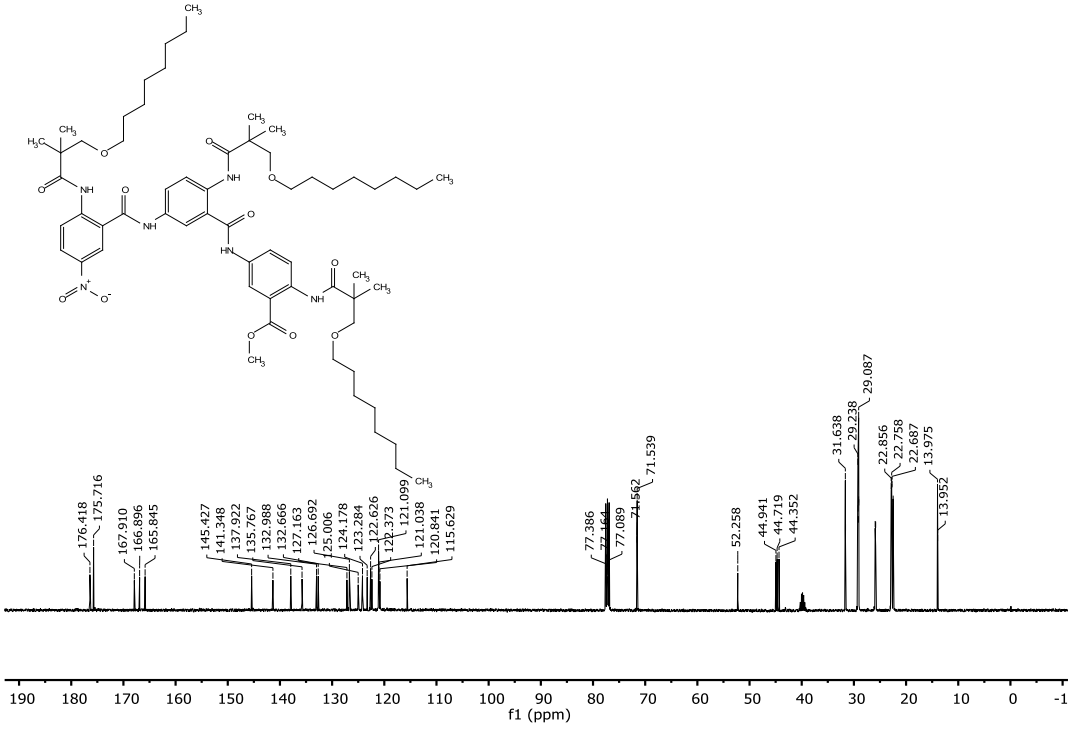

Figure S21 | **^{13}C NMR spectrum** of compound **L3-NO$_2$** ($CDCl_3$, 75 MHz, 25 °C).

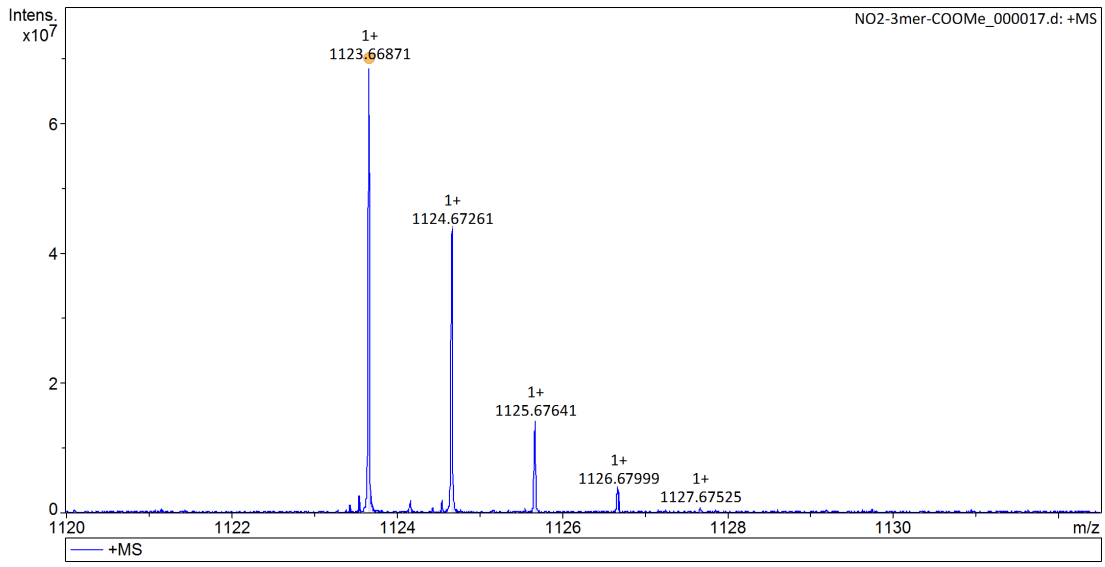

Figure S22 | HRMS-ESI spectrum of compound **L3-NO$_2$** (positive mode).

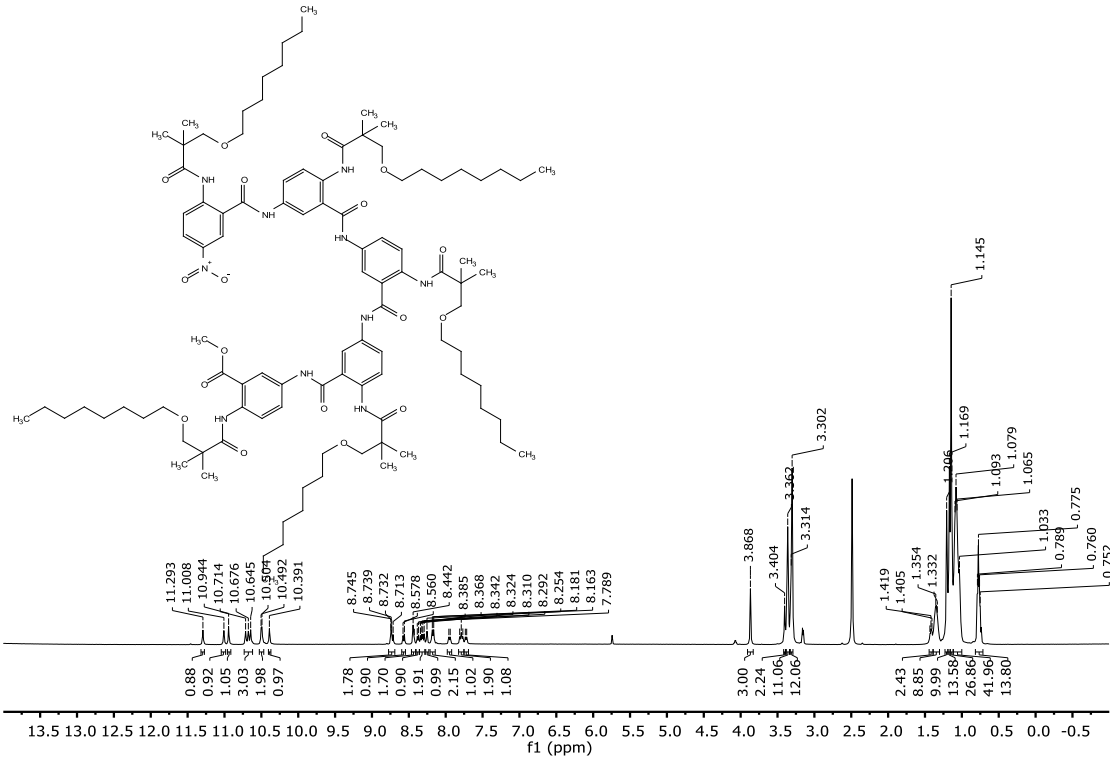

Figure S23 | ^{1}H NMR spectrum of compound **L5-NO$_2$** (DMSO-d_6, 400 MHz, 25 °C).

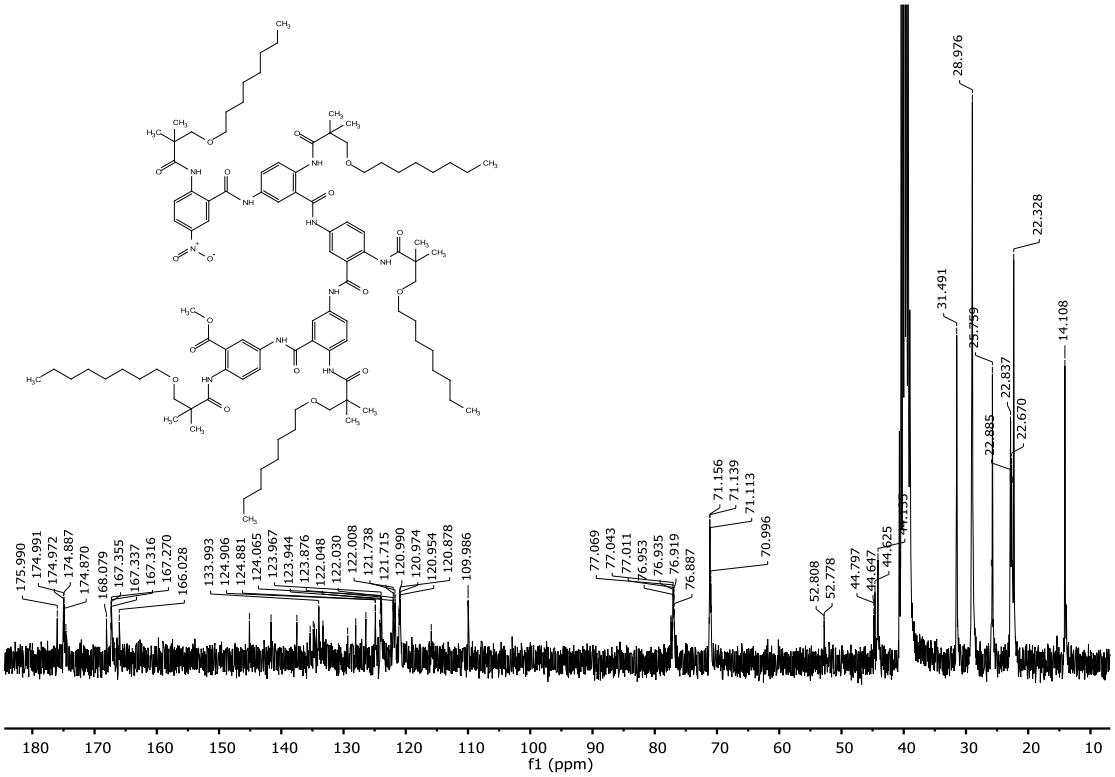

Figure S24 | **^{13}C NMR spectrum** of compound **L5-NO$_2$** (DMSO-d_6, 75 MHz, 25 °C)

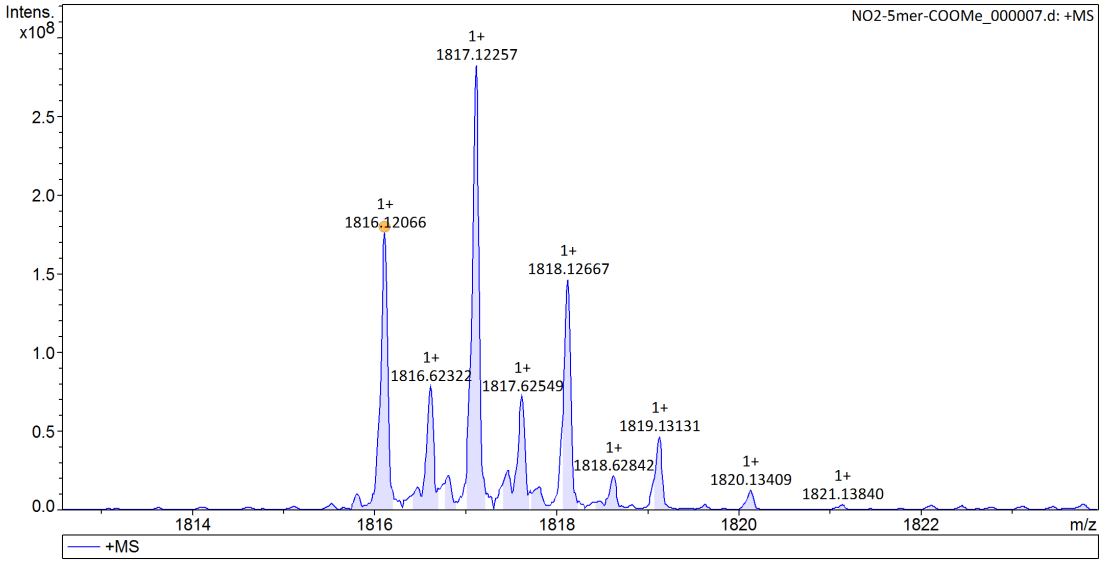

Figure S25 | **HRMS-ESI spectrum** of compound **L5-NO$_2$** (positive mode)

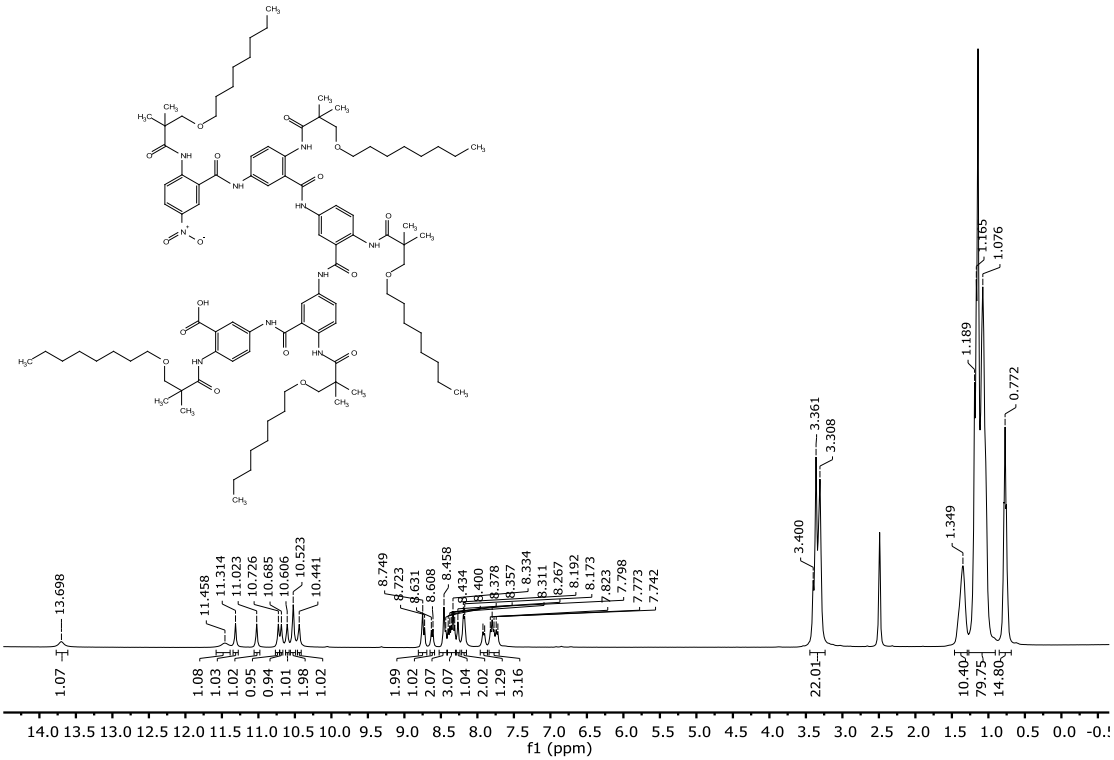

Figure S26 | **^{1}H NMR spectrum** of compound **L5-COOH** (DMSO-d_6, 400 MHz, 25 °C)

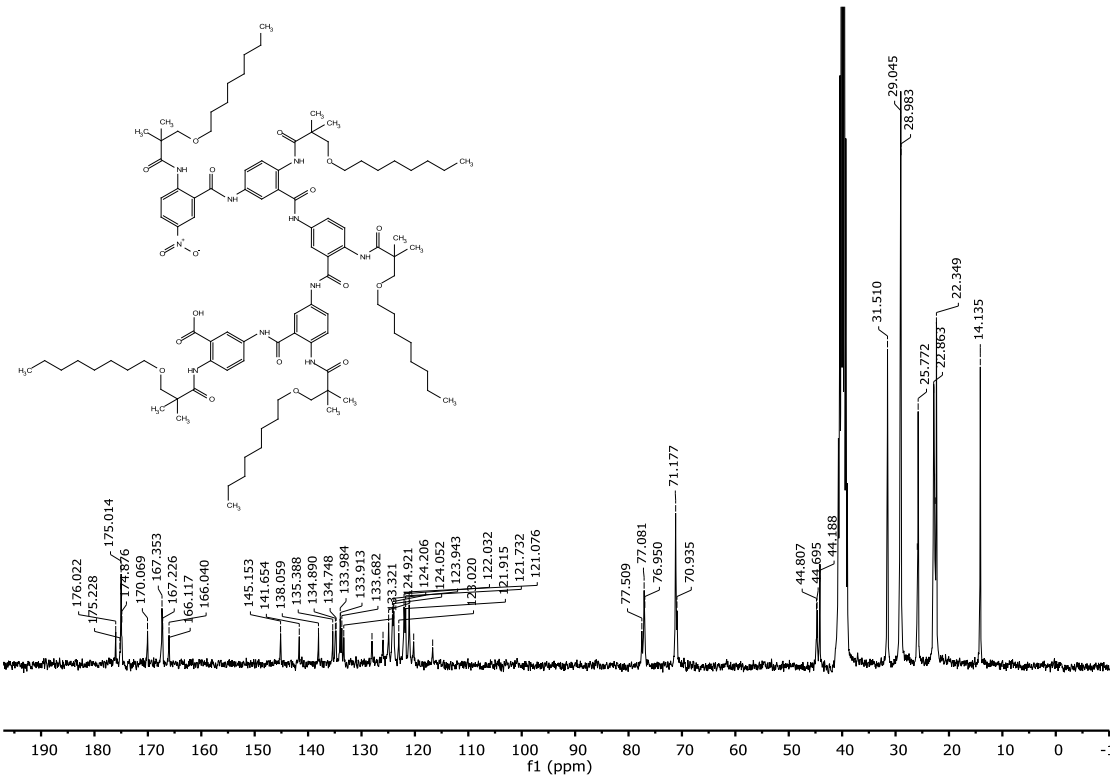

Figure S27 | **^{13}C NMR spectrum** of compound **L5-COOH** (DMSO-d_6, 75 MHz, 25 °C)

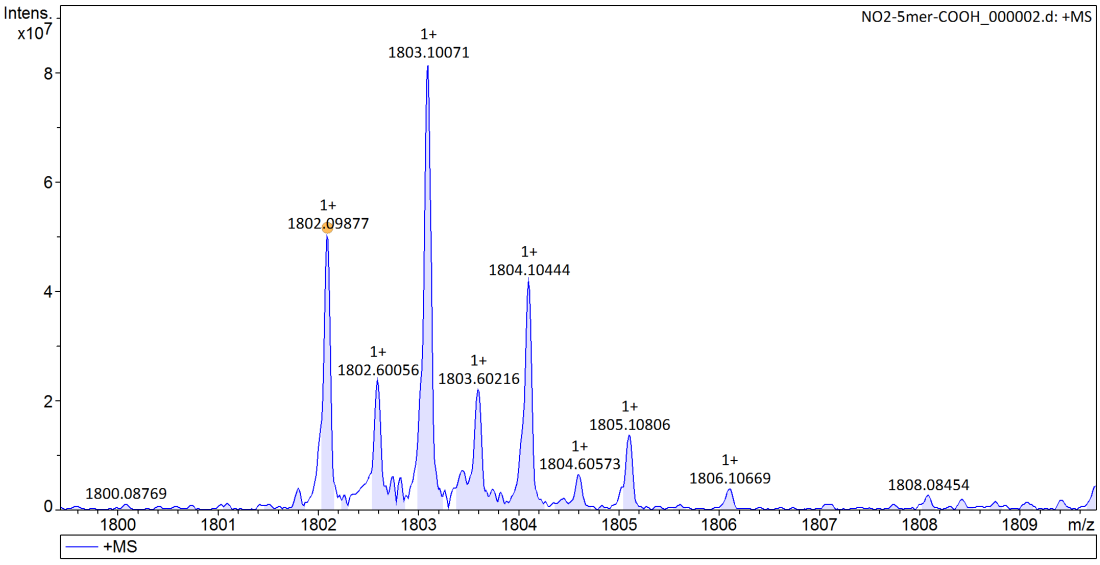

Figure S28 | **HRMS-ESI spectrum** of compound **L5-COOH** (positive mode).

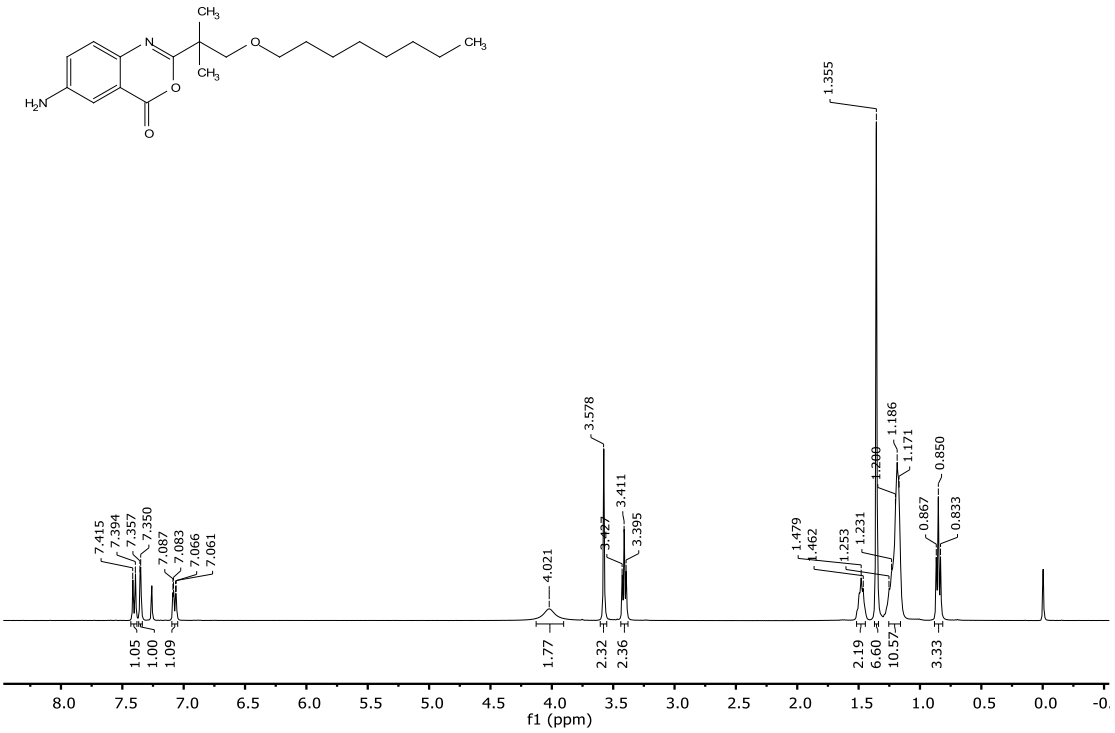

Figure S29 | **^{1}H NMR spectrum** of compound **2a** ($CDCl_3$, 400 MHz, 25 °C)

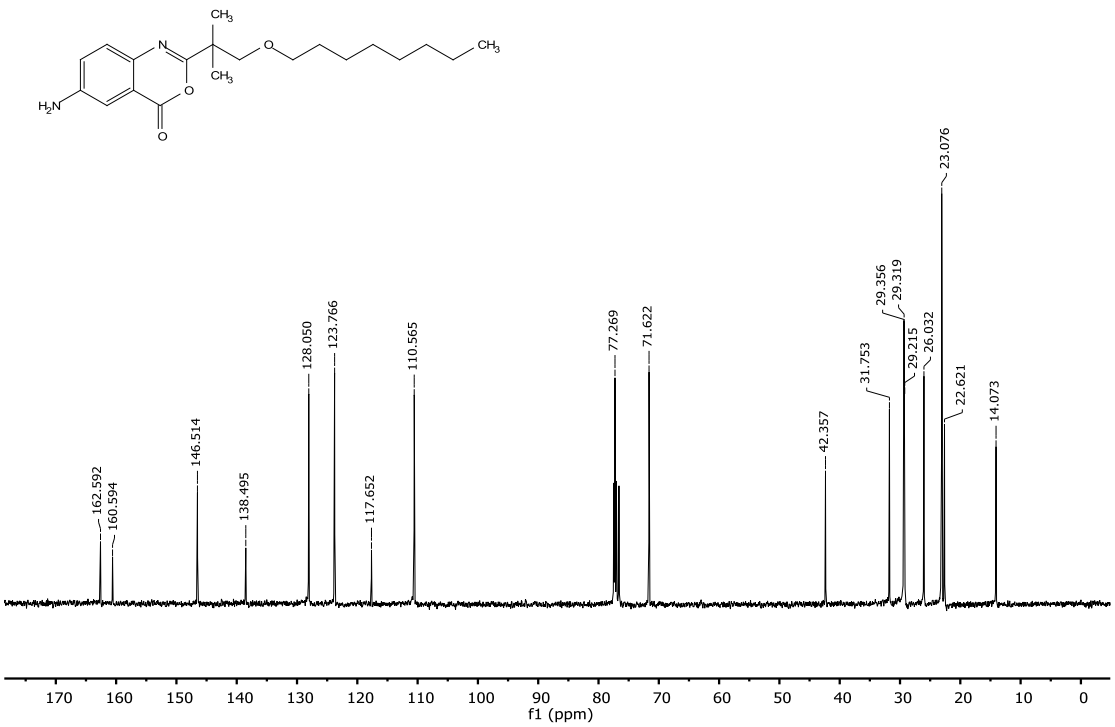

Figure S30 | **^{13}C NMR spectrum** of compound **2a** ($CDCl_3$, 75 MHz, 25 ºC).

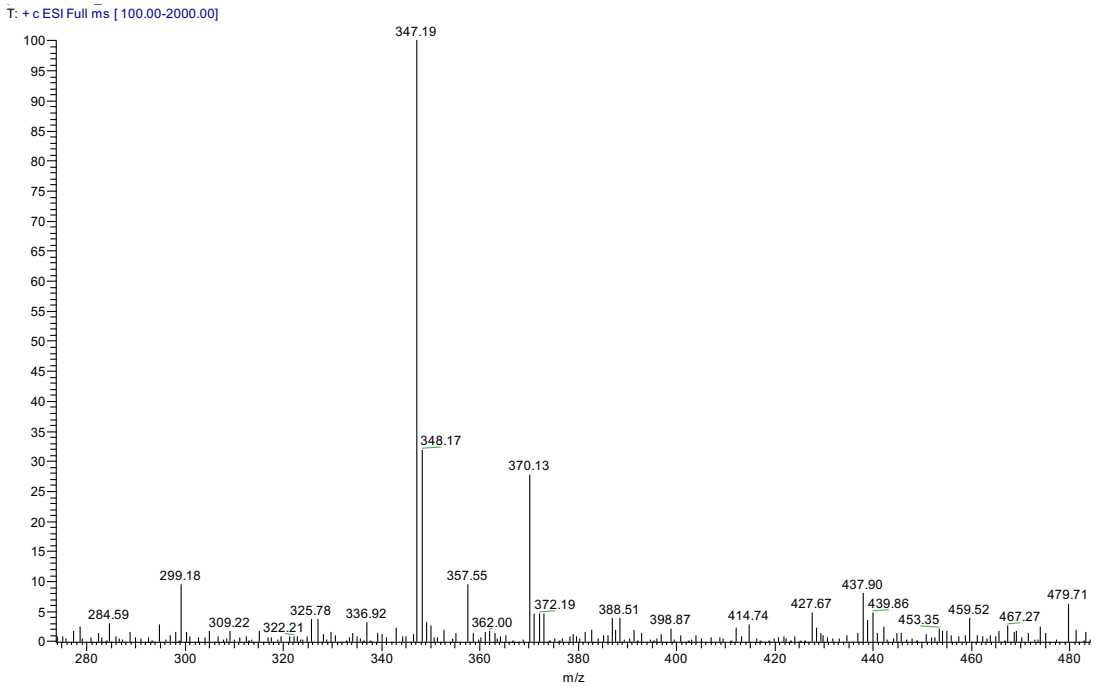

Figure S31 | **MS-ESI spectrum** of compound **2a** (positive mode)

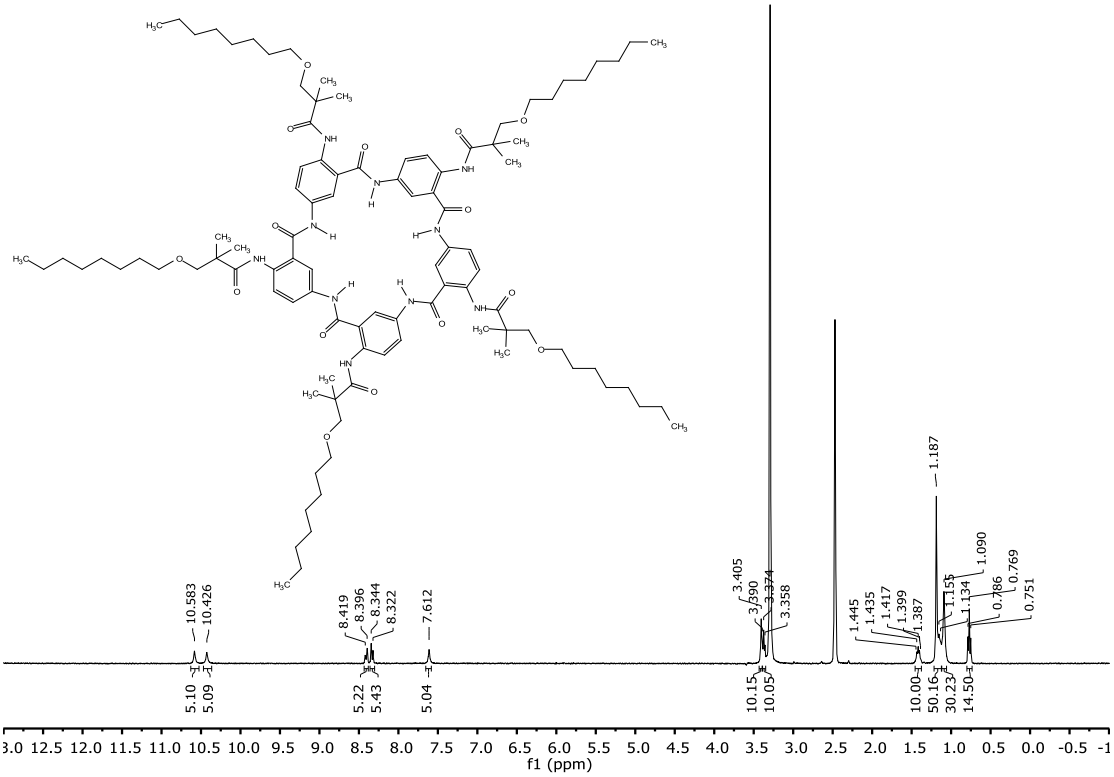

Figure S32 | **^{1}H NMR spectrum** of compound **c5a** (DMSO-d_6, 400 MHz, 25 °C)

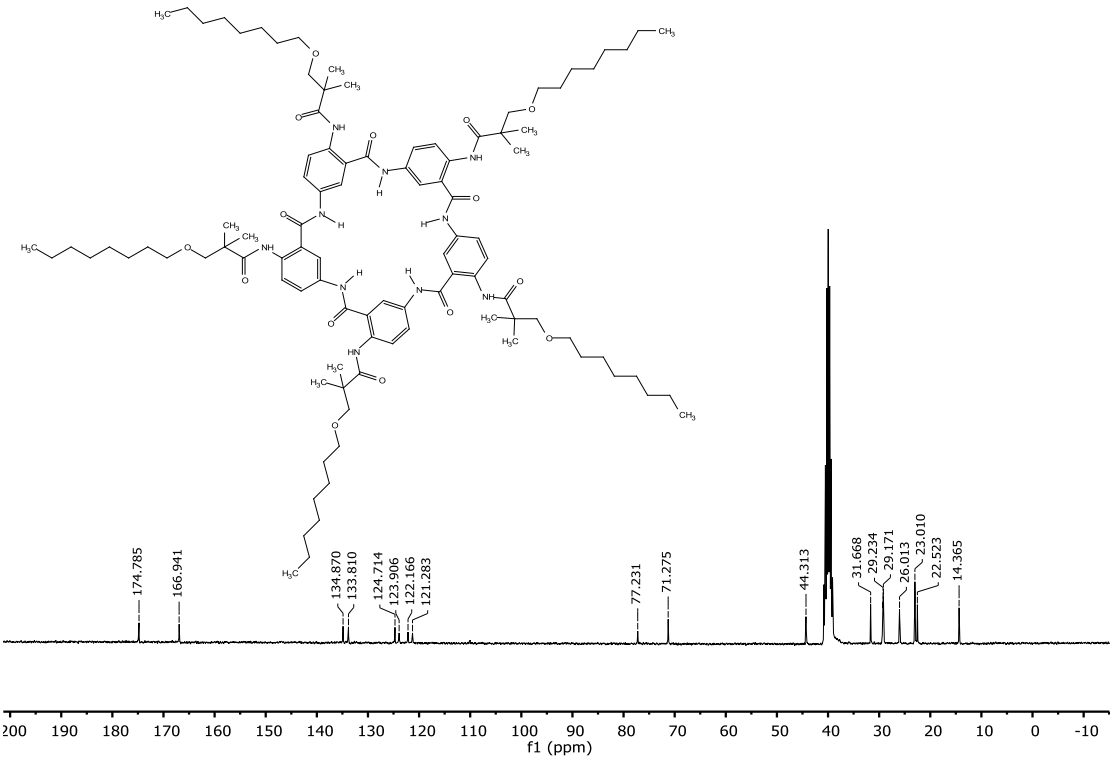

Figure S33 | **^{13}C NMR spectrum** of compound **c5a** (DMSO-d_6, 75 MHz, 25 °C).

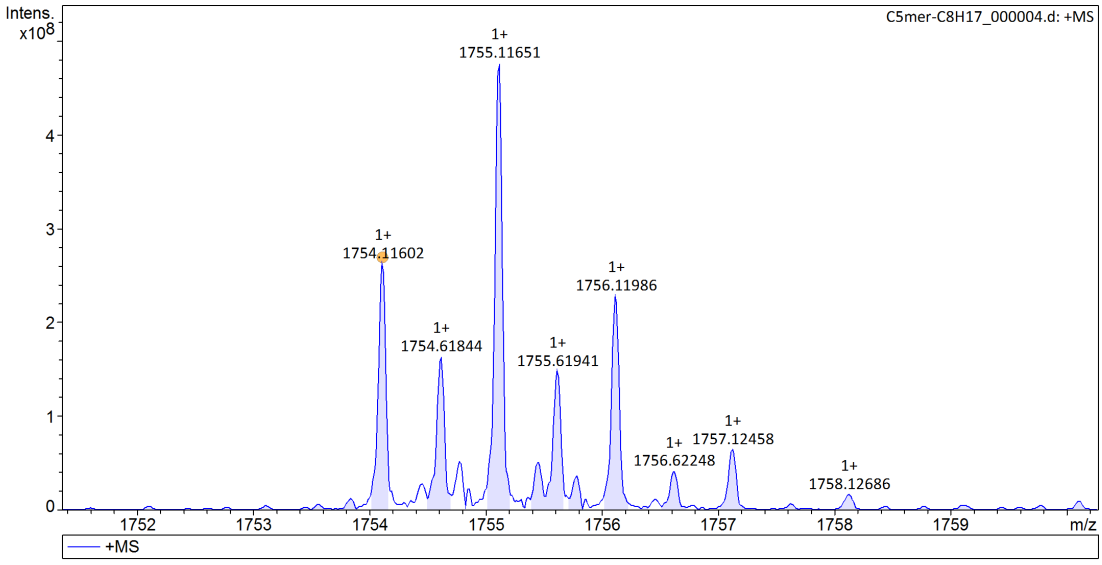

Figure S34 | **HRMS-ESI spectrum** of compound **c5a** (positive mode).

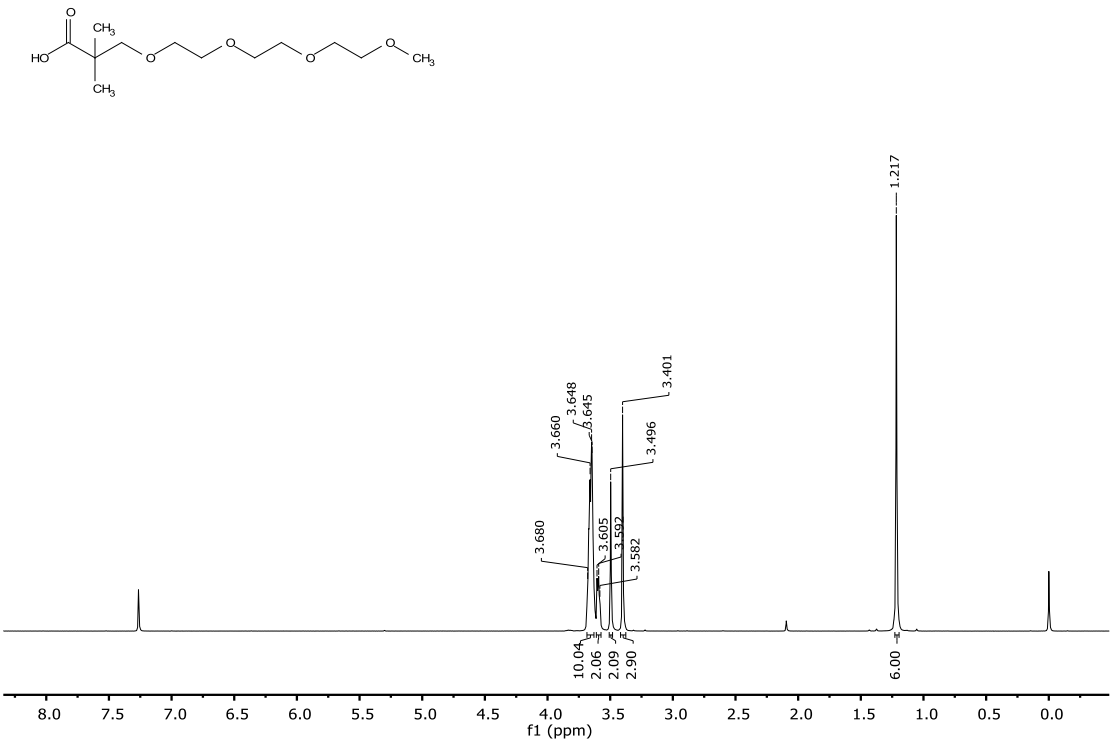

Figure S35 | **^{1}H NMR spectrum** of compound **2b-SC** ($CDCl_3$, 400 MHz, 25 °C).

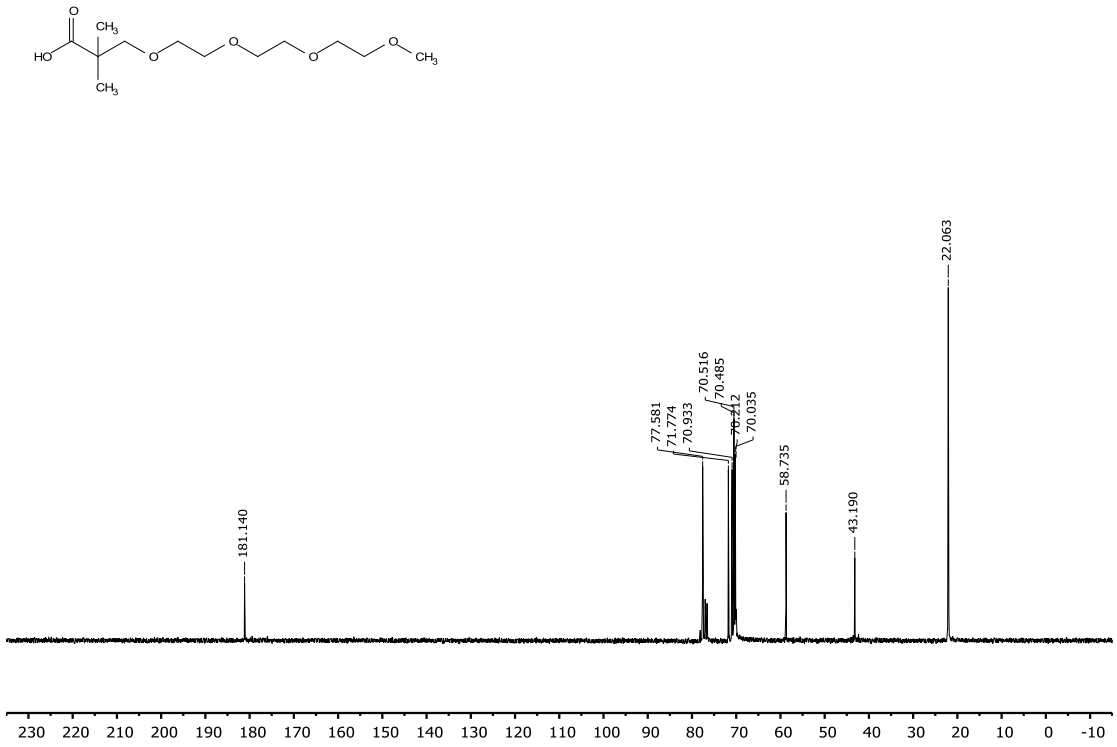

Figure S36 | **^{13}C NMR spectrum** of compound **2b-SC** ($CDCl_3$, 75 MHz, 25 °C)

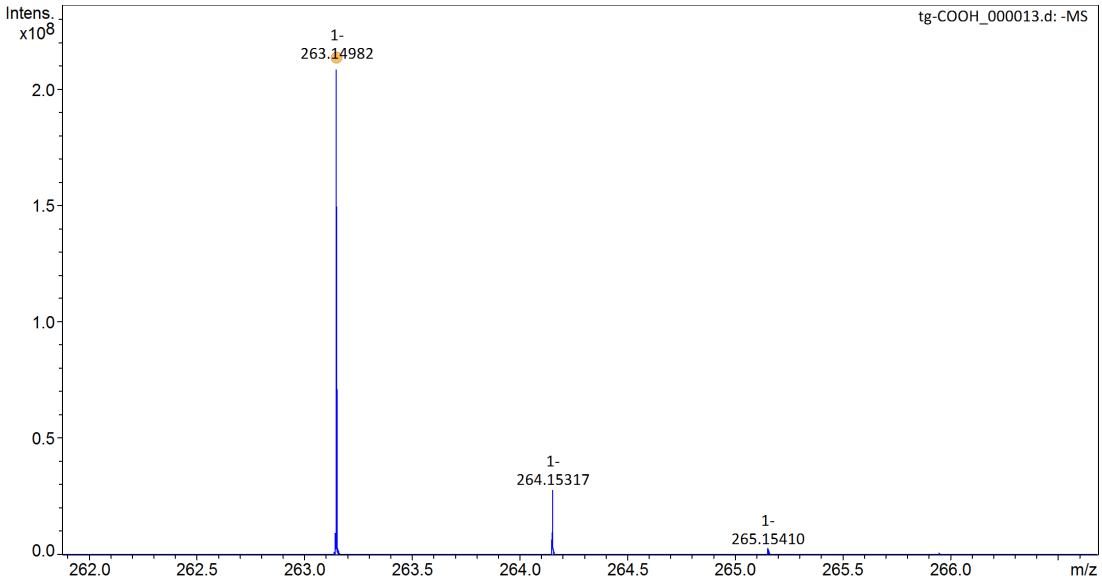

Figure S37 | **HRMS-ESI spectrum** of compound **2b-SC** (negative mode)

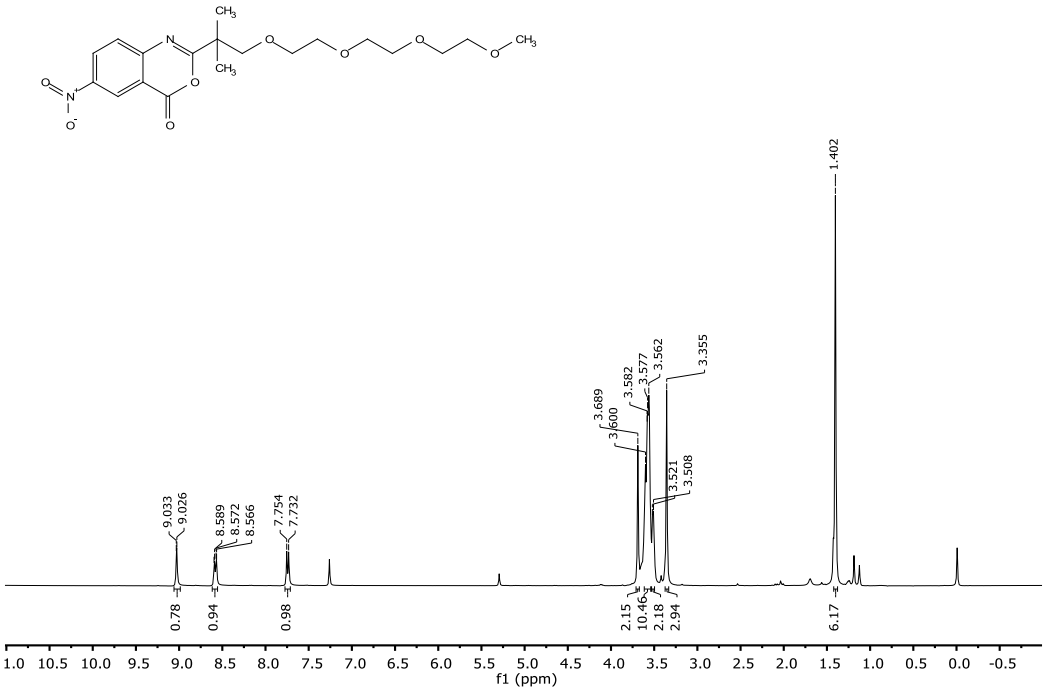

Figure S38 | ^{1}H NMR spectrum of compound **2b-NO$_2$** ($CDCl_3$, 400 MHz, 25 °C)

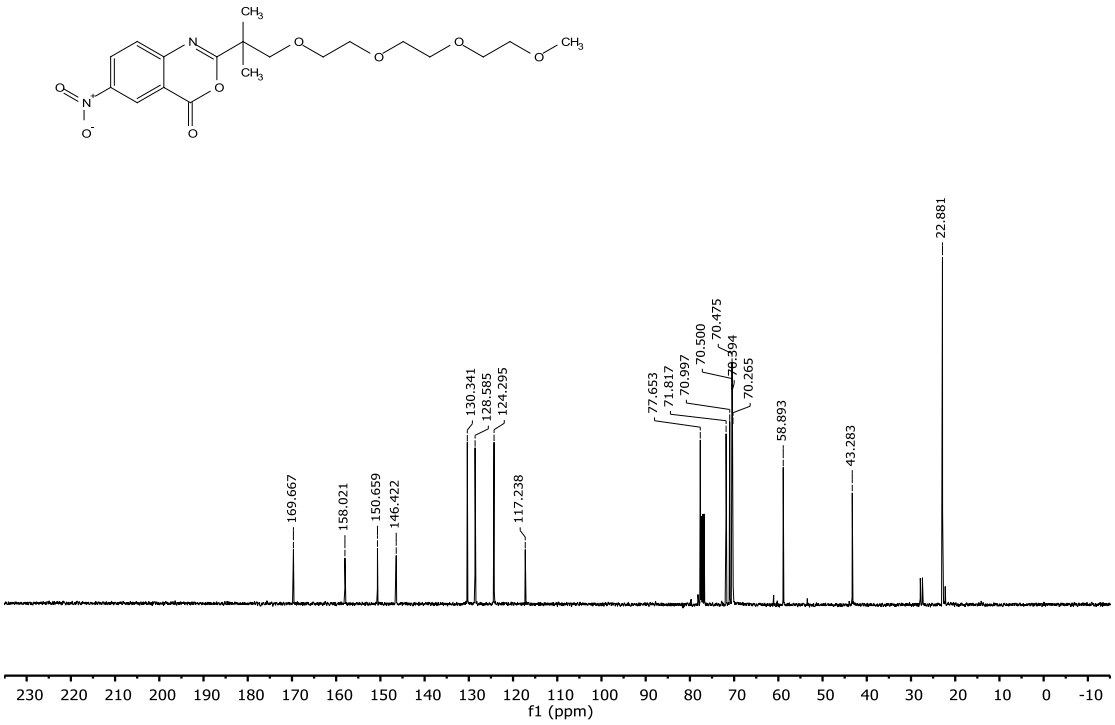

Figure S39 | ^{13}C NMR spectrum of compound **2b-NO$_2$** ($CDCl_3$, 75 MHz, 25 °C).

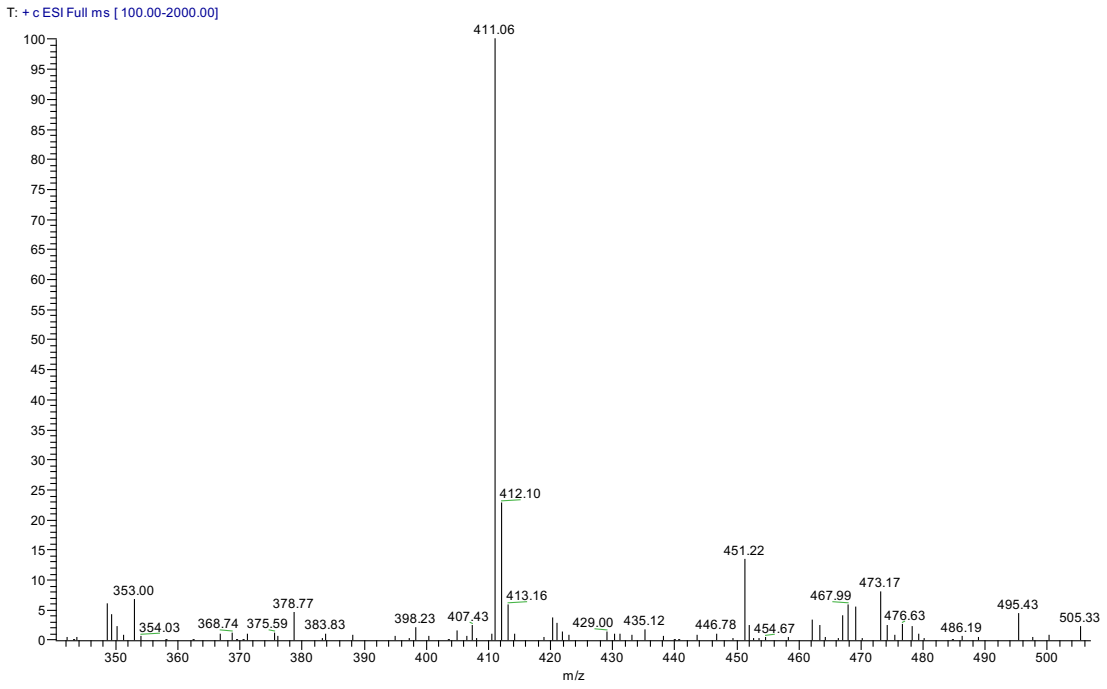

Figure S40 | MS-ESI spectrum of compound **2b-NO$_2$** (positive mode).

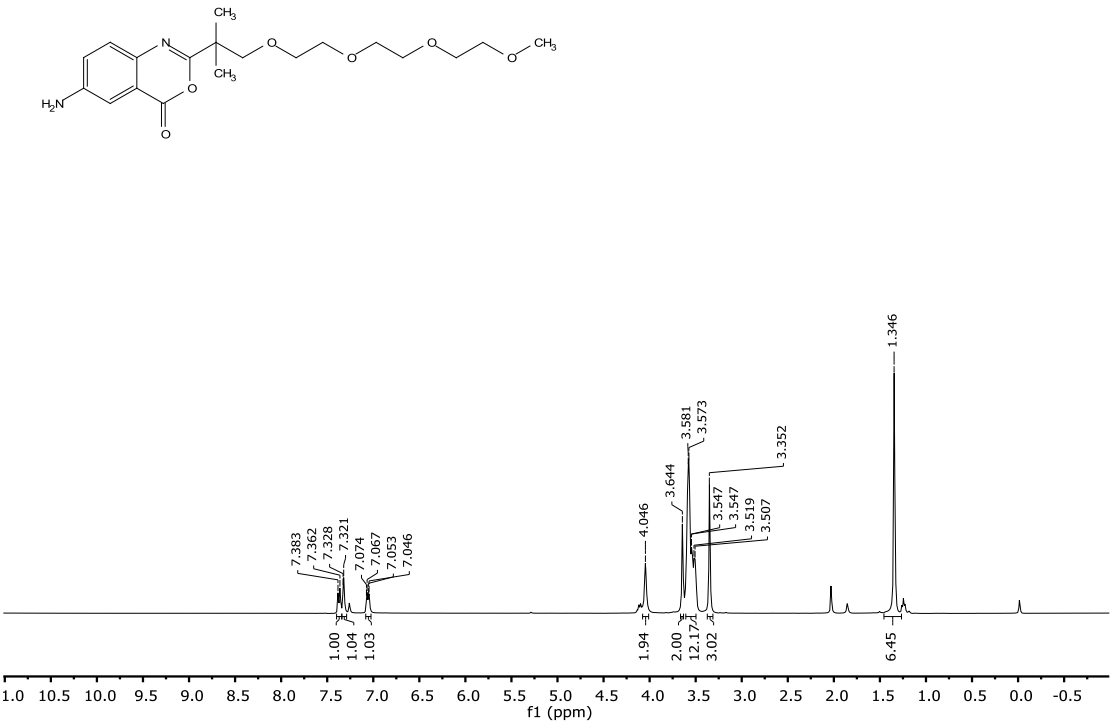

Figure S41 | ^{1}H NMR spectrum of compound **2b** ($CDCl_3$, 400 MHz, 25 °C).

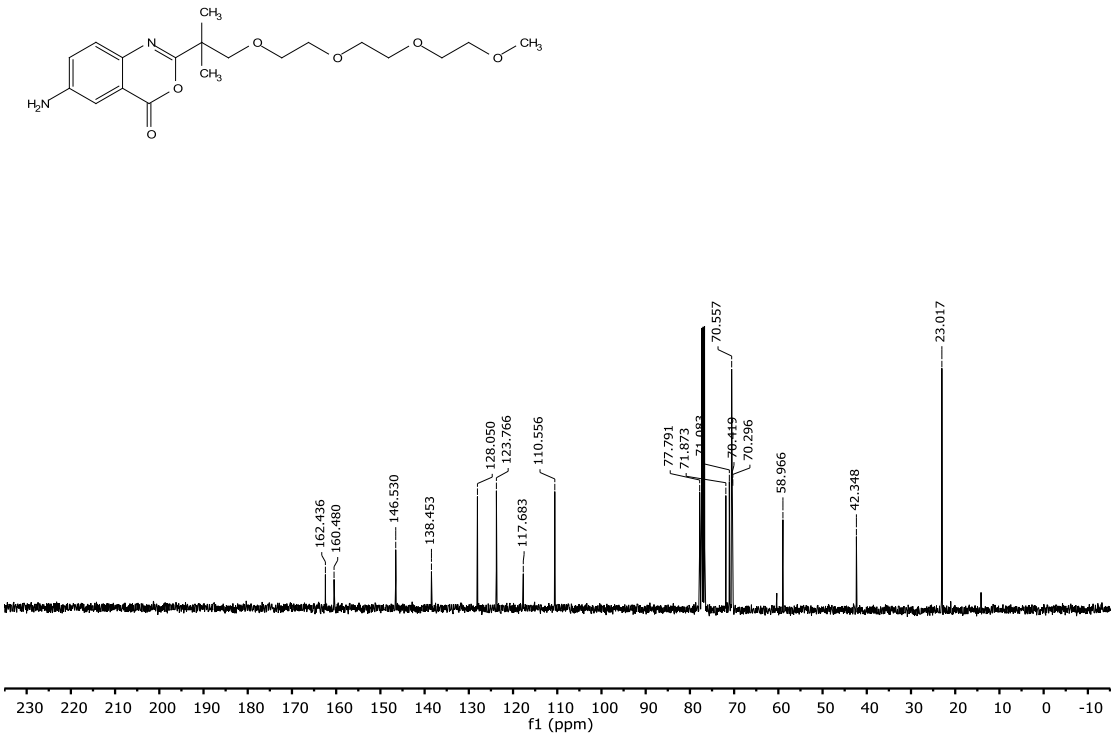

Figure S42 | ^{13}C NMR spectrum of compound **2b** ($CDCl_3$, 75 MHz, 25 ºC)

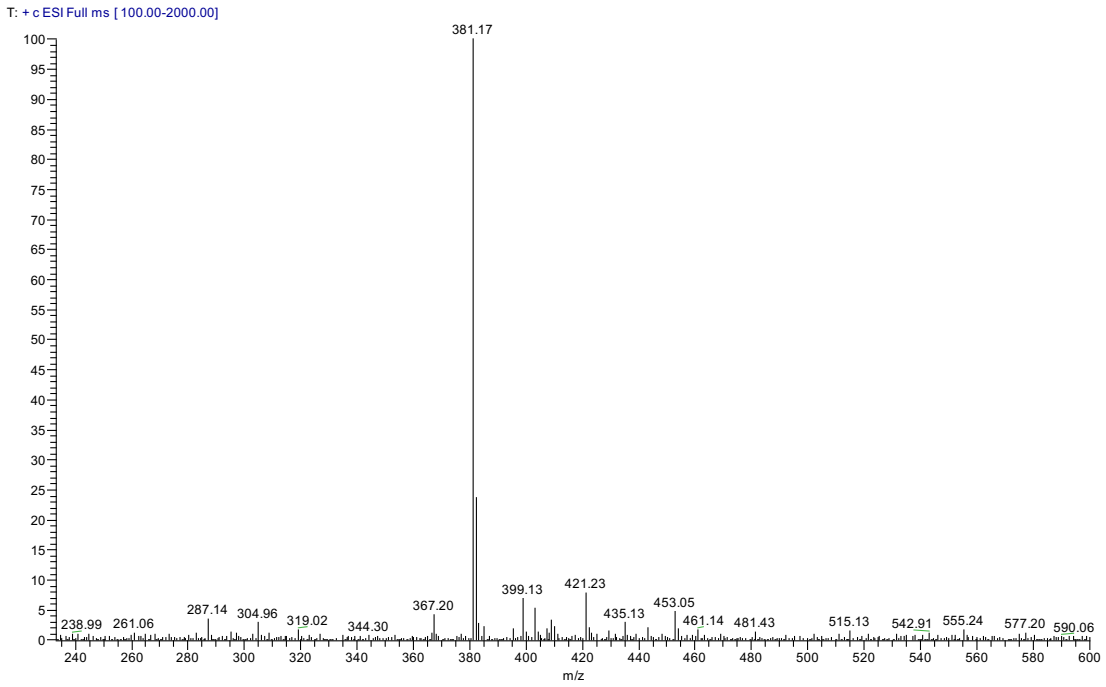

Figure S43 | MS-ESI spectrum of compound **2b** (positive mode).

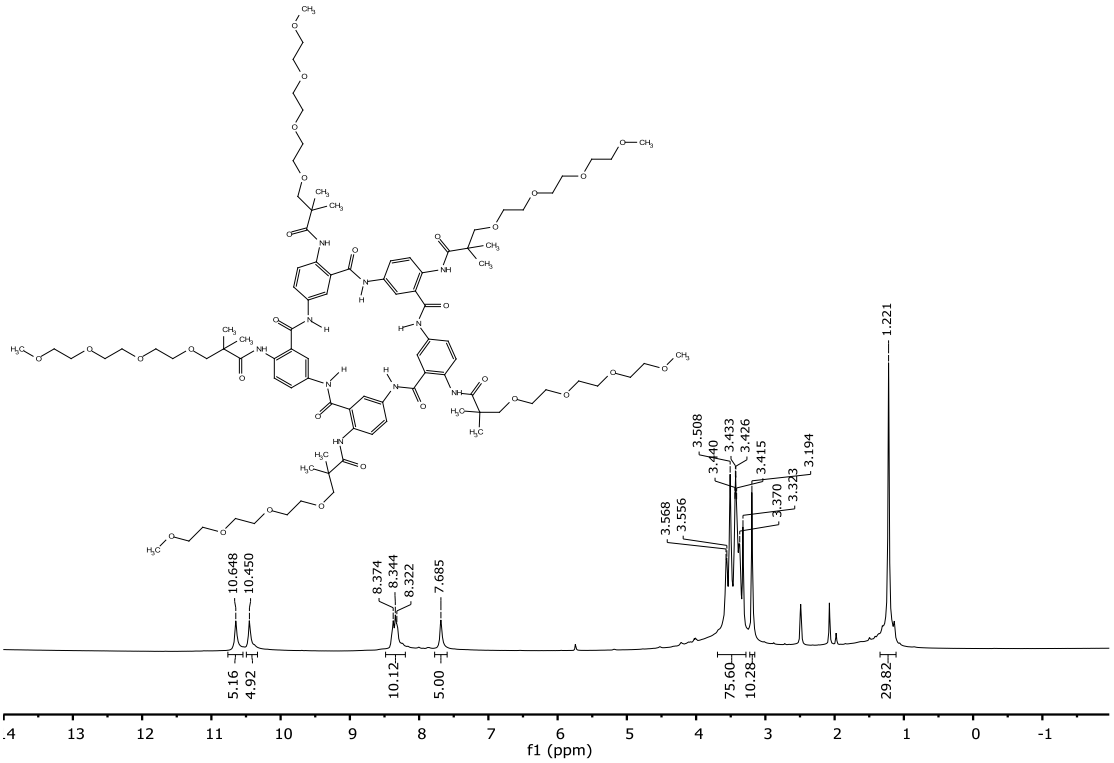

Figure S44 | **^{1}H NMR spectrum** of compound **c5b** (DMSO-d_6, 75 MHz, 25 °C).

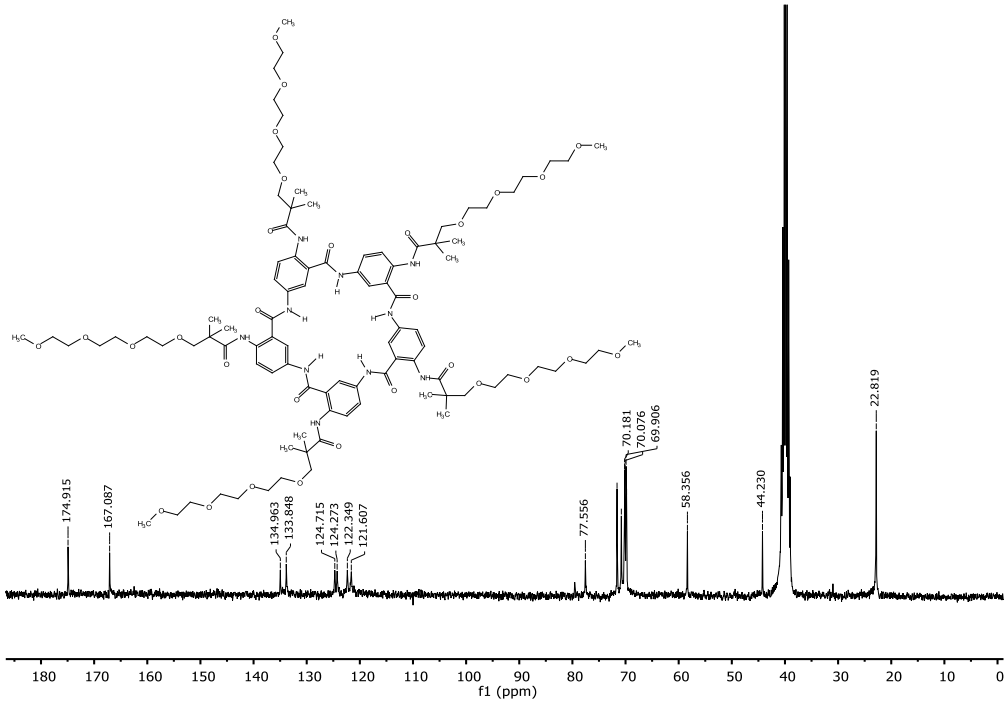

Figure S45 | **^{13}C NMR spectrum** of compound **c5b** (DMSO-d_6, 75 MHz, 25 °C).

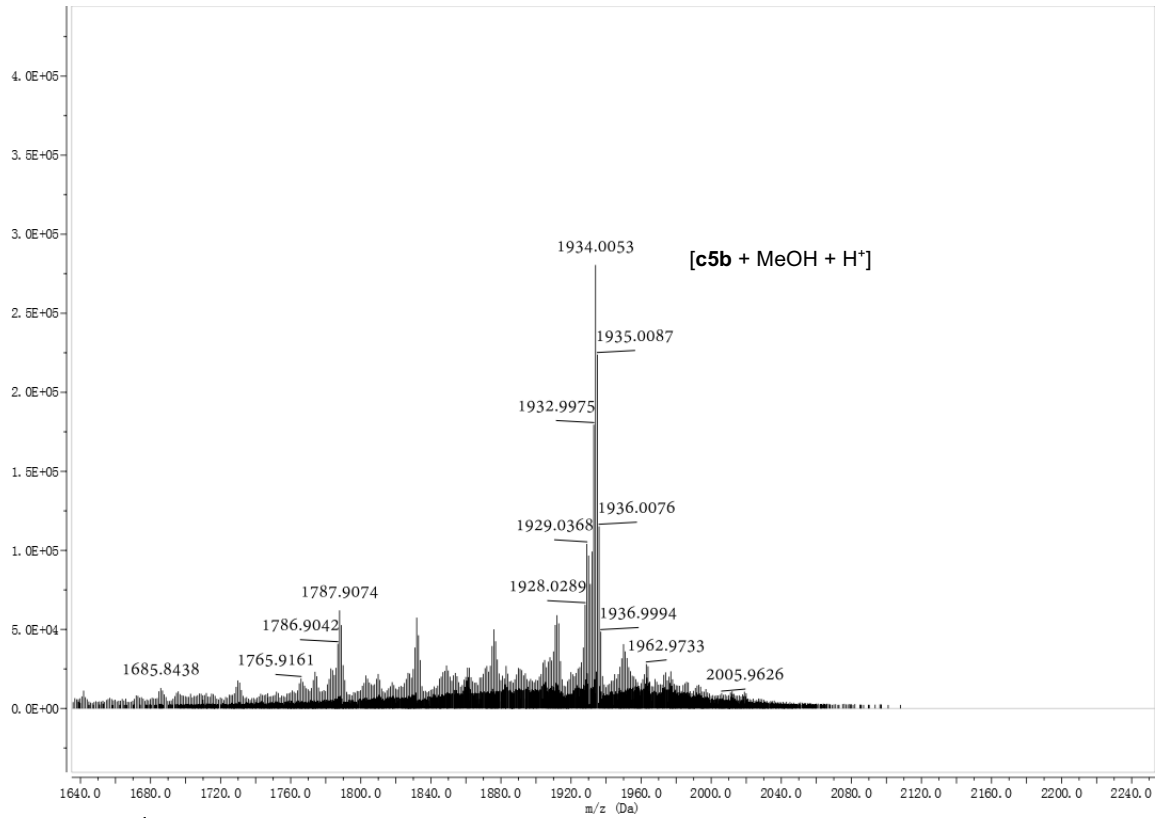

Figure S46 | HRMS-ESI spectrum of compound **c5b** (positive mode).

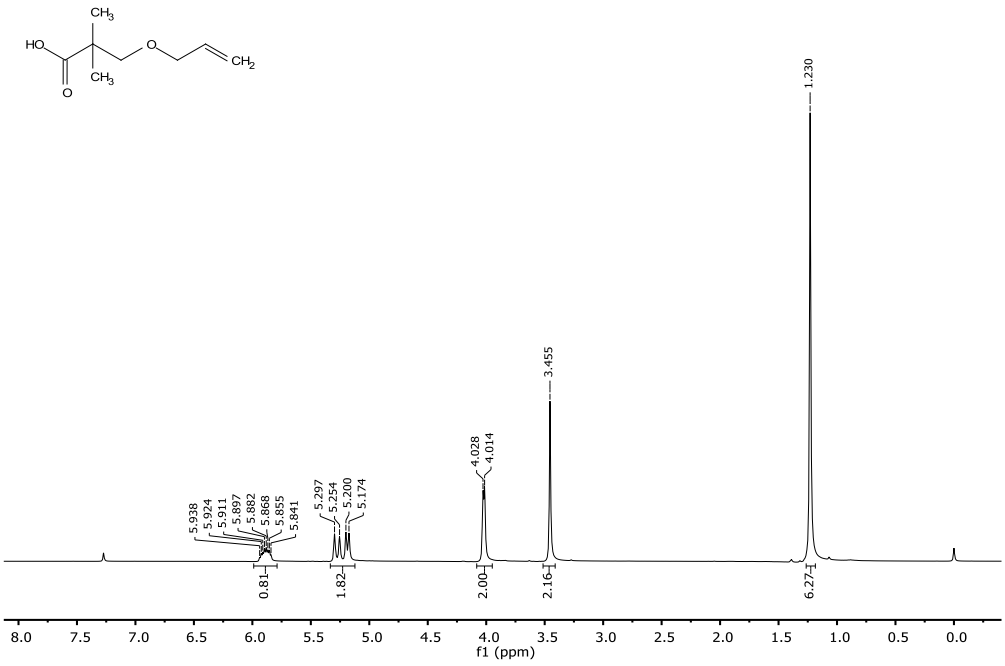

Figure S47 | ^{1}H NMR spectrum of compound **2c-SC** ($CDCl_3$, 400 MHz, 25 °C).

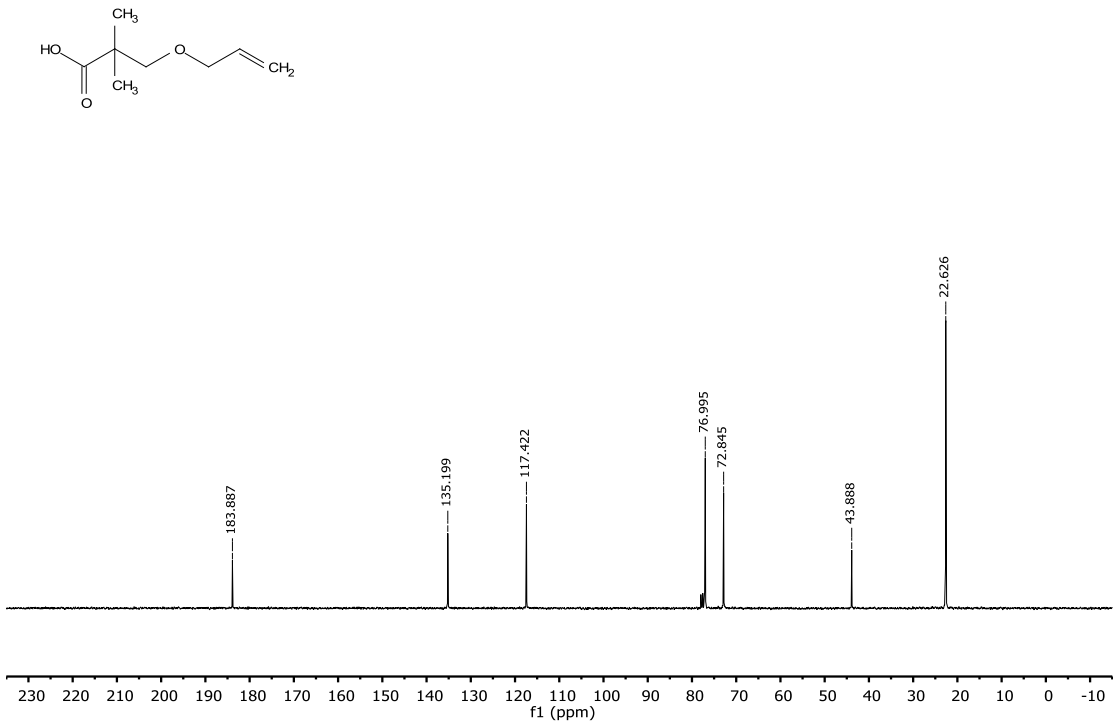

Figure S48 | **^{13}C NMR spectrum** of compound **2c-SC** ($CDCl_3$, 75 MHz, 25 °C).

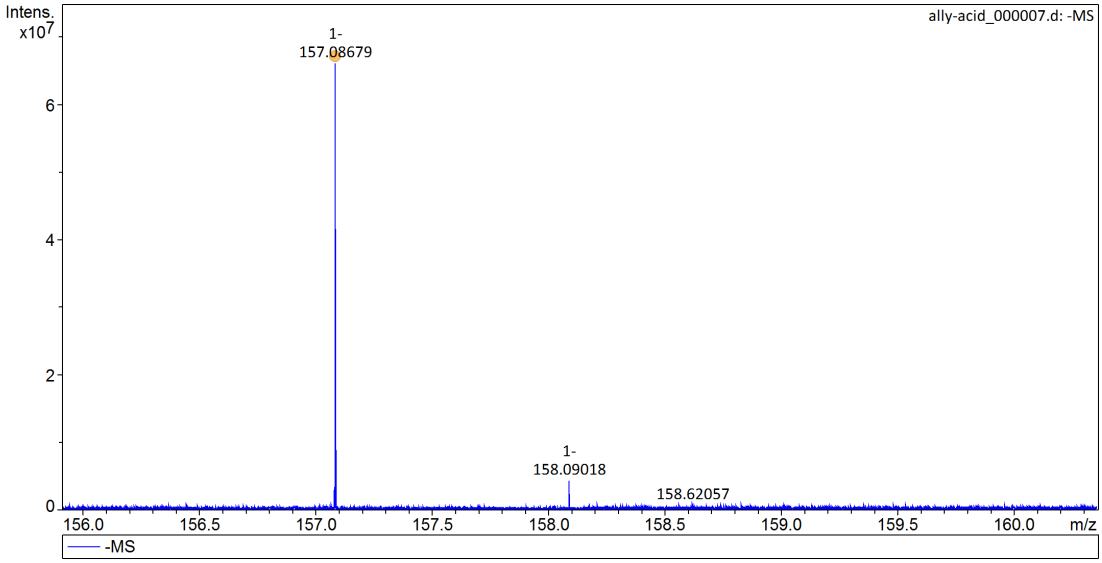

Figure S49 | **HRMS-ESI spectrum** of compound **2c-SC** (negative mode).

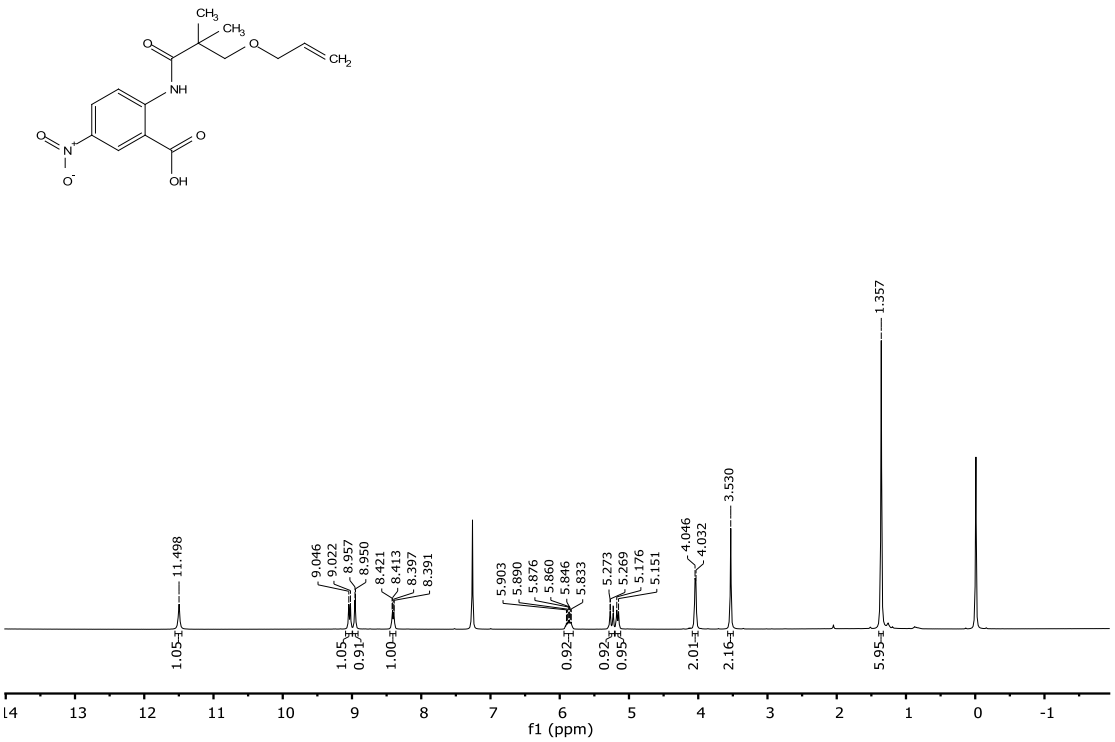

Figure S50 | **^{1}H NMR spectrum** of compound **2c-1** ($CDCl_3$, 400 MHz, 25 ºC).

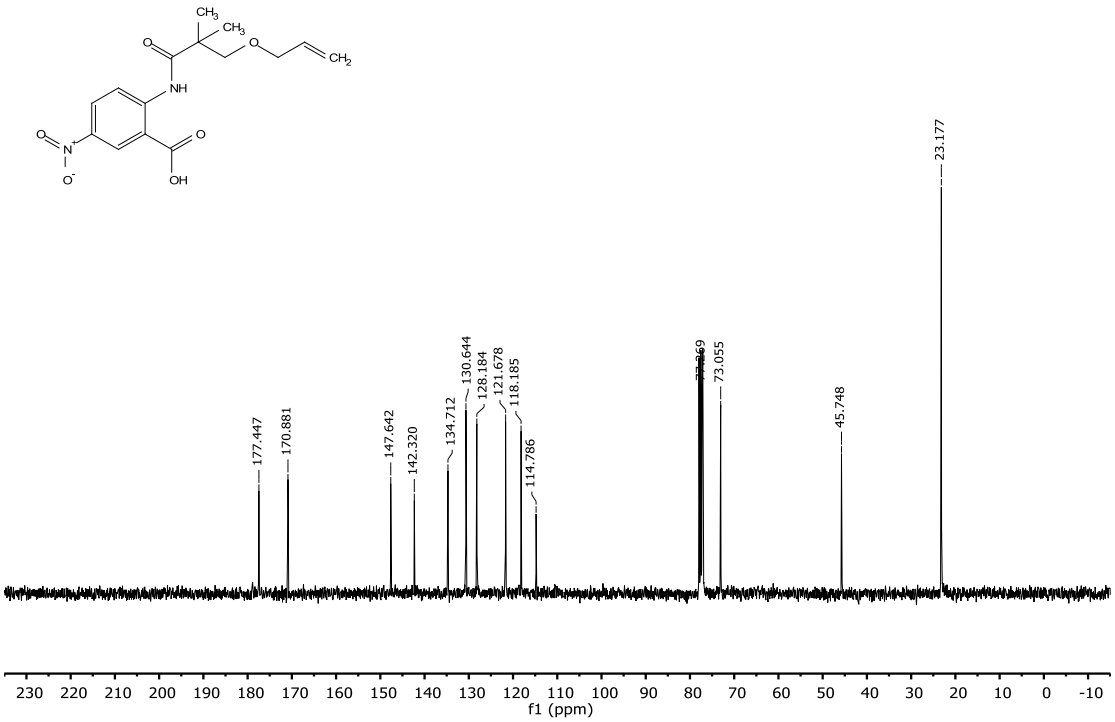

Figure S51 | **^{13}C NMR spectrum** of compound **2c-1** ($CDCl_3$, 75 MHz, 25 ºC).

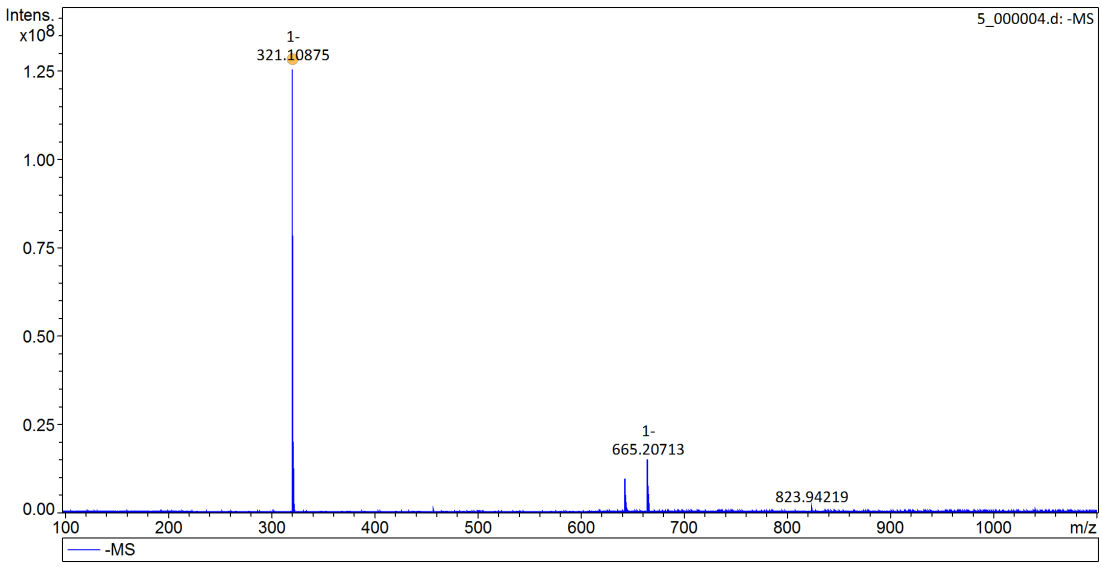

Figure S52 | HRMS-ESI spectrum of compound **2c-1** (negative mode).

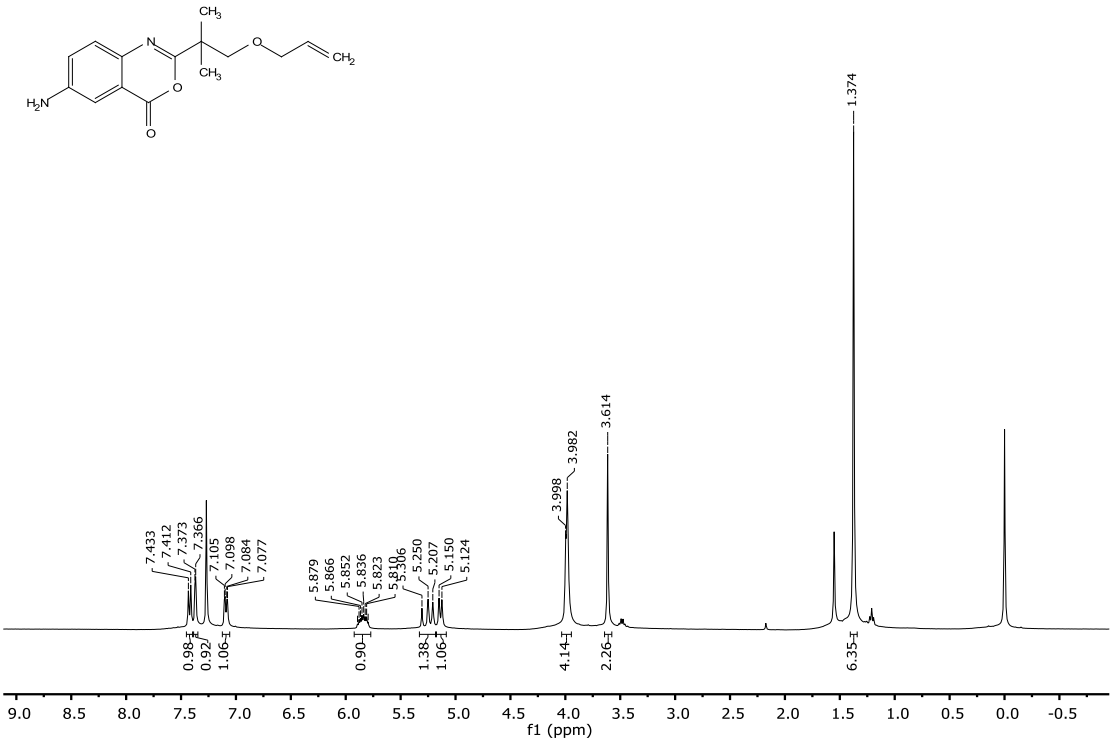

Figure S53 | ^{1}H NMR spectrum of compound **2c** ($CDCl_3$, 400 MHz, 25 °C).

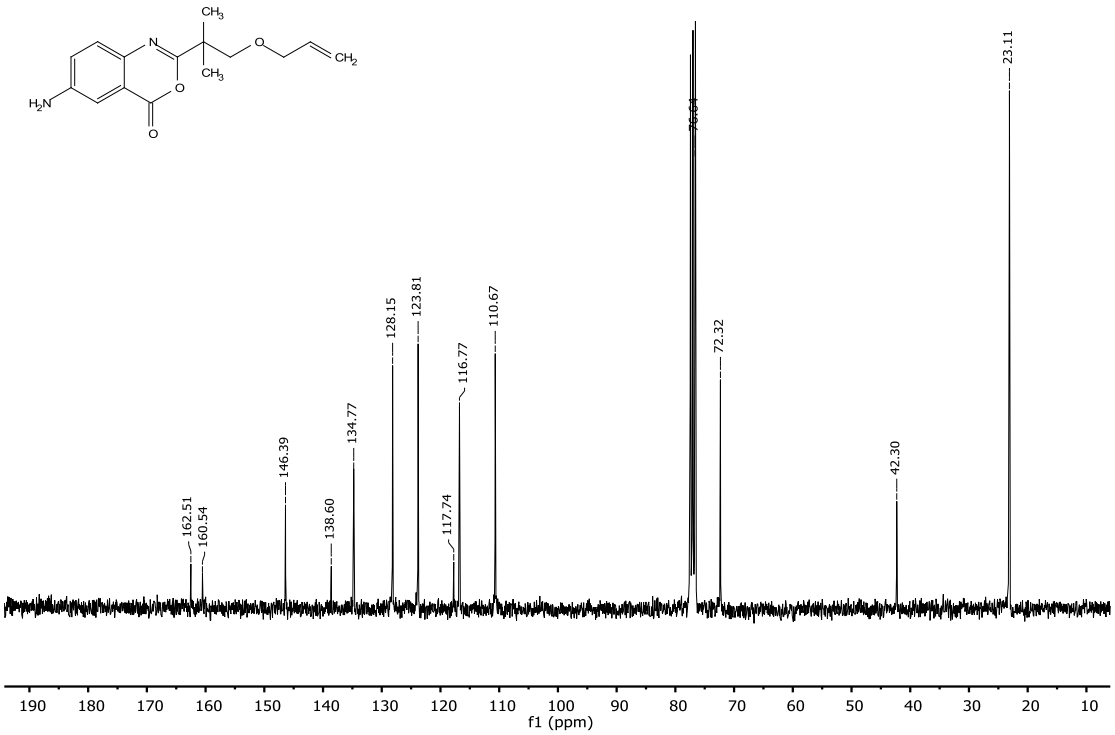

Figure S54 | **^{13}C NMR spectrum** of compound **2c** ($CDCl_3$, 75 MHz, 25 ºC)

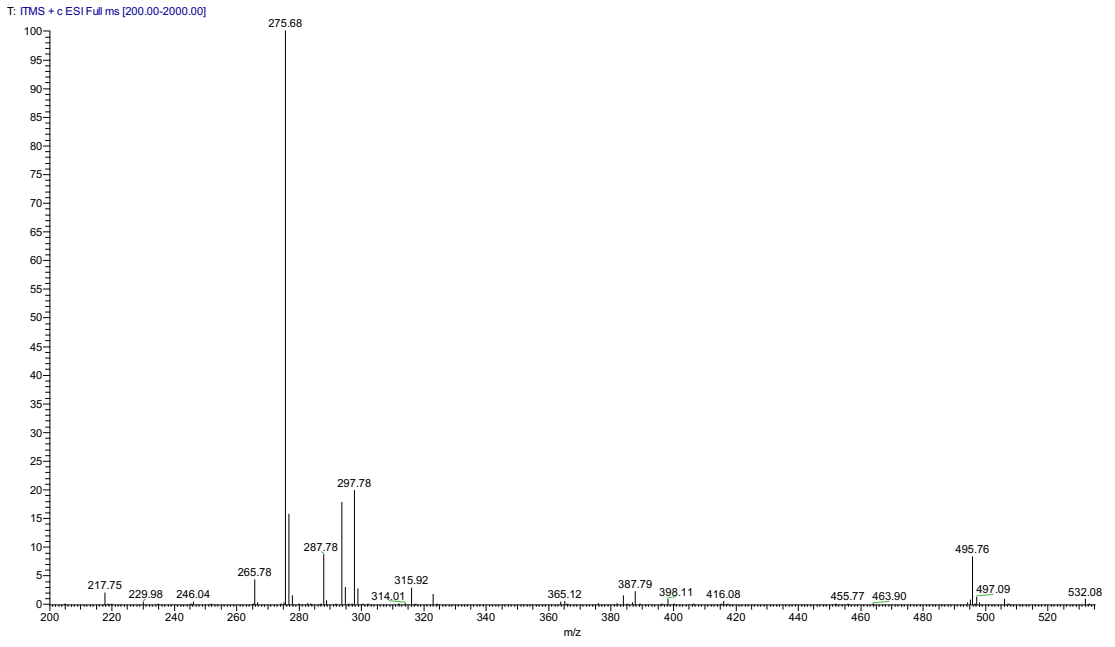

Figure S55 | **MS-ESI spectrum** of compound **2c** (positive mode).

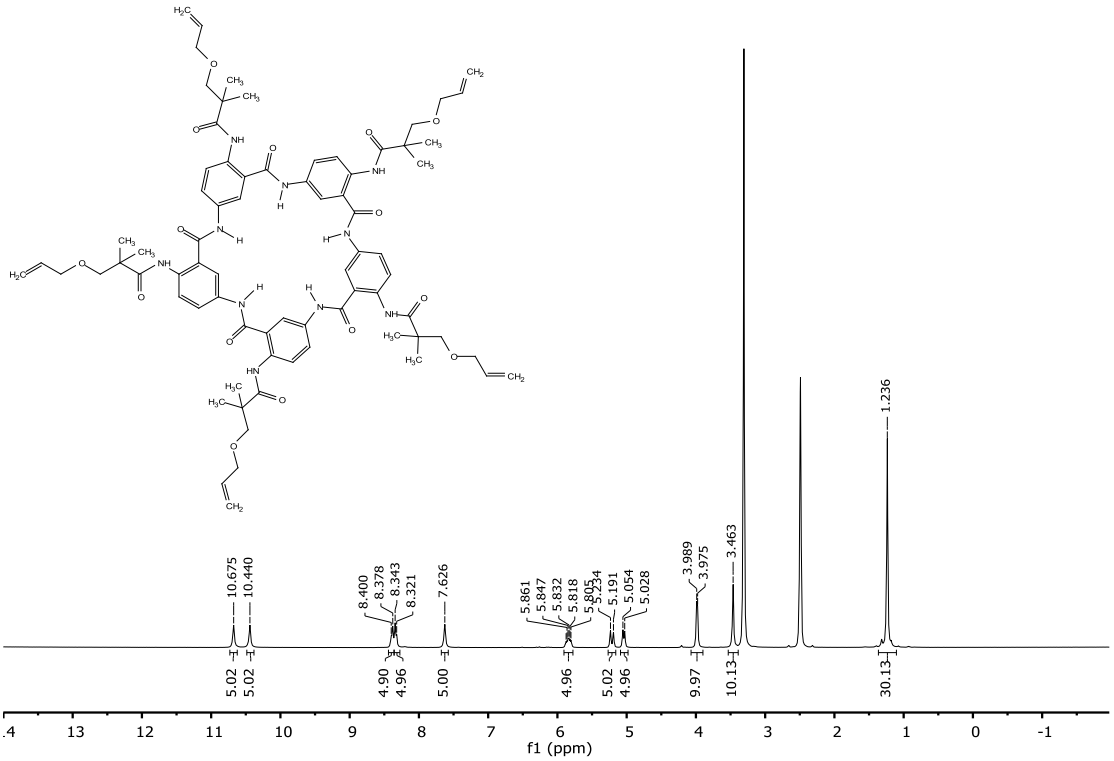

Figure S56 | ^{1}H NMR spectrum of compound **c5c** (DMSO-d_6, 400 MHz, 25 °C).

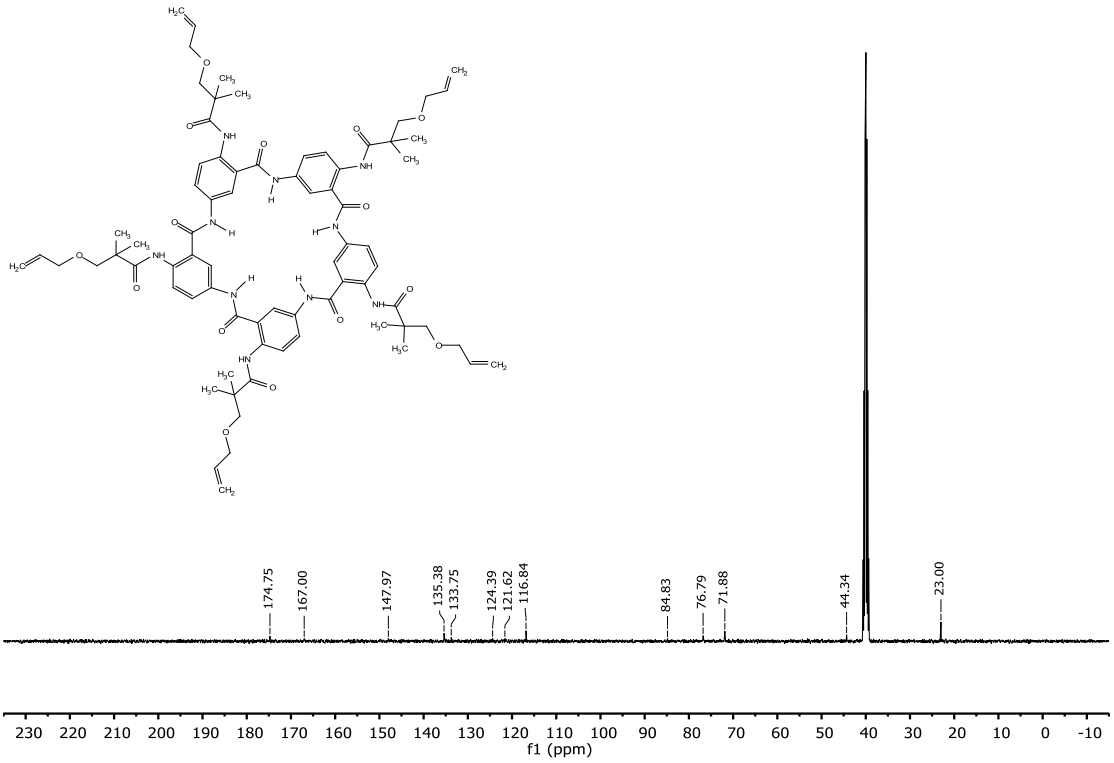

Figure S57 | ^{13}C NMR spectrum of compound **c5c** (DMSO-d_6, 75 MHz, 25 °C).

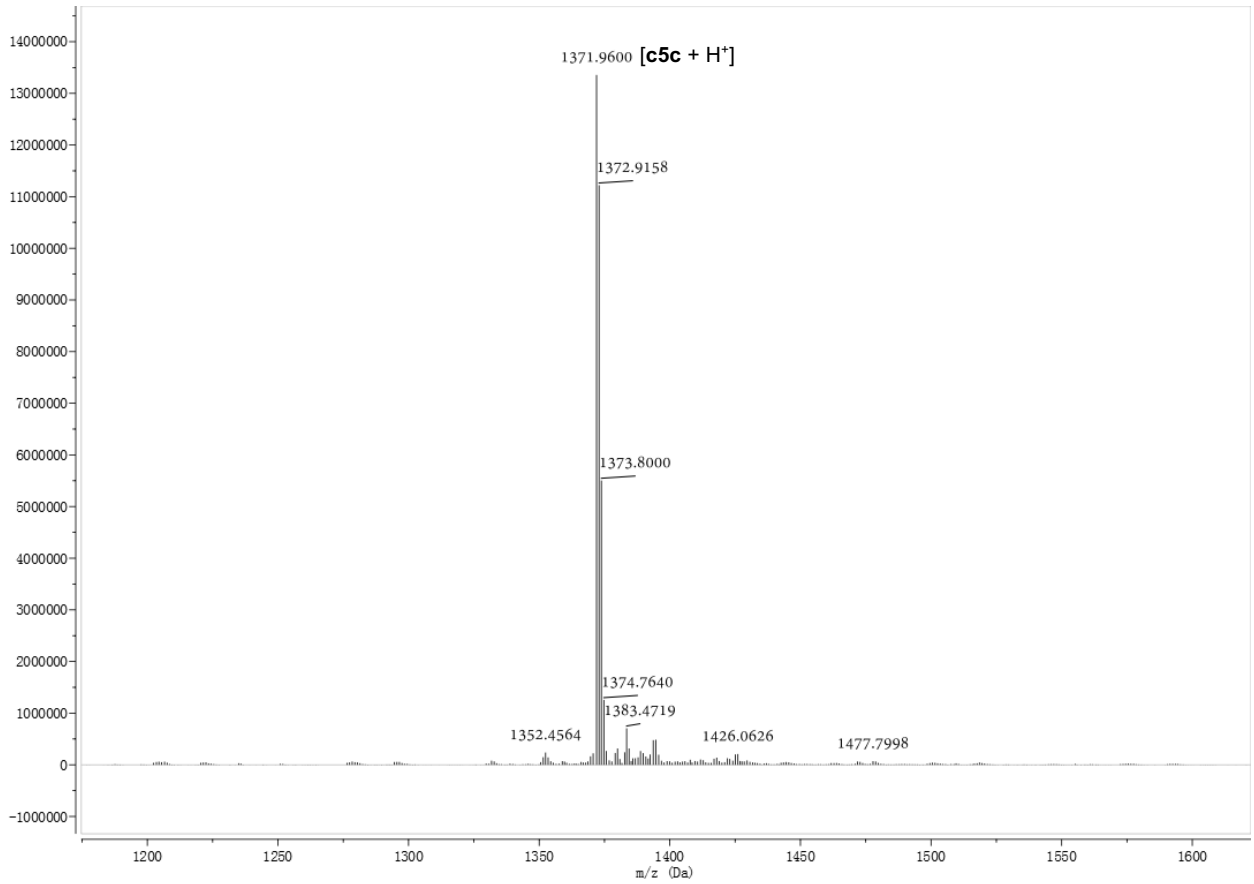

Figure S58 | HRMS-ESI spectrum of compound **c5c** (positive mode)

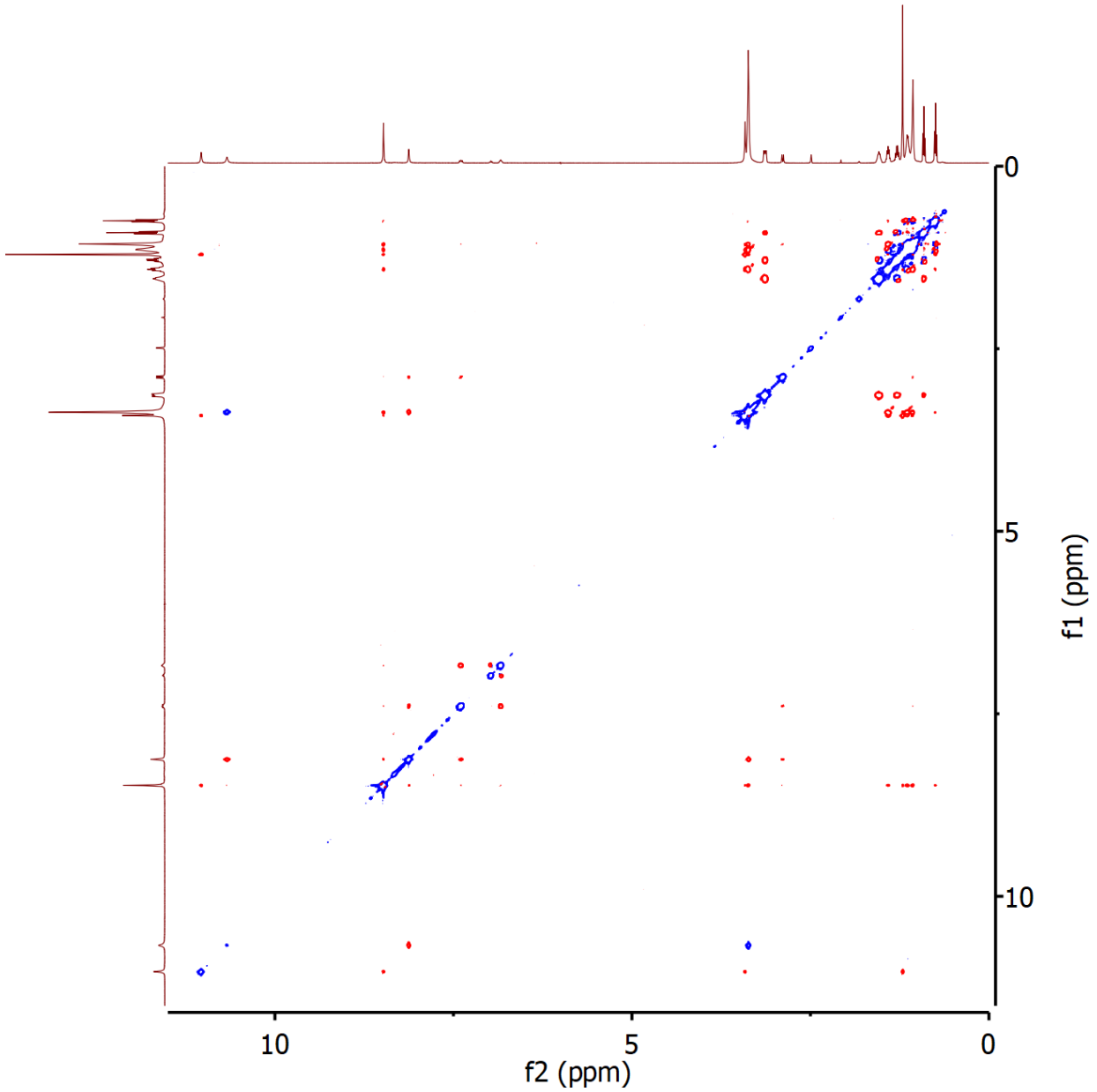

Figure S59 | 2D ROESY spectrum of the 1:1 mixture of **c5a** and TBA·MPP (DMSO-d_6, 20 mM, 500 MHz, mixing time = 0.4 s, 25°C).

4. X-ray Crystallography

Single crystals of **c5c** were obtained from $CHCl_3$/acetonitrile (1/1, v/v) by slow evaporation of solvents at room temperature. X-ray diffraction data were collected on a Rigaku XtaLAB Synergy diffractometer coupled to a Rigaku Hypix detector with Cu Kα radiation (λ = 1.54184 Å), from a PhotonJet micro-focus X-ray source at 100 K. Data of the single-crystal structure were solved by direct methods which revealed the positions of all non-hydrogen atoms, and were refined on F^2 by a full-matrix least squares procedure using anisotropic displacement parameters. All hydrogen atoms were placed in ideal geometry and were refined using a riding model.

5. Transmembrane Halide Transport

5.1. Vesicle Preparation. A portion (200 μL) of a solution of 1-palmitoyl-2-oleoyl-sn-glycero-3-phosphocholine (POPC) or dipalmitoylphosphatidylcholine (DPPC) (from Avanti Polar Lipids, US) in chloroform (25 mg/mL) was first diluted into 10 mL of chloroform. A thin lipid film was prepared by evaporating the solution on a rotary evaporator *in vacuo* for at least 3 hours.

5.1.1. For POPC-LUVs with encapsulated HPTS and an intravesicular pH of 11.5, the POPC thin film was hydrated with a buffer (10 mM HEPES, 100 mM NaCl, pH 11.5) containing 8-hydroxypyrene-1,3,6-trisulfonic acid trisodium salt hydrate (HPTS, from Sigma-Aldrich, US) (0.03 mM) at 37 °C for >30 min, with the final concentration of the lipid being 0.1 mg/mL. The resultant lipid suspension was subjected to 5 freeze–thaw cycles (liquid nitrogen–37 °C water bath), followed by extrusion through a 0.1-μm polycarbonate membrane (Sigma-Aldrich, US) to produce a solution of large unilamellar vesicles (LUVs). The LUVs were separated from the extravesicular HPTS and other components by size exclusion chromatography using Sephadex G-50 (GE Healthcare, US), pre-equilibrated with the buffer of 10 mM HEPES, 100 mM NaCl, pH 11.5.

5.1.2. For POPC-LUVs with encapsulated HPTS and an intravesicular pH of 7.0, the POPC thin film was hydrated with a buffer (10 mM HEPES, 100 mM NaCl, pH 7.0) containing 1 mM of HPTS (from Sigma-Aldrich, US) at 37 °C for >30 min, with the final concentration of the lipid being 0.1 mg/mL. The resultant lipid suspension was subjected to 5 freeze–thaw cycles (liquid nitrogen–37 °C water bath), followed by extrusion through a 0.1-μm polycarbonate membrane (Sigma-Aldrich, US) to produce a solution of large unilamellar vesicles (LUVs). The LUVs were separated from the extravesicular HPTS and other components by size exclusion chromatography using Sephadex G-50 (GE Healthcare, US), pre-equilibrated with the buffer of 10 mM HEPES, 100 mM NaCl, pH 7.0.

5.1.3. For POPC-LUVs with encapsulated lucigenin, the thin film was hydrated with a buffer (10 mM HEPES, 100 mM $NaNO_3$, pH 7) containing with 1 mL of 1 mM *N*, *N*′-dimethyl-9, 9′-biacridinium dinitrate (lucigenin, from TCI, Japan) at 37 °C for >30 min, with the final concentration of the lipid being 1 mg/mL. The resultant lipid suspension was subjected to 5 freeze–thaw cycles (liquid nitrogen–37 °C water bath), followed by extrusion through a 0.1-μm polycarbonate membrane (Sigma-Aldrich, US) to produce a solution of LUVs. The LUVs were separated from the extravesicular lucigenin and other components by size exclusion chromatography using Sephadex G-50 (GE Healthcare, US), pre-equilibrated with the buffer of 10 mM HEPES, 100 mM NaCl, pH 7.0.

5.1.4. For DPPC-LUVs with encapsulated HPTS, the thin film was hydrated with a buffer (10 mM HEPES, 100 mM NaCl, pH 7) containing 0.03 mM of 8-hydroxypyrene-1,3,6-trisulfonic acid trisodium salt hydrate (HPTS, from Sigma-Aldrich, US) at 45 °C for >30 min, with the final concentration of the lipid being 0.1 mg/mL. The resultant lipid suspension was subjected to 5 freeze–thaw cycles (liquid nitrogen–45 °C water bath), followed by extrusion through a 0.1-μm polycarbonate membrane (Sigma-Aldrich, US) at 45 °C to

produce a solution of LUVs. The LUVs were separated from the extravesicular lucigenin and other components by size exclusion chromatography using Sephadex G-50 (GE Healthcare, US), pre-equilibrated with the buffer of 10 mM HEPES, 100 mM NaCl, pH 7.0.

5.2. Determination of the transmembrane permeability of halide transport mediated by c5a with the HPTS assay. An aliquot (10μL) of macrocycle **c5a** (0.5 mM) in DMF was added to 1.8 mL of a buffer comprising of 10 mM HEPES, 100 mM NaX (X = Cl, Br or I) at pH 6.5, to which 200 μL POPC LUVs with intravesicular components of 10 mM HEPES, 100 mM NaCl, pH 11.5, was added. The fluorescence emission of the intravesicular HPTS was monitored with a fluorescence spectrometer (Cary Eclipse, Agilent, US) at the excitation wavelengths of 405 nm and 450 nm simultaneously, based on which the ratio of emission intensities corresponding to the 405-nm and 450-nm excitation was obtained. After 400 s, the vesicles were lysed by adding Triton X-100 (20 μL, 10% v/v) to obtain the minimal fluorescence intensity for normalization.

Each of the normalized time-lapse fluorescence emission curves was fitted with the quantitative model (black lines) according to the Goldman-Hodgkin-Katz flux theory[1] and the carrier-mediated transport model developed by Behr *et al*[2], based on which the anion permeability of vesicles with or without **c5a** was determined. The total anion permeability (ΔP_X-) of each halide ion elicited by **c5a** was calculated by subtracting the anion permeability measured with vesicles in the absence of **c5a**.

*5.2.1. Quantitative model for vesicle-based halide transport HPTS assay, t*o describe the process of cross-membrane transport of **c5a**-halide, a quantitative flux model with a combining of the Goldman-Hodgkin-Katz theory and carrier-mediated transport model was developed here. According to the Goldman-Hodgkin-Katz theory, the ion flux across the vesicle membrane can be calculated as:

$$j = \mu n P \frac{[A]_{out} - [A]_{in} e^{n\mu}}{1 - e^{n\mu}}$$

where $\mu = \frac{FE_m}{RT}$, F is the Faraday constant, E_m is the membrane potential, R is the molar gas constant,. T is the temperature, n is the charge valence, P is the permeability and $[A]_{out}$ is the concentration of ion-carrier complex at the outer membrane – solution interface, $[A]_{in}$ is the concentration at the inner membrane – solution interface. According to the carrier-mediated transport model developed by Behr et. al, $[A]_{out}$ and $[A]_{in}$ can be calculated as follow:

$$[A]_{out} = K_a[C]\frac{[S]_{out}}{1 + K_a[S]_{out}}$$

$$[A]_{in} = K_a[C]\frac{[S]_{in}}{1 + K_a[S]_{in}}$$

where K_a is the association constants for the binding of carrier with ion, $[C]$ is the concentration of carriers in the membrane, $[S]_{out}$ and $[S]_{in}$ is the extra-vesicular and intra-vesicular ion concertation. So the ion flux j can be re-written as:

$$j = \mu n P K_a[C]\frac{\frac{[S]_{out}}{1+K_a[S]_{out}} - \frac{[S]_{in}}{1+K_a[S]_{in}}e^{n\mu}}{1 - e^{n\mu}}$$

Base on this formula, the change in intra-vesicular halide ion and further resulting pH variation were numerically calculated iteratively with a given time-step (10^{-7} s) for the whole duration of experimental measurements. The calculations were carried out with Matlab (MathWork, Natick, USA). All the codes are available upon request.

5.3. Determination of the EC50 values of halide transport mediated by c5a with the HPTS assay. An aliquot (20 μL) POPC LUVs (intravesicular components: 10 mM HEPES, 100 mM NaCl, pH 11.5) was added to 1.98 mL of a buffer comprised of 10 mM HEPES, 100 mM NaCl, pH 7, followed by adding 20 μL of **c5a** in DMF. The emission of the intravesicular HPTS was monitored at 510 nm with a fluorescence

spectrometer (Cary Eclipse, Agilent, US) at the excitation wavelengths of 405 nm and 450 nm. After 200 s, the vesicles were lysed by adding Triton X-100 (20 μL, 10% v/v) to obtain the maximum fluorescence intensity for normalization.

The time course of the emission intensity of intravesicular HPTS, I_t, was obtained first by ratiometric analysis ($R_t = I_{t,450} / I_{t,405}$), followed by normalization according to the following equation,

$$Nomalized\ intensity\ ratio = \frac{R_t - R_0}{R_\infty - R_0}$$

where $R_0 = R_t$ at t = 100 s, before the addition of **c5a**; $R_\infty = R_t$ at t = 350 s upon the addition of Triton X-100. Normalized intensity ratio at 300 s just before addition of Triton X-100 was defined as the transmembrane activity (Y) which was analyzed with the Hill equation shown below to give effective concentration EC50 and the Hill coefficient n,

$$Y = Y_\infty + \frac{Y_0 - Y_\infty}{(1 + \frac{c}{EC50})^n}$$

where Y_0 is Y in absence of carrier, Y_∞ is Y with excess carrier, and c is the carrier concentration in a cuvette.

5.4. Determination of halide transport with the lucigenin assay. An aliquot (20 μL) POPC LUVs (intravesicular components: 10 mM HEPES, 100 mM $NaNO_3$, pH 7.0) was added to 1.98 mL of each of the buffers comprised of 10 mM HEPES, 100 mM NaX (X = Cl, Br, or I), pH 7, followed by adding 20 μL of **c5a** (0.2 mM) in DMF, with the final concentration of **c5a** being 10 μM. The emission of the intravesicular lucigenin was monitored at 505 nm with a fluorescence spectrometer (Cary Eclipse, Agilent, US) at the excitation wavelength of 430 nm. After 200 s, the vesicles were lysed by adding Triton X-100 (20 μL, 10% v/v) to obtain the minimal fluorescence intensity for normalization.

5.5. Differentiation of carrier vs channel chloride transport with DPPC LUVs. An aliquot (20 μL) DPPC LUVs (intravesicular components: 10 mM HEPES, 100 mM NaCl, pH 7.0) was added to 1.98 mL of a buffer comprised of 10 mM HEPES, 100 mM NaCl, pH 7, followed by incubating at 45 °C for 3 min. An aliquot (20 μL) of **c5a** (0.2 mM) in DMF was added to the LUVs, with the final concentration of **c5a** being 5 μM, and the solution was incubated for an additional 3 min at 45 °C. LUVs with **c5a** were incubated either at 45 °C or 25 °C for 3 minutes. The emission of the intravesicular HPTS was monitored at 510 nm with a fluorescence spectrometer (Cary Eclipse, Agilent, US) at the excitation wavelengths of 405 and 450 nm, followed by applying a base pulse (20 μL of 0.5 mM NaOH) at 50 s. After 200 s, the vesicles were lysed by adding Triton X-100 (20 μL, 10% v/v) to obtain the maximum fluorescence intensity for normalization.

6. Cell Culture and Confocal Imaging

6.1 Primary Cell Culture. Human bronchial epithelial (HBE) cells from cystic fibrosis (CF) patients (DF508 homozygous) were obtained from the UNC-CF Tissue Culture Core under the auspices of protocols approved by the UNC Institutional Review Board using previously reported methodologies[3]. Cultures on 12-mm permeable supports (Transwell-Clear; Costar) were maintained in a well-humidified (>95%) incubator (5% CO_2) at 37ºC during cellular differentiation (3-4 weeks after plating).

6.2. Confocal imaging studies. CF HBE cultures were treated with apically with **c5a** (5 μM in 1% DMSO) or vehicle control (1% DMSO in PBS) daily for 5 days prior to imaging. The height of the luminal airway surface layer (ASL) was visualized by adding a cell-impermeant dye (Texas Red-dextran 70kDa; 0.1%) to the **c5a** and vehicle control on the evening prior to imaging[4]. The cultures were mounted on the stage of a scanning confocal microscope (SP5, Leica) outfitted with an environmental chamber that regulated temperature to 37°C, humidity at >50%, and CO_2 at 5%[5]. The thickness of the ASL layer in **c5a** and control cultures were measured by high-speed X-Z confocal scanning. A custom Matlab script was used to make thickness measurements from the resulting images.

7. Computational Studies

The density functional theory calculations were performed with the ADF[6] software package. The revPBE-D3[7,8] functional and dispersion correction, along with a TZP basis set[9], were used to geometry optimize all structures involving the macrocycle **c5**, amide molecular units based on macrocycle **c5**, linear pentamer **L5**, and macrocycle **c6**. The core electrons were frozen for the oxygen, nitrogen, carbon, sulfur, phosphorus, chlorine, bromine, and iodine atoms. Models detailing the host-guest interaction of chloride, bromide, iodide, nitrate, perchlorate, bisulfate, methyl phenylphosphonate, and diphenyl phosphate with the macrocycle **c5** were treated with a -1 overall charge on the system. The Hirshfeld charges, dipole moments, and energy decomposition analyses (EDA) were obtained from relaxed structures of macrocycle **c5**, linear pentamer **L5**, and/or amide molecular units based on the macrocycle **c5**.

As confirmation, an energy decomposition analysis (EDA) reveals that, compared to the linear pentamer **L5**, macrocycle **c5** is 16.9 kcal/mol less stable, but gains stability through greater orbital interactions (-9.6 kcal/mol). Consequently, macrocycle c5, with its highly electropositive cavity, as shown with DFT computed Hirshfeld charges of +0.12 e and +0.04 e for each of the NH and CH protons, is in a high-energy unbound state and is predisposed for binding anions.

8. References

1. Shen, Y. *et al*. Ultrasensitive liposome-based assay for the quantification of fundamental ion channel properties. *Anal. Chim. Acta* **1112**, 8-15 (2020).
2. Behr, J.-P., Kirch, M., & Lehn, J.-M. Carrier-mediated transport through bulk liquid membranes: dependence of transport rates and selectivity on carrier properties in a diffusion-limited process. *J. Am. Chem. Soc*. **107**, 241–246 (1985).
3. Fulcher ML, Gabriel S, Burns KA, Yankaskas JR, Randell SH. Well-differentiated human airway epithelial cell cultures. *Methods Mol Med*. **107**,183–206 (2005). PMID: 15492373
4. Button B, Picher M, Boucher RC. Differential effects of cyclic and constant stress on ATP release and mucociliary transport by human airway epithelia. The Journal of physiology. **580**(Pt. 2), 577–592 (2007).
5. Goralski JL, Wu D, Thelin WR, Boucher RC, Button B. The in vitro effect of nebulised hypertonic saline on human bronchial epithelium. *Eur. Respir. J*. **51**, 1702652 (2018). PMCID: PMC6000726
6. te Velde, G., *et al*., Chemistry with ADF. *J. Comput. Chem*. **22**, 931-967 (2001).
7. Zhang, Y., Yang, W. Comment on “Generalized Gradient Approximation Made Simple”. *Phys. Rev. Lett*. **80**, 890 (1998).
8. Grimme, S., Antony, J., Ehrlich, S., Krieg, H. A consistent and accurate ab initio parametrization of density functional dispersion correction (DFT-D) for the 94 elements H-Pu. *J. Chem. Phys*. **132**, 154104 (2010).
9. van Lenthe, E., Baerends, E. Optimized Slater-type basis sets for the elements 1–118. *J. Comput. Chem*. **24**, 1142-1156 (2003).